www.aging-us.com AGING 2017, Vol. 9, No. 7

Research Paper

The effects of graded levels of calorie restriction: XI. Evaluation of the main hypotheses underpinning the life extension effects of CR using the hepatic transcriptome

Davina Derous[1,2], Sharon E. Mitchell[1], Lu Wang[3], Cara L. Green[1], Yingchun Wang[3], Luonan Chen[4], Jing-Dong J. Han[5], Daniel E.L. Promislow[6,7], David Lusseau[1], Alex Douglas[1,2], John R. Speakman[1,3]

[1]Institute of Biological and Environmental Sciences, University of Aberdeen, Aberdeen, Scotland, UK
[2]Centre for Genome Enabled Biology and Medicine, University of Aberdeen, Aberdeen, Scotland, UK
[3]State Key laboratory of Molecular Developmental Biology, Institute of Genetics and Developmental Biology, Chinese Academy of Sciences, Chaoyang, Beijing, China
[4]Chinese Academy of Sciences Key Laboratory of Computational Biology, Chinese Academy of Sciences-Max Planck Partner Institute for Computational Biology, Shanghai Institutes for Biological Sciences, Chinese Academy of Sciences, Shanghai, China
[5]Key laboratory of Systems Biology, Innovation Center for Cell Signaling Network, Institute of Biochemistry and Cell Biology, Shanghai Institute of Biological Sciences, Chinese Academy of Sciences, Shanghai, China
[6]Department of Pathology, University of Washington, Seattle, WA 98195, USA
[7]Department of Biology, University of Washington, Seattle, WA 98195, USA

Correspondence to: John R. Speakman, Alex Douglas; **email:** j.speakman@abdn.ac.uk, a.douglas@abdn.ac.uk

Keywords: aging, calorie restriction, gene expression, liver, transcriptomics
Received: April 27, 2017 **Accepted:** July 27, 2017 **Published:** July 31, 2017

ABSTRACT

Calorie restriction (CR) may extend longevity by modulating the mechanisms involved in aging. Different hypotheses have been proposed for its main mode of action. We quantified hepatic transcripts of male C57BL/6 mice exposed to graded levels of CR (0% to 40% CR) for three months, and evaluated the responses relative to these various hypotheses. Of the four main signaling pathways implied to be linked to the impact of CR on lifespan (insulin/insulin like growth factor 1 (IGF-1), nuclear factor-kappa beta (NF-κB), mechanistic target of rapamycin (mTOR) and sirtuins (SIRTs)), all the pathways except SIRT were altered in a manner consistent with increased lifespan. However, the expression levels of SIRT4 and SIRT7 were decreased with increasing levels of CR. Changes consistent with altered fuel utilization under CR may reduce reactive oxygen species production, which was paralleled by reduced protection. Downregulated major urinary protein (MUP) transcription suggested reduced reproductive investment. Graded CR had a positive effect on autophagy and xenobiotic metabolism, and was protective with respect to cancer signaling. CR had no significant effect on fibroblast growth factor-21 (FGF21) transcription but affected transcription in the hydrogen sulfide production pathway. Responses to CR were consistent with several different hypotheses, and the benefits of CR on lifespan likely reflect the combined impact on multiple aging related processes.

INTRODUCTION

Aging is accompanied by many metabolic changes and elevated risks of metabolic, cardiovascular, neurodegenerative and other non-communicable diseases. Obesity, insulin resistance, inflammation and hypertension are predisposing conditions that increase in prevalence during aging and contribute to the disease state known as the metabolic syndrome of aging [1]. In 1935, evidence emerged that mammalian longevity could be increased by restricting food intake [2]. Nowadays, it is well established that restricting the amount of calories contributes to an increased lifespan and healthspan in many species [3–8], including non-human primates [9]. CR also delays the onset of diseases related to the metabolic syndrome of aging, such as atherosclerosis, type 2 diabetes mellitus and cardiovascular diseases [10–12]. The mechanism(s) by which CR mediates its beneficial effects on aging are yet to be fully comprehended and are likely a result of changes simultaneously in many tissues and pathways. Mathematical models applied to mortality rates have been used to understand if CR postpones or slows the aging process [13]. Here, we analyzed the liver transcriptome as a part of a systems level description of graded CR responses [14–22]. From a clinical perspective the liver is well protected against aging relative to the other organs, but changes still occur in hepatic structure and function, such as declining liver regeneration, decreasing drug clearance and increasing bile cholesterol production [23]. Interestingly only four weeks of CR was able to reverse the majority of the aging-associated changes observed in murine liver [24]. Due to its central role in energy metabolism and glucose homeostasis, the liver is of great interest for genome-wide analysis to understand whole-body aging.

Different theories of aging have been proposed and over 25 years ago it was estimated that there were already more than 300 aging theories [25]. Many of these old theories have laid the ground for the progress that has been made in the current aging research field. Explanations of the impact of CR on longevity have focused on a limited set of hypotheses derived from these different theories. These hypothetical impacts of different systems in the longevity effects of CR may converge on common pathways and are hence not mutually exclusive.

Lifelong 40% CR alters hepatic fat metabolism by reducing lipogenesis, and increasing lipolysis and ketogenesis [26], while during aging there is a shift towards lipogenesis [27]. This alteration in lipid metabolism is believed to contribute to the CR-observed increase in lifespan [28,29]. During short-term CR, β-oxidation is increased and triglyceride synthesis inhibited, which leads to an improvement of liver function [30]. The disposable soma theory of aging argues that organisms reallocate energy sources to maintain the soma, at the cost of investment in reproduction [31,32]. In addition, CR also induces a shift to β–oxidation of fatty acids, which produces flavin adenine dinucleotide (FADH). Unlike carbohydrate utilization (nicotinamide adenine dinucleotide (NADH) production) FADH bypasses complex I in the electron transport chain, which is a primary site for reactive oxygen species (ROS) production [33]. The free radical theory of aging argues that accumulation of damage due to ROS leads to a gradual decline in cellular function [34]. CR could be protective against oxidative stress damage achieved by a decrease in the rate at which ROS are generated, an increase in the rate at which ROS are detoxified and/or an up-regulation of degradation and repair processes (reviewed in [4]).

Several major pathways have also been implicated to impart the beneficial effects associated with CR. These are reduced insulin/insulin like growth factor (IGF-1) signaling [15,35,36], reduced mechanistic target of rapamycin (mTOR) signaling [37], reduced nuclear factor-kappa beta (NF-κB) signaling [38] and increased sirtuin signaling [39]. Downregulation of the evolutionary conserved insulin/IGF-1 signaling pathway is associated with increase in lifespan in worms, flies and rodents [40–44]. The insulin/IGF-1 signaling pathway regulates its downstream effects via regulation of phosphoinositide-3-kinase (PI3K) and protein kinase B (AKT). In addition, the insulin/IGF-1 pathway has downstream effects on the mTOR complex 1 via AKT/Tuberous sclerosis 1 (TSC1). In response to nutrients and hormones, the mTOR signaling pathway can regulate protein synthesis, cellular growth and metabolism (reviewed in [45]). Inhibition of this pathway can increase lifespan in model organisms and inhibition is protective against aging-associated diseases (reviewed in [37]). NF-κB signaling is also associated with aging, mainly as its activation is linked with inflammation and known lifespan regulators insulin/IGF-1 and mTOR (reviewed in [38]). Increased sirtuin signaling has been found to increase lifespan in numerous species [46–49] and can also interact with the insulin signaling pathway [50]. Sirtuin signaling is linked to autophagy, and the increased autophagy under CR may contribute to the increase in lifespan [51,52]. Lastly the beneficial effects of CR on cancer are well known and its anti-cancer effect may also be involved in extending lifespan (reviewed in [53]).

Many of these pathways have common signaling cascades and therefore might coincide in their effects. Hence, we concentrated on the main mechanisms proposed for the anti-aging effects of CR: modulated insulin/IGF-1, mTOR, NF-κB and Sirtuin signaling, reduced oxidative stress, the disposable soma theory, anti-cancer mechanisms and increased autophagy. In addition, the role of fibroblast growth factor-21 (FGF21), a hormone secreted by liver during fasting, has gained recent prominence in the aging field [54] and hydrogen sulfide (H_2S) was also recently proposed to play a key role in aging [55]. We therefore included these in our analysis. Lastly, we also included xenobiotic metabolism as a separate mechanism from oxidative stress as suggested by studies in worms [56]. In most rats and mice increasing levels of CR in both sexes are linearly related to the increase in lifespan [3,4,57]. Hence the use of graded levels of CR as a research tool has gained much prominence in recent years [58–60]. C57BL/6 mice that are both known responders to CR and a well-studied strain, were the subject of the mouse genome project and are therefore ideal to study the graded effects of CR. Linear changes in gene expression with the level of restriction may likely be key components driving the longevity response. We therefore used a correlation approach across different levels of CR to investigate if the hypothesized mechanisms mediating the CR effect responded in a linear fashion when mice were exposed to graded levels of CR.

RESULTS

General correlation approach mapped onto pathways from IPA and custom built pathways

We used 6 levels of restriction (5 month old male mice, restricted for 3 months until 8 months old): 24 hours *ad libitum* (AL) feeding, 12 hours AL feeding (time restricted feeding), 10% CR, 20% CR, 30% CR and 40% CR which will be referred to as 24AL, 12AL, 10CR, 20CR, 30CR and 40CR respectively. The gene expression levels were correlated with the increase in restriction. If a pathway mediated the effect of CR on lifespan, we expected gene expression in this pathway to correlate with the increase in CR level. We constructed several pathways that represent the different mechanisms related to aging. The pathways were custom built based on expert knowledge and curated databases using Ingenuity Pathway Analysis (IPA) software. The pathways were colored based on a cut-off of an absolute correlation coefficient higher than 0.3. Regulation of the downstream pathways from the aging mechanisms are identified by pathway analysis in IPA. In addition to the p-value for individual pathways we also calculated a z-value reflecting up or down regulation of the entire pathway (for more details see methods).

The effect of graded CR on the insulin/IGF-1 signaling pathway

Insulin activates the insulin receptor (INSR) and downstream the insulin receptor substrate (IRS) family. Phosphorylated IRS proteins expose binding sites for signaling partners including PI3K which ultimately activates AKT. IGF-1 binds to its receptor (IGF1R) and induces a signaling cascade also via PI3K/AKT. In addition, AKT regulates mTOR via TSC1/TSC2. The INSR correlated positively with the increase in CR, probably reflecting the lowered levels of circulating insulin [15], while members of IRS family, PI3K, ATP citrate lyase (*Acly*) correlated negatively. Further downstream several target genes correlated negatively with the extent of CR (Figure1, Table S1). However, other components in this pathway correlated positively (Figure 1, Table S1). The PI3K/AKT (z-score: -3.138, p-value: 0.019) and IGF-1 signaling (z-score: -1.091, p-value: 0.002) pathways were both significantly downregulated and hence the insulin/IGF-1 signaling appeared to be reduced in direct proportion to the increasing severity of CR. Significantly altered pathways downstream from Insulin/IGF-1 included changes in gluconeogenesis (z-score: 0.370, p-value: <0.001), lipolysis (z-score: NA, p-value: 0.046), and protein synthesis (z-score: -2.115, p-value: <0.001).

We previously measured urinary major urinary proteins (MUPs), food anticipatory activity (FAA) and basal metabolic rate (BMR) in the same animals [15,18,21]. We assessed whether changes in urinary MUPs, FAA and BMR were associated with gene expression levels of genes involved in the insulin/IGF-1 signaling pathway. In total, gene expression levels of 13 genes involved in insulin/IGF-1 signaling correlated significantly with FAA, 7 with urinary MUPs and 10 with BMR (Table 1).

The effect of graded CR on the mTOR pathway

mTOR exists in two complexes: mTORC1 and mTORC2. Complex one contains the regulatory associated protein of MTOR, complex 1 (RAPTOR or *Rptor*), MTOR associated protein, LST8 homolog (GBL or *Mlst8*) and AKT1 substrate 1 (PRAS40 or *Akt1s1*) while complex two contains GBL, RPTOR independent companion of MTOR, complex 2 (RICTOR), the PROTOR group and mitogen-activated protein kinase associated protein 1 (SIN1 or *Mapkap1*). Both mTOR complexes are stimulated by Ras homolog enriched in brain (RHEB) which is downstream from insulin, growth factor and nutrient signaling pathways. RHEB is negatively regulated by TSC1/2. Gene expression of the components of both mTORC1 and mTORC2 were negatively correlated with increasing CR level, indicating significantly reduced signaling of mTOR under increasing CR (Figure 2, Table S2). Based on the correlation coefficient of the genes involved in mTORC1 and mTORC2, these 2 complexes were predicted in IPA to be negatively correlated with the increase in CR. However, no differences were observed between mTORC1 and mTORC2 in the extent of downregulation. The overall mTOR signaling pathway was indeed downregulated (z-score: -0.18, p-value: <0.001). Genes clustered together by IPA as the RHO group downstream from mTORC2 also correlated negatively with the increase in CR. RICTOR on the other hand correlated positively with the increase in CR. Expression levels of ribosomal protein S6 kinase beta-1 (*S6k1*) did not correlate with the increase in CR. Graded CR significantly altered several pathways downstream from mTOR including: autophagy (z-score: 0.833, p-value: <0.001), lipid metabolism (z-score: NA, p-value: <0.001), angiogenesis (z-score: 0.829, p-value: <0.001), cell proliferation (z-score -0.357, p-value: <0.001) and protein synthesis (z-score: -2.115, p-value: <0.001).

The effects of graded CR on NF-κB signaling

The IKK complex (inhibitor of kappaB kinase beta (IKKβ) and conserved helix-loop-helix ubiquitous kinase (IKKα)) phosphorylates IκB proteins, and is activated by cytokines, growth factors and antigen receptors. Phosphorylation of IκB leads to downstream inactivation of the NF-κB/Rel complex via ubiquitination and proteasomal degradation. NF-κB/Rel proteins include NF-κB2 p52/p100, NF-κB1 p50, p65/v-rel reticuloendotheliosis viral oncogene homolog A (avian) (RelA), and avian reticuloendotheliosis viral (v- rel)

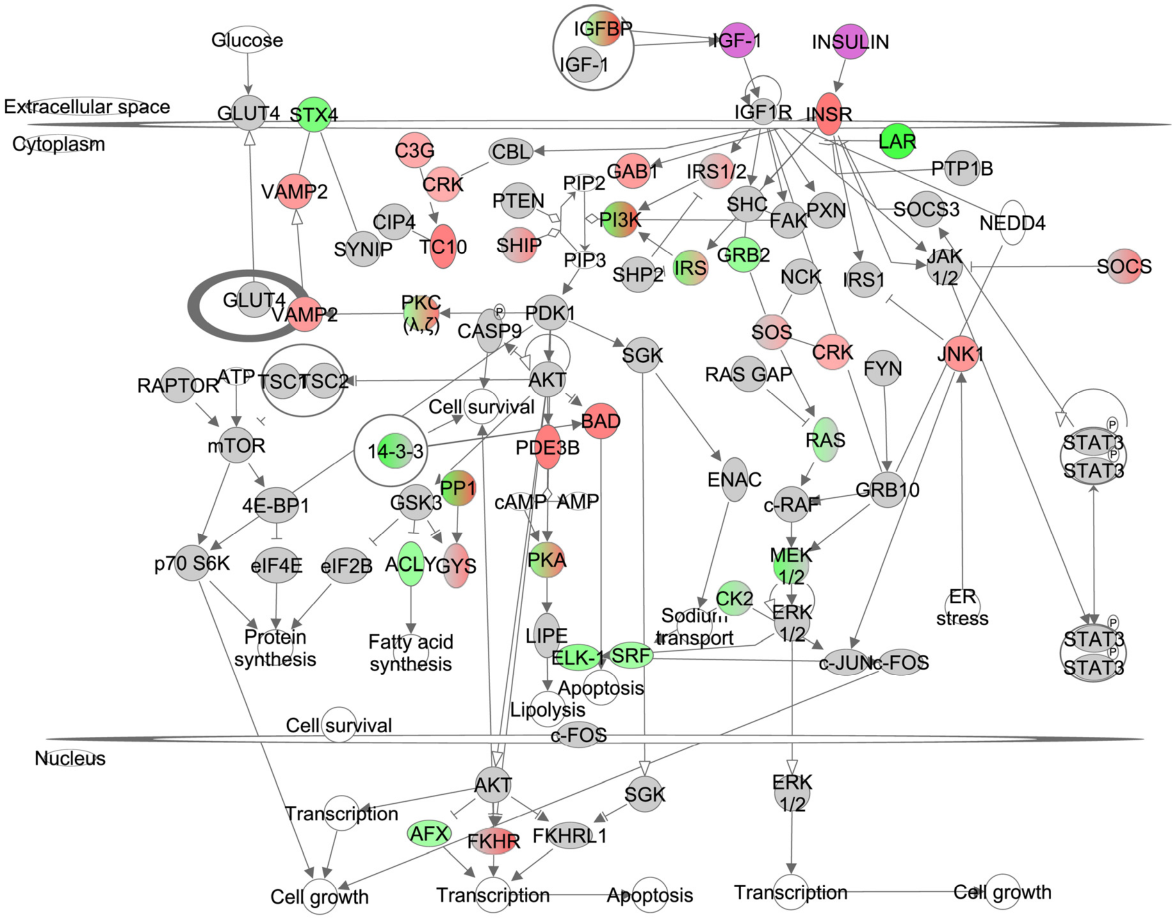

Figure 1. The insulin like growth factor (IGF-1)/insulin pathway created in the Ingenuity Pathway Analysis (IPA, www.qiagen.com/ingenuity) program. The normalized counts for each gene were correlated with the increase in calorie restriction (CR) level by Pearson correlation method. The pathway is colored based on a cut-off of an absolute correlation coefficient higher than 0.3.. Red indicates a positive correlation with increasing CR level while green indicates a negative correlation. Circulating levels of insulin and IGF-1 were significantly reduced in these CR mice [15] and this is indicated by a purple color.

oncogene related B (RelB) and transcribes target genes in the nucleus. In addition, IKKα can phosphorylate NF-κB2 p100 via an alternative pathway. This leads to downstream activation of RelB and induces target gene transcription in the nucleus. IκB was positively correlated with the increase in CR level and the NF-κB/RelB complexes were negatively correlated, indicating the increasing levels of CR progressively reduced signaling of this pathway (Figure 3, Table S3). NF-κB induced significant changes in the inflammation and immune response, cell proliferation (z-score -0.357, p-value: <0.001) and lymphogenesis (z-score: -0.539, p-value: <0.001).

We previously measured circulating hormone levels of the same mice [15] and assessed whether expression levels of genes involved in the NF-κB signaling pathway were significantly associated with these hormones. In total 4 genes correlated with leptin, 5 with insulin, 1 with interleukin 6 (IL6), 7 with tumor necrosis factor-alpha (TNF-α) and 11 with IGF-1 (Table 2).

The effects of graded CR on sirtuin signaling

The sirtuin signaling pathway has shared signaling cascades with mTOR signaling, NF-κB and insulin signaling, and gene expression of some members of these pathways correlated negatively with the increase of CR (Figure 2-3, Table S2-S3). There are seven sirtuins in mammals (SIRT1-7) which are involved in various biological functions. We constructed this pathway based on the Sirtuins at a glance publication by Nakagawa and Guarente (2011) [61]. Of these 7 SIRTs only *Sirt4* and *Sirt7* correlated negatively with the increase in CR (Figure 4, Table S4). Target genes of *Sirt4*, insulin degrading enzyme (IDE) and solute carrier family 25 (mitochondrial carrier, adenine nucleotide translocator), member 5 (SLC254A), correlated negatively and positively respectively with graded CR.

Table 1. Expression levels of gene involved in insulin/IGF-1 signaling pathway correlated with urinary major urinary proteins (MUPs), food anticipatory activity (FAA) and basal metabolic rate (BMR).

	MUPs		FAA		BMR	
	r	p-value	r	p-value	r	p-value
Acly	0.425	0.019				
Bad			0.419	0.042	-0.350	0.031
Casp9			-0.488	0.016		
Eif4ebp1			-0.486	0.016		
Elk1			-0.428	0.037	0.407	0.011
Foxo4	0.431	0.018				
Fyn			-0.442	0.031	0.457	0.004
Grb2					0.423	0.008
Insr			0.408	0.048	-0.461	0.004
Irs1	0.419	0.021				
Lipe			-0.410	0.047		
Mapk8			0.495	0.014	-0.334	0.041
Nck1	0.495	0.005				
Pde3b			0.530	0.008	-0.443	0.005
Ptprf	0.440	0.015	-0.648	0.001	0.549	<0.001
Rapgef1	-0.378	0.039				
Rhoq			0.490	0.015	-0.322	0.049
Socs3			-0.441	0.031		
Srf			-0.405	0.049		
Stx4a	0.680	<0.001			0.481	0.002

Normalized gene counts for each individual was correlated with their corresponding physiological and behavioral data.

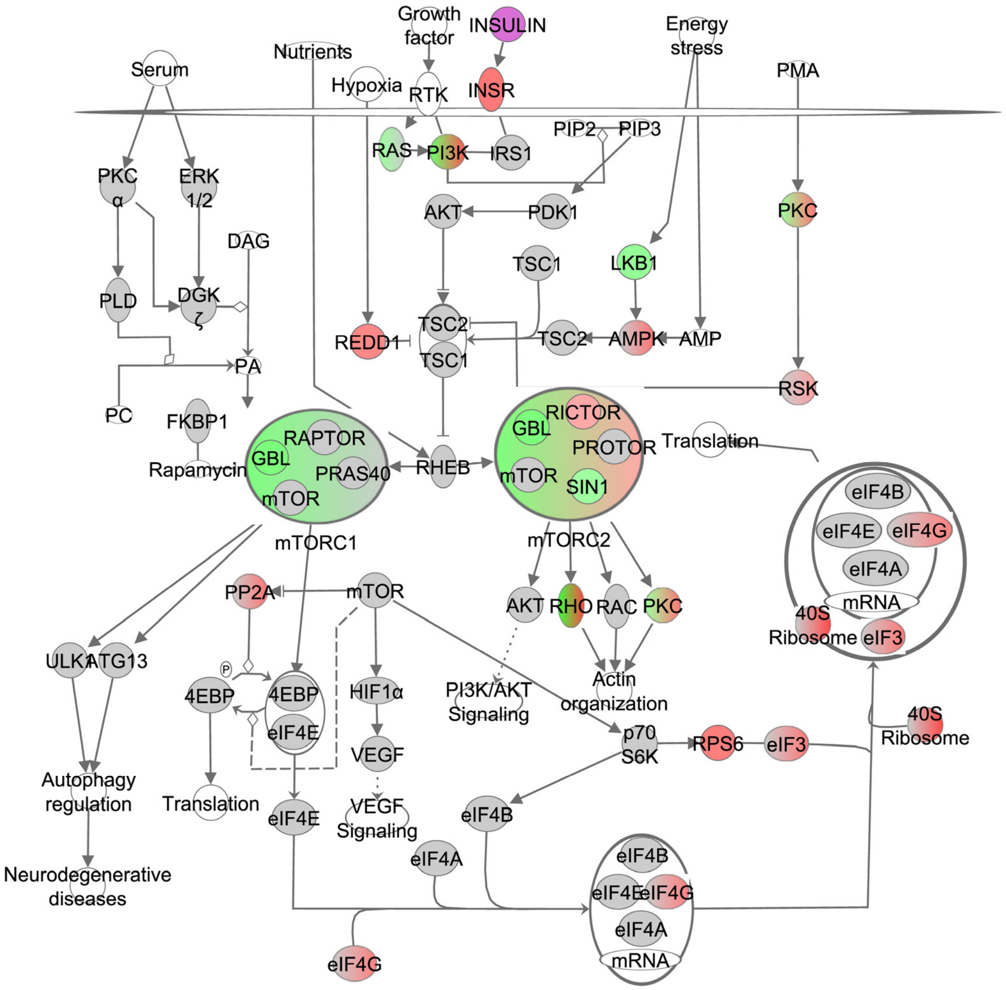

Figure 2. The mechanistic target of rapamycin (mTOR) signaling pathway obtained from the Ingenuity Pathway Analysis (IPA, www.qiagen.com/ingenuity) program. The normalized counts for each gene were correlated with the increase in calorie restriction (CR) level by Pearson correlation method. The pathway is colored based on a cut-off of an absolute correlation coefficient higher than 0.3. Red indicates a positive correlation with increasing CR level while green indicates a negative correlation. Circulating levels of insulin were significantly reduced in these CR mice [15] and this is indicated by a purple color.

The effects of graded CR on oxidative stress signaling

It has been hypothesized that CR may modulate oxidative stress by decreasing the rate at which ROS are generated, increasing the rate at which ROS are detoxified and upregulating degradation and repair processes (reviewed in [4]). This pathway includes processes such as nitric oxide (NO) production, nuclear factor erythroid derived 2 (NRF2) signaling, hypoxia-inducible factor 1-alpha (HIF1-α) signaling, eukaryotic initiation factor 2 (eIF2) signaling, inducible nitric oxide synthase (iNOS) signaling and NF-κB signaling. Interleukins, TNF-α and insulin have been suggested to induce expression in this pathway. Under graded CR, gene expression in this pathway indicated that genes involved in the eIF2 signaling (z-score: 4.718, p-value: <0.001) were positively correlated with the extent of restriction while NRF2 (z-score: NA, p-value: 0.001) correlated negatively (Figure 5, Table S5). In addition, the production of ROS was predicted to be decreased (z-score: -0.305, p-value: <0.001).

Table 2. Expression levels of gene involved in NF-κB signaling pathway correlated with levels of circulating hormones.

	leptin		insulin		IL6		TNF-α		IGF-1	
	r	p	r	p	r	p	r	p	r	p
Azi2			-0.508	0.003			-0.376	0.031	-0.517	0.002
Card11							0.391	0.024		
Cd4			0.417	0.016			0.429	0.013		
Chuk					-0.400	0.038				
Fadd							0.577	<0.001		
Gsk3b	-0.371	0.034	-0.427	0.013					-0.568	0.001
Malt1									-0.347	0.048
Mapk8									-0.534	0.001
Peli1			-0.361	0.039						
Prkcz									0.513	0.002
Rela							0.360	0.039		
Ripk1	-0.416	0.016							-0.433	0.012
Tab1									-0.367	0.036
Tbk1									-0.368	0.035
Tbp	-0.374	0.032							-0.386	0.027
Tdp2									-0.455	0.008
Tirap	0.362	0.038	0.477	0.005						
Tradd							0.435	0.011		
Traf6									-0.492	0.004
Ube2n							0.544	0.001		

Normalized gene counts for each individual was correlated with their corresponding physiological and behavioral data.

We previously measured activity levels of antioxidants in livers of the same individual mice [15] and we assessed whether their expression levels correlated with the corresponding enzyme activity levels. The expression levels of the gene catalase (*Cat*) correlated positively with the measured actively levels of this antioxidant (r: 0.378, p-value: 0.019). Gene members of the superoxide dismutase family correlated negatively with activity levels of superoxide dismutase (*Sod1* r: -0.325 p-value: 0.046; *Sod2* r: -0.335 p-value: 0.039). None of the gene members of the glutathione peroxidase (GPx) family correlated significantly with the anti-oxidant activity level of GPx. In total, 10 genes involved in oxidative stress correlated with SOD activity levels, 29 with catalase and 9 with GPx (Table 3). Gene expression levels were also correlated with circulating hormone levels of the same mice [15] (Table 4). In total 30 genes correlated significantly with leptin, 33 with insulin, 23 with TNF-α, 10 with IL6, 34 with IGF-1 and 36 with resistin.

The effects of graded CR on reproduction pathways

Major urinary proteins (MUPs) are used by male mice in scent marking to attract females and their synthesis is a major cost of reproduction [31,62,63]. The p53 signaling pathway has also been implicated to play are role in reproduction [64,65]. However downstream genes of p53 signaling did not correlate significantly with CR. Gene expression of the different MUPs all correlated negatively with the extent in restriction (Figure 6, Table S6). Expression levels of MUPs genes also correlated strongly in a positive manner with several circulating hormones measured in the same mice (Table 5). Other gene products involved in reproduction such as PPARGC1A, RAR-related orphan receptor gamma (RORC), phosphoenolpyruvate carboxykinase 1, cytosolic (PCK1) and nuclear receptor subfamily 1, group I, member 2 (NR1I2) correlated strongly in a positive manner with the increase in CR (Table S6).

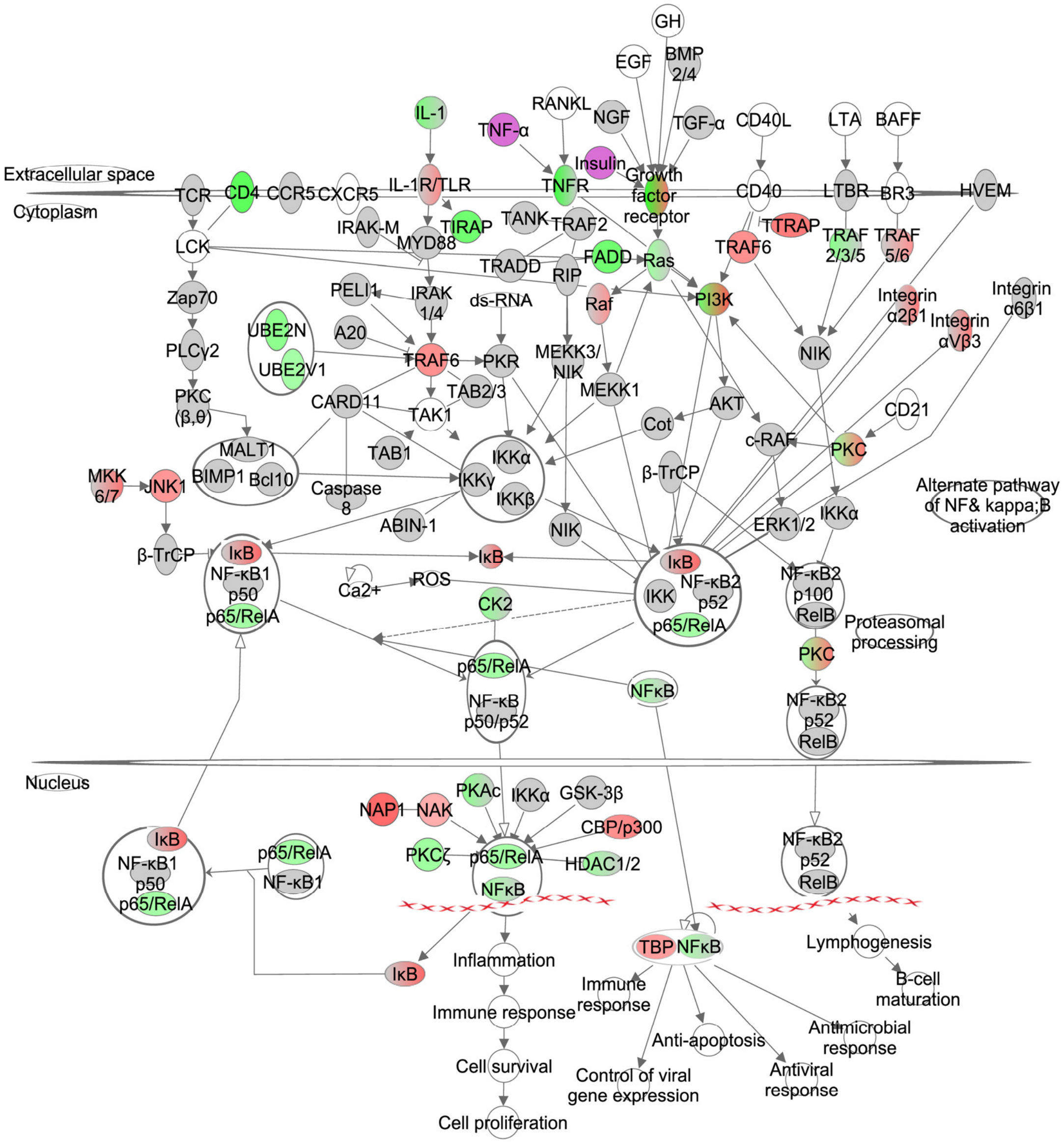

Figure 3. The nuclear factor kappa B (NF-κB) signaling pathway constructed in the Ingenuity Pathway Analysis (IPA, www.qiagen.com/ingenuity) program. The normalized counts for each gene were correlated with the increase in calorie restriction (CR) level by Pearson correlation method. The pathway is colored based on a cut-off of an absolute correlation coefficient higher than 0.3. Red indicates a positive correlation with increasing CR level while green indicates a negative correlation. Circulating levels of insulin and TNF-α were significantly reduced in these mice [15] and this is indicated by a purple color.

The effects of graded CR on cancer signaling pathways

A number of pathways are involved in cancer signaling, and show overlap with the oxidative stress signaling pathway (e.g. HIF1-α, NO, NRF2, iNOS). Expression of genes downstream from p53 did not correlate with the increase in CR but NF-κB correlated negatively with the increase in CR. Hedgehog, TGF-β and Catenin beta 1 (CTNNβ) signaling all showed negative correlations to the extent of increasing CR (Figure 7, Table S7). The tumor suppressor genes of the SMAD family also correlated positively with CR (Figure 7, Table S7). The 'disease function' cancer was predicted to be strongly decreased (z-score: -3.285, p-value: <0.001).

Table 3. Expression levels of gene involved in oxidative stress signaling correlated with activity levels of antioxidants.

	SOD		catalase		GPx	
	r	p-value	r	p-value	r	p-value
Apex1			0.385	0.017	0.339	0.037
Atf4	0.343	0.035			0.432	0.007
Brca1	-0.329	0.044				
Calr			0.333	0.041		
Casp3			0.323	0.048	0.539	<0.001
Cat			0.380	0.019		
Cbr1	-0.345	0.034	-0.382	0.018		
Crebbp			-0.340	0.037		
Cul2			0.377	0.020		
Eif2a	-0.423	0.008				
Eif2s1			0.324	0.047		
Eif4e			0.382	0.018		
Fkbp5			-0.457	0.004		
Fmo1			-0.472	0.003		
Fth1	-0.445	0.005	-0.387	0.016		
Hsp90aa1			0.415	0.010		
Hsp90b1	0.344	0.034	0.359	0.027	0.377	0.020
Hspa5			0.388	0.016		
Insr			-0.329	0.044		
Map2k1	0.371	0.022	0.379	0.019		
Map2k5	-0.321	0.049				
Mapk14	-0.370	0.022	-0.437	0.006		
Ncf4			0.392	0.015		
Nfkbia			-0.419	0.009		
Ppib			0.334	0.040		
Prkcb					0.351	0.031
Scarb1			-0.323	0.048		
Serpine1						
Shc1					0.410	0.011
Stip1			0.438	0.006		
Taok3			-0.451	0.004		
Tdp1					0.412	0.010
Trp53bp1			0.371	0.022		
Ube2e3			-0.427	0.008		
Usp14			0.340	0.037		
Vcp			0.448	0.005	0.330	0.043

Normalized gene counts for each individual was correlated with their corresponding physiological and behavioral data.

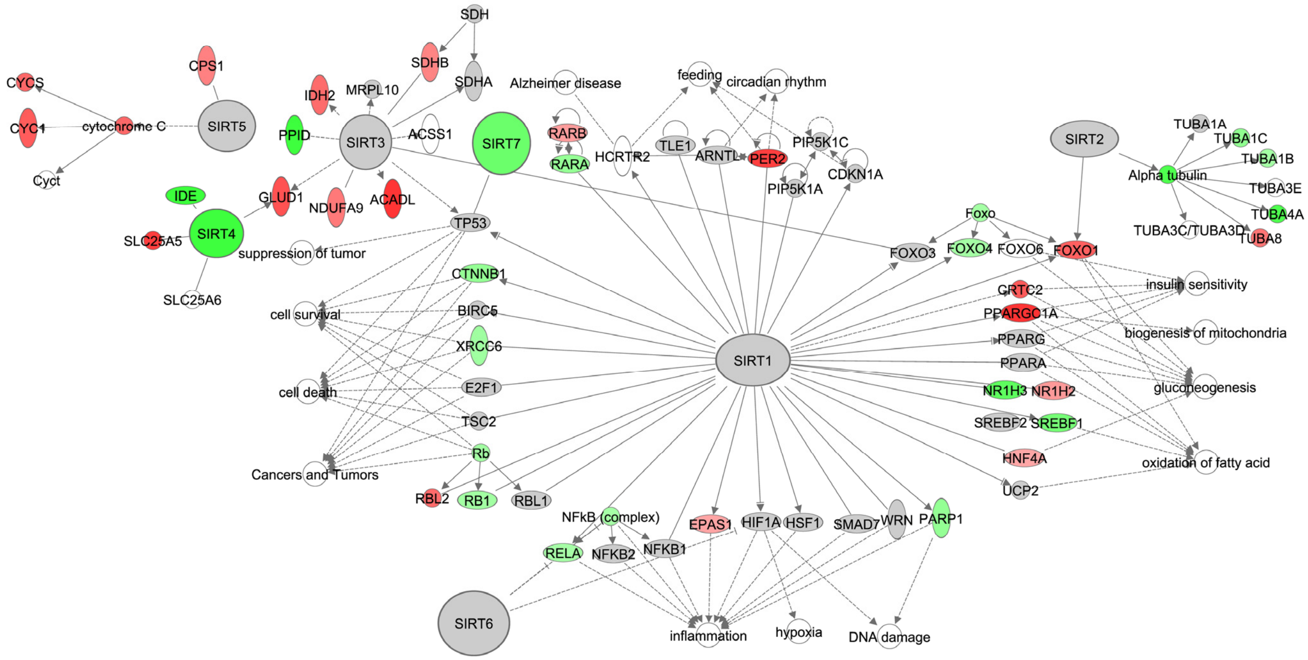

Figure 4. The sirtuin signaling pathway constructed in the Ingenuity Pathway Analysis (IPA, www.qiagen.com/ingenuity) program. The normalized counts for each gene were correlated with the increase in calorie restriction (CR) level by Pearson correlation method. The pathway is colored based on a cut-off of an absolute correlation coefficient higher than 0.3. Red indicates a positive correlation with increasing CR level while green indicates a negative correlation.

The effects of graded CR on autophagy

Starvation and nutrient deprivation induce autophagy. In addition, PI3K/AKT (insulin pathway) signaling activates mTOR and ERK/MAPK signaling negatively regulates mTOR, which both lead to an activation of mTOR and suppression of autophagy. Downstream from mTOR, UNC-51 like kinase 1 (ULK1) forms a large complex with autophagy related 13 (AGT13) and the scaffold protein FIP200. PI3K class III is required for the induction of autophagy. The ATG genes control autophagosome formation through ATG12/ATG5 which requires ATG7 and ATG10. This induces the lipidated form of LC3 (LC3-II) which is attached to the autophagosome membrane. FIP200 and the further downstream AGT genes correlated positively with CR (Figure 8, Table S8). Similar results were found for LC3, LC3-I and LC3-II. Hence, autophagy was significantly increased with increasing levels of CR (z-score: 0.833, p-value: <0.001). Gene expression levels of genes involved in autophagy correlated negatively with circulating levels of IGF-1 measured in the same mice (Table 6).

The effects of graded CR on mitochondrial biogenesis and fuel utilization

We split mitochondrial biogenesis and fuel utilization into 5 separate pathways: Glycolysis, the tricarboxylic acid cycle (TCA) cycle, fatty acid β-oxidation, and the electron transport chain (ETC) combined with mitochondrial biogenesis genes and gluconeogenesis. The genes involved in glycolysis (z-score: NA, p-value: 0.016), TCA cycle (z-score: NA, p-value: <0.001), fatty acid β-oxidation (z-score: 2.872, p-value: <0.001) and gluconeogenesis (z-score: 0.370, p-value: <0.001) all showed positive correlations with the extent of restriction (Figure 9A-D). Genes involved in the ETC were also positively correlated with the increase of CR, especially at complexes II, IV and V. Genes signaling mitochondrial dysfunction and apoptosis (z-score: -1.504, p-value <0.001) were negatively correlated with CR (Figure 10, Table S9). In addition genes involved in ETC, gluconeogenesis, glycolysis and TCA correlated in general positively with FAA and negatively with circulating levels of leptin and insulin, body temperature and BMR measured in the mice (Figure 11).

Table 4. Expression levels of gene involved in oxidative stress signaling correlated with levels of circulating hormones.

	leptin		insulin		TNF-α		IL6		IGF-1		resistin	
	r	p	r	p	r	p	r	p	r	p	r	p
Abcc1											-0.422	0.028
Abcc2	-0.471	0.006	-0.418	0.016					-0.563	0.001		
Abl1	-0.365	0.037										
Aox1					0.354	0.044						
Apex1					0.365	0.037						
Arnt	-0.413	0.017							-0.556	0.001		
Atf2			-0.464	0.007					-0.544	0.001		
Bach1			-0.477	0.005								
Calr	0.374	0.032	0.621	<0.001	0.517	0.002			0.545	0.001		
Casp9							0.429	0.026				
Cat	0.523	0.002	0.428	0.013	0.509	0.002	-0.497	0.008	0.625	<0.001		
Cbr1	-0.570	0.001	-0.514	0.002	-0.383	0.028			-0.654	<0.001		
Cbx5			-0.392	0.024								
Cdc25a	-0.371	0.033	-0.373	0.033					-0.451	0.008		
Cdc34											-0.382	0.049
Cdkn1a											-0.403	0.037
Clpp							0.554	0.003			-0.444	0.020
Cops5											-0.410	0.034
Crebbp	-0.525	0.002	-0.419	0.015					-0.579	<0.001		
Csf2ra											-0.411	0.033
Csf2rb2											-0.424	0.028
Cul2			0.416	0.016	0.465	0.006					-0.453	0.018
Cybb											-0.437	0.023
Eif1a											-0.382	0.049
Eif2a	-0.396	0.023	-0.504	0.003					-0.433	0.012		
Eif2ak4									-0.478	0.005		
Eif2s1											-0.404	0.037
Eif2s3x									-0.553	0.001		
Eif4e											-0.425	0.027
Enc1	-0.404	0.020							-0.509	0.002		
Erp29			0.420	0.015	0.458	0.007			0.361	0.039	-0.495	0.009
Fkbp5	-0.581	<0.001	-0.487	0.004	-0.597	<0.001			-0.515	0.002		
Fmo1	-0.605	<0.001	-0.548	0.001	-0.647	<0.001			-0.569	0.001		
Fth1			-0.415	0.016			0.427	0.027	-0.458	0.007		
Gclc					0.354	0.043						
Gsk3b	-0.371	0.034	-0.427	0.013					-0.568	0.001		
Gsr											-0.447	0.019

H2afx											-0.461	0.015
Herpud1	-0.408	0.018										
Hif1a							-0.401	0.038				
Hsp90aa1											-0.501	0.008
Hsp90b1			0.522	0.002	0.488	0.004						
Hspa5											-0.431	0.025
Icam1											-0.397	0.040
Insr	-0.466	0.006	-0.546	0.001	-0.407	0.019			-0.481	0.005		
Maf	-0.344	0.050	-0.478	0.005	-0.479	0.005						
Map2k1			0.427	0.013	0.354	0.043			0.373	0.032	-0.444	0.020
Map3k1											-0.399	0.039
Map3k5	-0.485	0.004	-0.644	<0.001	-0.557	0.001			-0.394	0.023		
Mapk14	-0.560	0.001	-0.496	0.003	-0.380	0.029			-0.462	0.007		
Mapk8									-0.534	0.001		
Mdm2									-0.457	0.008		
Mdm4			-0.353	0.044					-0.578	<0.001		
Ncf2											-0.417	0.030
Ncf4											-0.460	0.016
Ncoa1									-0.554	0.001		
Nfkbia	-0.453	0.008	-0.507	0.003	-0.390	0.025			-0.478	0.005		
Pdpk1			-0.390	0.025					-0.525	0.002		
Plat											-0.453	0.018
Pmf1							0.388	0.046				
Ppara			-0.392	0.024							0.508	0.007
Ppib	0.427	0.013	0.650	<0.001	0.492	0.004			0.530	0.002		
Ppp1r15a	-0.356	0.042										
Prdx1	0.360	0.039										
Scarb1	-0.383	0.028					0.400	0.039				
Serpine1							0.460	0.016			-0.452	0.018
Shc1											-0.423	0.028
Sirpa											-0.433	0.024
Sqstm1											-0.441	0.021
Stip1			0.357	0.041							-0.411	0.033
Taok3	-0.456	0.008	-0.507	0.003					-0.473	0.005		
Tlr4											-0.439	0.022
Trim28	-0.415	0.016										
Trp53											-0.422	0.028
Trp53bp1											-0.520	0.005
Txn1	0.406	0.019			0.403	0.020					-0.454	0.017
Txnrd1											-0.458	0.016

Ube2k									-0.430	0.013
Vcam1	-0.506	0.003	-0.422	0.015					-0.437	0.011
Vcp			0.509	0.003	0.499	0.003				
Xbp1	0.438	0.011			0.370	0.034			0.485	0.004

Normalized gene counts for each individual was correlated with their corresponding physiological and behavioral data.

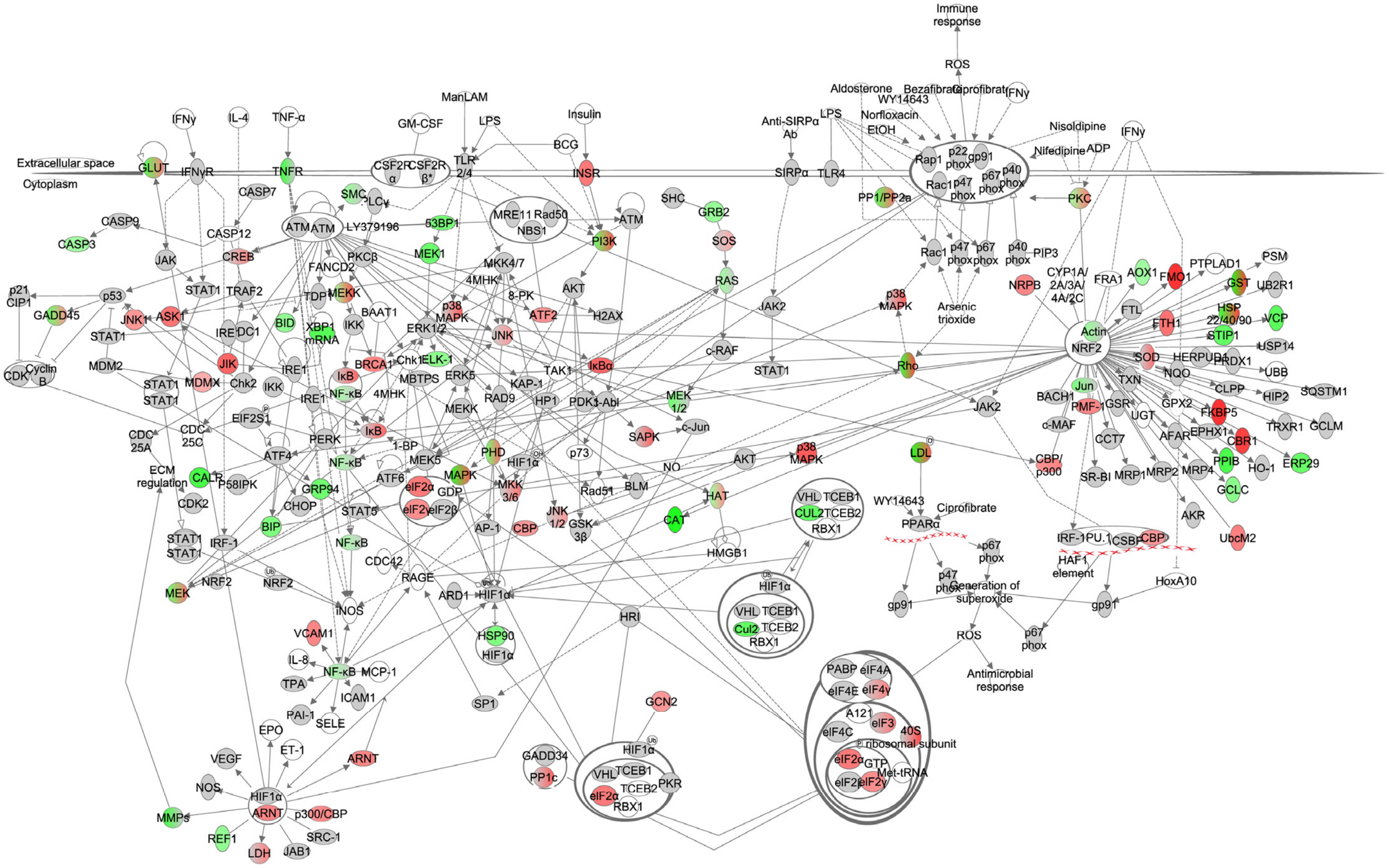

Figure 5. The oxidative stress signaling pathway constructed in the Ingenuity Pathway Analysis (IPA, www.qiagen.com/ingenuity) program. The normalized counts for each gene were correlated with the increase in calorie restriction (CR) level by Pearson correlation method. The pathway is colored based on a cut-off of an absolute correlation coefficient higher than 0.3. Red indicates a positive correlation with increasing CR level while green indicates a negative correlation.

The effects of graded CR on FGF21 and the H_2S pathway

Gene expression levels of *Fgf21* did not correlate with the extent of restriction (Table S10). H_2S is generated *in vivo* by cystathionine-γ-lyase (CSE or *Cth*) and cystathionine-β-synthase (CBS) and was shown to have an effect on circadian rhythm genes in a NAD/NAD+ ratio and *Sirt1* dependent manner [66]. Expression levels of genes involved in circadian rhythm such as period circadian clock 1 (*Per1*), *Per2*, cryptochrome 1 (*Cry1*) and *Cry2* were significantly positively correlated with CR. The circadian pathway itself however was not significantly altered with increasing CR levels (z-score: NA, p-value: 0.080). *Cth* correlated positively with CR while *Cbs* correlated negatively (Figure 12, Table S10).

Table 5. Gene expression levels of major urinary proteins (MUPs) correlated with circulating hormone levels.

	Insulin		IGF-1		TNF-α		Leptin	
	r	p-value	r	p-value	r	p-value	r	p-value
Mup1	0.345	0.049	0.414	0.017	0.292	0.099	0.475	0.005
Mup3	0.475	0.005	0.654	<0.001	0.443	0.010	0.732	<0.001
Mup4	0.279	0.116	0.565	0.001	0.418	0.016	0.579	<0.001
Mup5	0.319	0.070	0.595	<0.001	0.306	0.083	0.686	<0.001
Mup6	0.338	0.055	0.521	0.002	0.343	0.051	0.645	<0.001
Mup7	0.456	0.008	0.497	0.003	0.434	0.012	0.582	<0.001
Mup8	0.486	0.004	0.431	0.012	0.452	0.008	0.618	<0.001
Mup9	0.528	0.002	0.603	<0.001	0.450	0.009	0.592	<0.001
Mup10	0.534	0.001	0.661	<0.001	0.464	0.006	0.739	<0.001
Mup11	0.491	0.004	0.553	0.001	0.375	0.031	0.556	0.001
Mup12	0.320	0.070	0.397	0.022	0.326	0.064	0.466	0.006
Mup14	0.553	0.001	0.486	0.004	0.439	0.011	0.571	0.001
Mup16	0.495	0.003	0.489	0.004	0.457	0.007	0.626	<0.001
Mup17	0.440	0.010	0.516	0.002	0.382	0.028	0.636	<0.001
Mup20	0.581	<0.001	0.640	<0.001	0.529	0.002	0.714	<0.001
Mup21	0.447	0.009	0.558	0.001	0.368	0.035	0.669	<0.001

Normalized gene counts for each individual was correlated with their corresponding physiological and behavioral data.

Table 6. Expression levels of genes involved in autophagy correlated with circulating hormone levels.

	Insulin		IGF-1		TNF		Leptin	
	r	p-value	r	p-value	r	p-value	r	p-value
Atg10	-0.062	0.731	0.094	0.602	0.116	0.520	0.052	0.775
Atg13	0.138	0.443	-0.166	0.356	0.185	0.303	-0.044	0.809
Atg16l1	-0.297	0.093	-0.566	0.001	-0.148	0.412	-0.359	0.040
Atg7	0.043	0.811	0.422	0.014	0.033	0.854	0.180	0.317
Lamp2	0.298	0.092	0.656	<0.001	0.302	0.088	0.701	<0.001
Map1lc3a	-0.229	0.200	-0.133	0.460	-0.180	0.316	-0.131	0.469
Map1lc3b	-0.433	0.012	-0.166	0.355	-0.278	0.118	-0.426	0.013
Rb1cc1	-0.502	0.003	-0.609	<0.001	-0.221	0.216	-0.296	0.095
Stx17	-0.500	0.003	-0.456	0.008	-0.323	0.067	-0.335	0.057
Wdfy3	-0.509	0.002	-0.466	0.006	-0.429	0.013	-0.446	0.009

Normalized gene counts for each individual was correlated with their corresponding physiological and behavioral data.

The effects of graded CR on xenobiotic metabolism

Constitutive active receptor (CAR, *Nr1I3*) is able to activate target genes by forming a complex with retinoid X receptor alpha (RXRα). Similar pregnane X receptor (PXR, *Nr1I2*) also forms a complex with RXRα. These activate transcription of enzymes involved in the xenobiotic metabolism. The xenobiotic metabolism consists of phase I, phase II and phase III enzymes. Phase I enzymes include the cytochrome P450 family (CYP), flavin containing monooxygenase (FMO) and aldehyde dehydrogenase (ALDH). Transcription levels of *Nr1I2*, *Nr1I3*, *Rxra*, *Fmo1*, *Fmo2*, *Fmo3*, *Fmo4*, *Cyp2c8*, *Cyp3a7*, *Aldh1a3*, *Aldh3a2*, *Aldh5a1*, *Aldh6a1* and *Aldh9a1* were all strongly positively associated with the increase in CR (Figure 13, Table S11). Overall metabolism of xenobiotics was predicted to be significantly upregulated (z-score: 1.183, p-value: <0.001).

DISCUSSION

In this strain of mouse graded increases in CR leads to a graded increase in lifespan [67]: hence we suggested that changes at the molecular level mimicking this effect are likely to be more important than non-linear effects or responses that are constant across all levels. Here we found that graded CR had a graded impact on several different pathways in such a way that the changes might facilitate an increase in lifespan. To

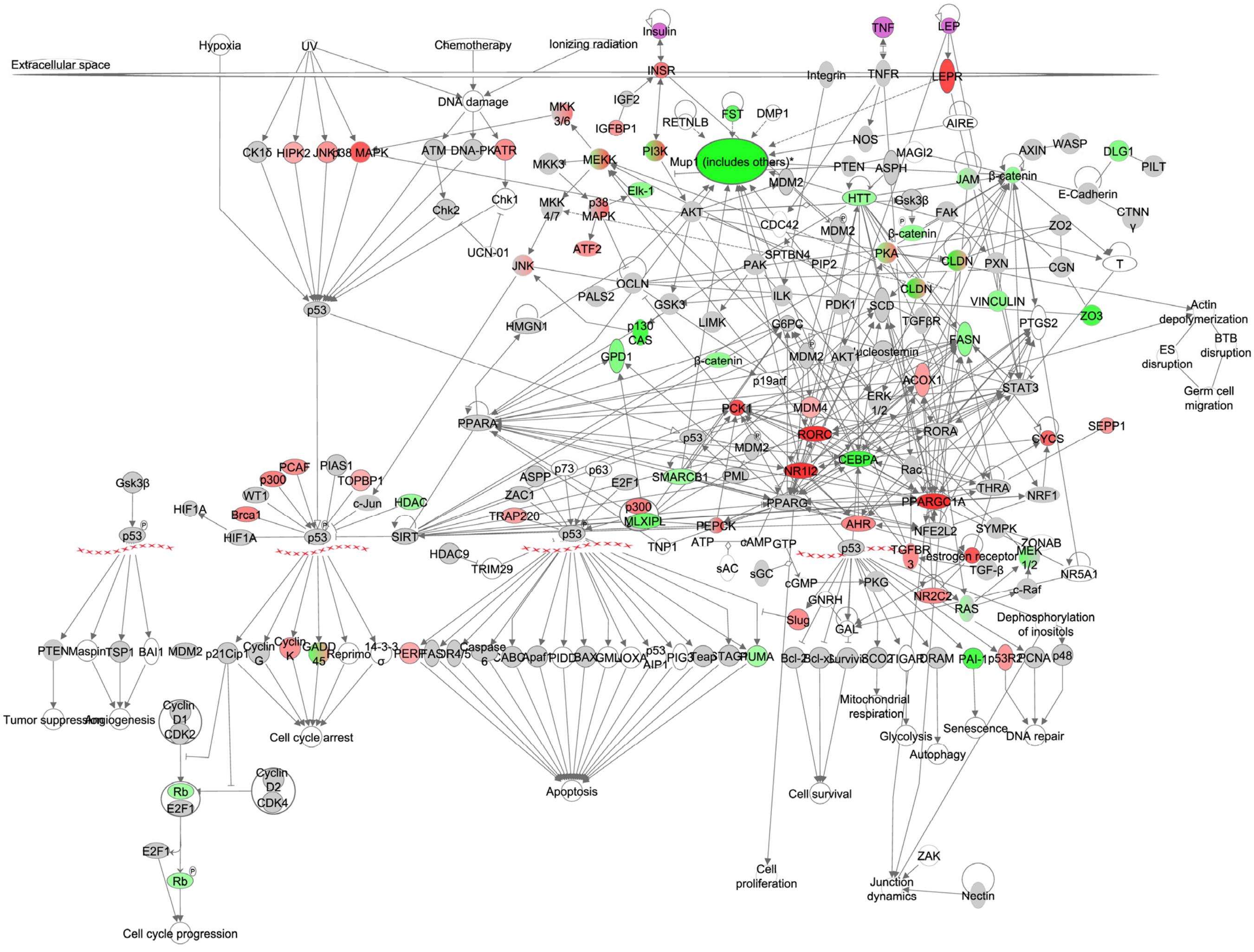

Figure 6. The reproduction pathway constructed in the Ingenuity Pathway Analysis (IPA, www.qiagen.com/ingenuity) program. The normalized counts for each gene were correlated with the increase in calorie restriction (CR) level by Pearson correlation method. The pathway is colored based on a cut-off of an absolute correlation coefficient higher than 0.3. Red indicates a positive correlation with increasing CR level while green indicates a negative correlation. Circulating levels of insulin, TNF-α and leptin were significantly reduced in these mice [15] and this is indicated by a purple color.

summarize, we found that insulin/IGF-1, NF-κB, and mTOR but probably not SIRT signaling pathways were correlated with graded CR in such a way that they may mediate the effect of CR on lifespan. The observed changes in fuel utilization related genes in relation to CR level may reduce oxidative stress. Reproductive investment in the form of MUPs were negatively associated with CR. Graded CR had a positive effect on autophagy and xenobiotic metabolism and CR was protective in cancer signaling. In addition, CR had no effect on transcription rates of FGF21 but did had a positive significant effect on the H_2S production mechanism. To aid the discussion of the results, we have included an integrated overview of the different pathways affected by graded CR (Figure 14).

CR has transcriptional impacts on three of the four evolutionary conserved signaling pathways related to longevity

The insulin/IGF-1 signaling pathway is evolutionary conserved and its role in aging came to light from stu-

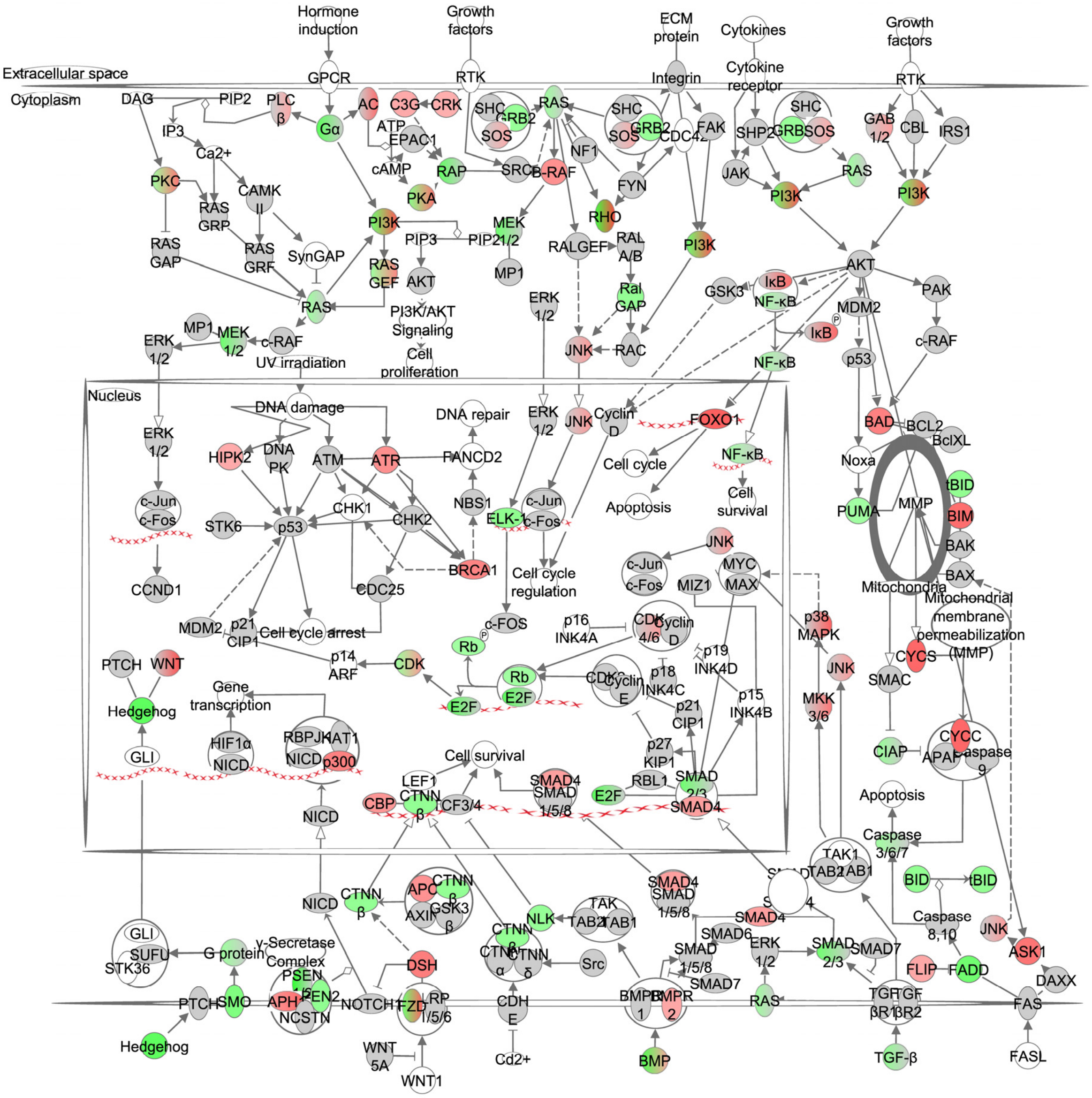

Figure 7. The cancer signaling pathway obtained from the Ingenuity Pathway Analysis (IPA, www.qiagen.com/ingenuity) program. The normalized counts for each gene were correlated with the increase in calorie restriction (CR) level by Pearson correlation method. The pathway is colored based on a cut-off of an absolute correlation coefficient higher than 0.3. Red indicates a positive correlation with increasing CR level while green indicates a negative correlation. The string of Xs represent DNA and indicate a transcriptional effect of a gene.

dies with *Caenorhabditis elegans* [40,68]. *C. elegans* mutants for the daf-2 gene (IGF-1 receptor), involved in insulin-like signaling, have a lifespan twice as long as wild types [41,50]. Mice lacking the insulin receptor substrate 1 (IRS1$^{-/-}$) but not IRS2 (IRS2$^{-/-}$) are long-lived, but strangely have lifelong insulin resistance, while being also resistant against age-sensitive markers [43,44]. The mice studied here exhibited lower circulating levels of insulin and IGF-1 under CR [15]. This was correlated with improved glucose tolerance and improved insulin sensitivity [15]. In the present paper, we found that expression levels of hepatic genes involved in the insulin/IGF-1 signaling pathway generally correlated negatively with increasing CR, including members of the IRS family: hence the pathway was inhibited and increasingly so at higher levels of restriction. Insulin signaling activates glycogen synthesis for energy storage, suppresses hepatic glucose output and initiates lipogenesis. These processes are all reduced under CR [26] and we found significant downregulation of *Acly* in this pathway which is involved in the synthesis of fatty acids [69,70]. In agreement with other studies that have focused on single levels of restriction [15,35,36], these results indicate insulin/IGF-1 signaling is reduced under CR in relation to the extent of restriction and hence may contribute to the graded increase in lifespan under graded CR [40–42]. However, elucidating the exact mechanism by which reduced insulin/IGF-1 regulates longevity is challenged by its complexity (reviewed in [71]). This pathway may mediate its beneficial effects via its impact on oxidative stress [72,73], the change in substrate utilization under CR [28,29], its impact in other pathways such as mTOR [74], xenobiotic detoxification mechanisms [75] and reproduction [76,77]. In addition, insulin and IGF-1 have been implicated to play a role in cancer [78].

Similar to insulin, the role of mTOR in longevity was first established in *C. elegans* where mutations in mTOR and mTORC1 component raptor (daf-15) extended longevity [79,80]. In *Drosophila melanogaster,* mutations of mTOR and several components

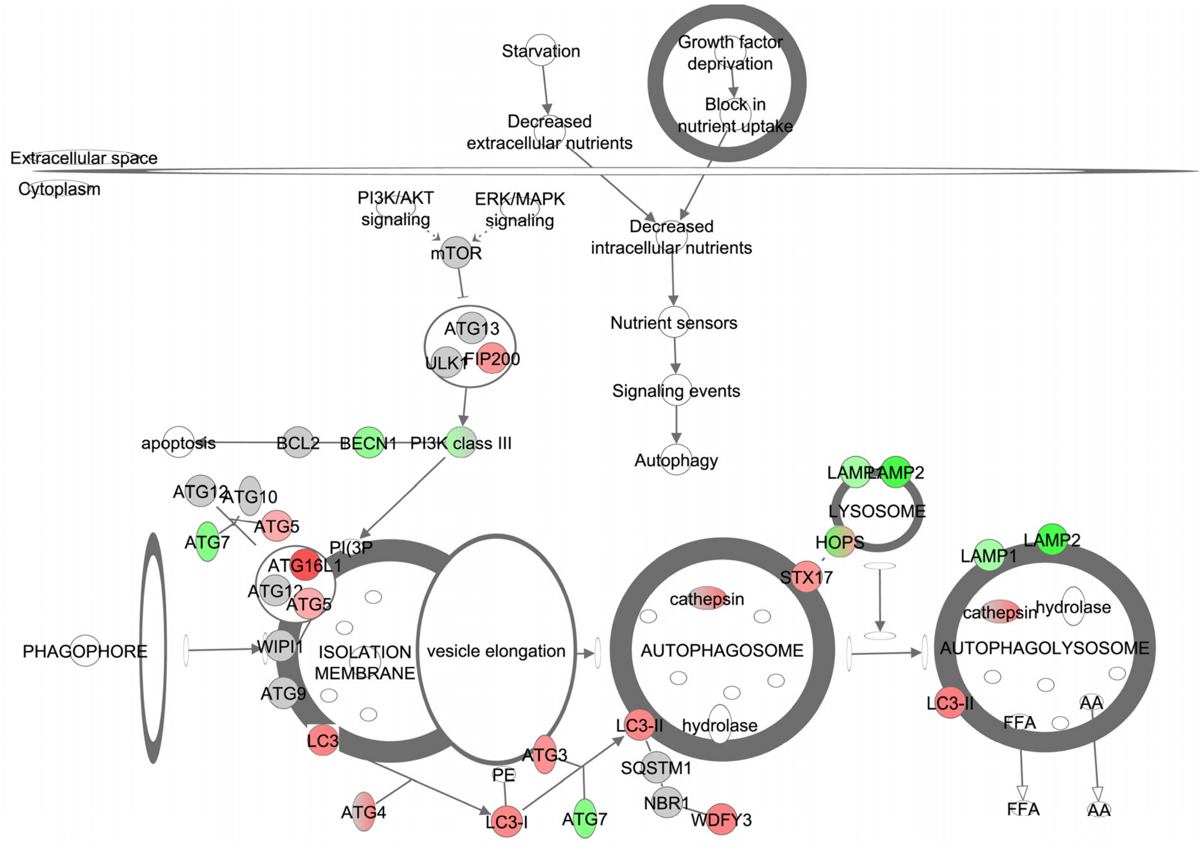

Figure 8. The autophagy signaling pathway obtained from the Ingenuity Pathway Analysis (IPA, www.qiagen.com/ingenuity) program. The normalized counts for each gene were correlated with the increase in calorie restriction (CR) level by Pearson correlation method. The pathway is colored based on a cut-off of an absolute correlation coefficient higher than 0.3. Red indicates a positive correlation with increasing CR level while green indicates a negative correlation.

of the mTORC1 also increased lifespan [81,82]. This was followed by studies in mice [83,84] indicating that mTOR is an evolutionary conserved regulator of longevity. Hence, reduced mTOR signaling as a result of CR may contribute to longevity and CR-induced health benefits (reviewed in [85]). mTORC1 regulates processes related to growth and differentiation while mTORC2 plays a regulatory role in the insulin cascade [86]. Disruption of mTORC1 leads to an increased lifespan [81,82] and is believed to be the primary complex to regulate longevity. In our graded CR study, expression levels of mTORC1 and mTORC2 were both strongly negatively associated with the increase in CR.

Deletion of S6K1, which is downstream from mTOR and insulin signaling, leads to an increased lifespan in female but not male mice [87]. S6K1 is a substrate of mTORC1 which is believed to be the main complex regulating longevity [88]. We found that graded CR had no effect on the expression levels of S6K1. However, activation of S6K1 is controlled via phosphorylation of at least 8 Ser/Thr residues [89]. mTOR can regulate S6K1 activation by either blocking an upstream S6K kinase or activating a phosphatase [89]. Although gene expression of S6K1 was not significantly altered in our data, its inhibition may be regulated via the down-regulated mTORC1. Hence, the results we found of the

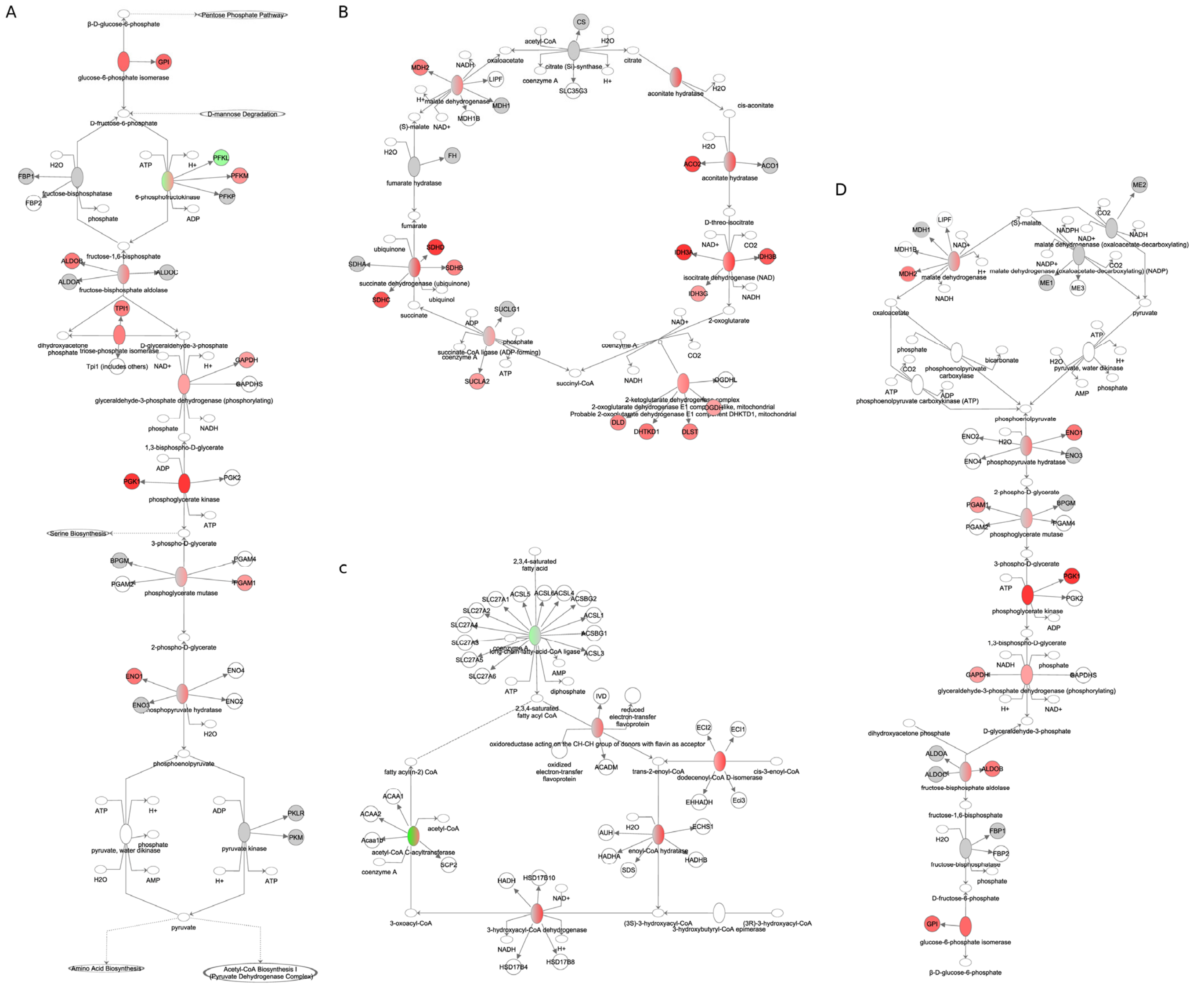

Figure 9. Fuel utilization pathways obtained from the Ingenuity Pathway Analysis (IPA, www.qiagen.com/ingenuity) program. The normalized counts for each gene were correlated with the increase in calorie restriction (CR) level by Pearson correlation method. The pathway is colored based on a cut-off of an absolute correlation coefficient higher than 0.3. Red indicates a positive correlation with increasing CR level while green indicates a negative correlation. (**A**) glycolysis. (**B**) TCA cycle (**C**) fatty acid β-oxidation. (**D**) gluconeogenesis.

downregulated mTORC1/2 may play a role in the effect of CR on longevity. However, the effects may be minimal in these male mice as suggested by the minor effect on lifespan of knocking out the S6K1 gene in male mice [87]. Given the strongly altered pathways downstream of mTOR (autophagy, protein synthesis etc) this suggests that mTOR may have CR responsive effects independent of S6K1 in male mice. Recent work suggested that downstream mTOR signaling in male mice may be regulated via eukaryotic translation initiation factor 4E binding protein 1 (4E-BP1) [90]. Transgenic 4E-BP1 male but not female mice are protected from ageing-induced obesity [90]. Our data suggests that processes downstream from mTOR may be activated in a S6K1 independent manner or that mTOR may not play a key role in extending lifespan in male mice under CR.

A third pathway linked to aging is NF-κB signaling, mainly as its activation is linked to known lifespan regulators including insulin/IGF-1, mTOR and the sirtuins (reviewed in [38]). Inducible genetic inhibition of NF-κB in the epidermis of aged mice for two weeks resulted in a gene expression profile similar to that of young mice [91]. NF-κB transcription factors are also evolutionary conserved and are mainly regulators of the immune system and inflammatory responses [92]. CR is known to reduce inflammation and decreased NF-κB signaling has been suggested to play a key role in this response [93]. TNF-α, a major pro-inflammatory cytokine, activates NF-κB and is also a transcriptional target of NF-κB [94]. The circulating levels of TNF-α were reduced in the mice studied here [15] and expression of NF-κB was negatively correlated with increasing CR level but examination of the direct correlation of NF-κB to TNF-α showed these correlations were not significant suggesting other factors were likely more important in the suppression of NF-κB reported here. In addition, RelA and its downstream genes were also downregulated. This would indeed suggest a reduced signaling of NF-κB under graded CR, resulting in less inflammation. In addition, NF-κB might also play a role in regulating energy metabolism that is independent of inflammation [95,96]. In cancer cells, RelA can regulate mito-chondrial function via binding to mitochondrial DNA and repressing gene expression affecting oxidative phosphorylation and ATP levels [97]. RelA can activate the p53

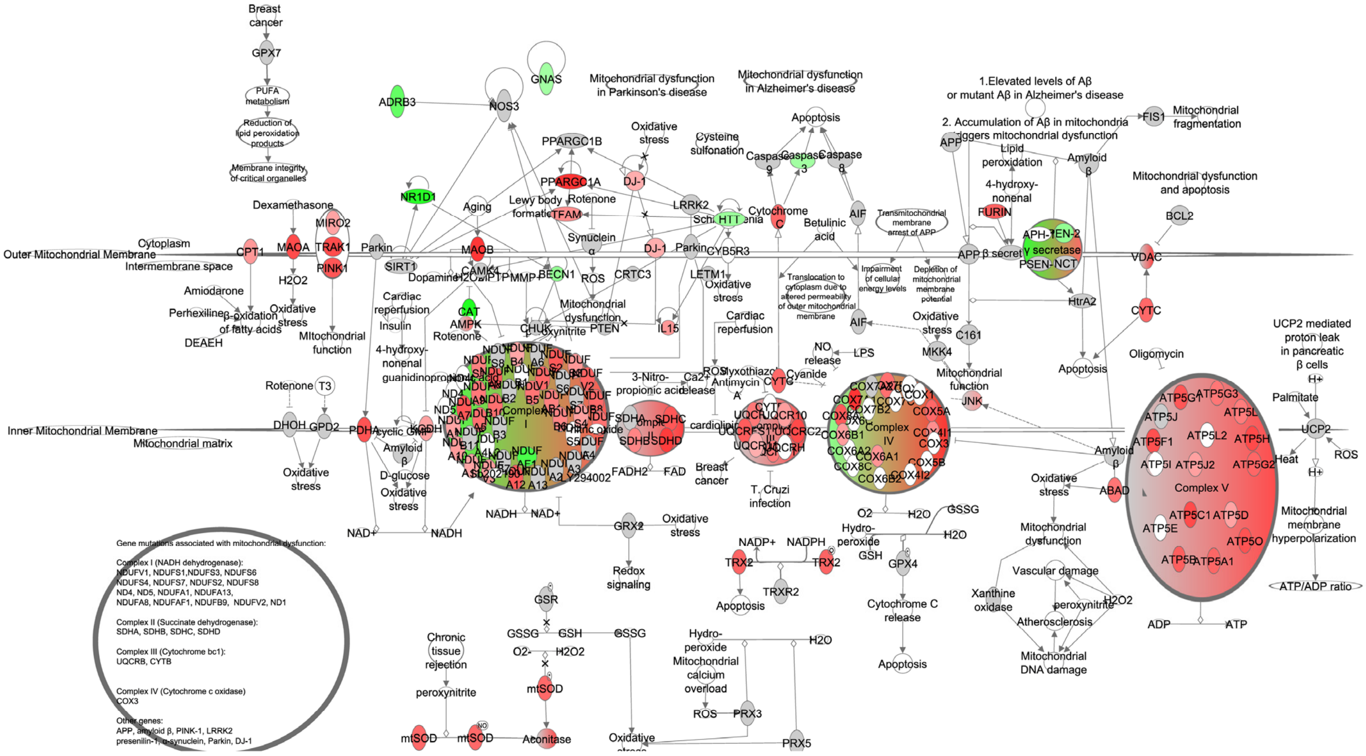

Figure 10. Electron transport chain and mitochondrial biogenesis constructed in the Ingenuity Pathway Analysis (IPA, www.qiagen.com/ingenuity) program. The normalized counts for each gene were correlated with the increase in calorie restriction (CR) level by Pearson correlation method. The pathway is colored based on a cut-off of an absolute correlation coefficient higher than 0.3. Red indicates a positive correlation with increasing CR level while green indicates a negative correlation.

gene and an increase in p53 levels leads to an increase in oxidative phosphorylation and a decrease in glycolysis [95]. Gene expression levels of p53 were not altered in our study but we did observe an increase in expression of genes involved in glycolysis. The RelA/p63 complex can also increase glucose uptake via transcriptional regulation of the glucose transporter GLUT3 [96]. However, no changes were found in GLUT3 expression levels in our data.

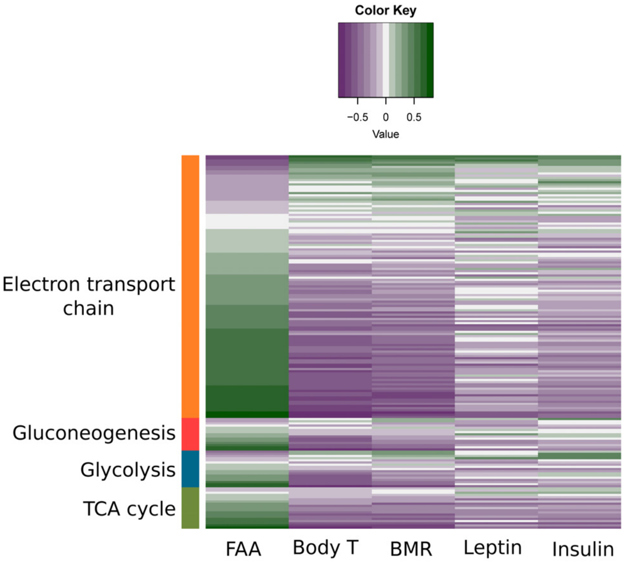

Figure 11. Association between physiological/behavior data and expression levels of genes involved in substrate metabolism. Previously measured leptin and insulin levels, food anticipatory activity (FAA), body temperature (body T) and basal metabolic rate (BMR) [15,16,18,21] for each individual mouse were correlated with the normalized counts of genes involved in electron transport chain, gluconeogenesis, glycolysis and tricarboxylic acid (TCA) cycle. Purple indicates a negative correlation between genes and the measured physiological/behavior data while green indicates a positive correlation.

Work with *Saccharomyces cerevisiae*, *C. elegans* and *D. melanogaster* indicated that lifespan can also be extended by overexpression of Sir2 [47–49] which may also interact with the insulin signaling pathway [50]. Mammals have 7 Sir2-like proteins (i.e. SIRT1-7) [98] and the loss of SIRT6 in SIRT6-deficient mice leads to abnormalities that were similar to ageing-associated degenerative processes [99]. Here we found little changes in expression levels of SIRTs and only *Sirt4* and *Sirt7* were negatively correlated with the increase in CR level. SIRT4 knock out (KO) mice have a 30% increase in circulating levels of insulin during *ad libitum* feeding [100]. After an overnight fast, the KO mice had higher insulin levels compared to their wild type littermates which was not due to due to glucose intolerance. In fact the fasted KO mice had a slightly improved glucose tolerance [100]. During CR, SIRT4 activity was downregulated and Haigis et al (2006) postulates this is due to the switch towards amino acid-stimulated insulin secretion they identified in the KO mice. This is in agreement with our results were we also found a decrease in expression levels of SIRT4 with increasing CR. Here, we found that fatty acid β-oxidation is upregulated during CR, which is in agreement with others [101]. This would lead to a reduction in NAD/NADH ratio in the liver. Hence Haigis et al (2006) suggests that the change in this ratio may downregulate SIRT4 during CR as SIRT4 is dependent on NAD for its activity. In addition, SIRT4 deacetylates and inhibits malonyl CoA decarboxylase 1 (MCD1) and deletion of SIRT4 would therefore prevent production of a key precursor for fat synthesis (i.e. malonyl CoA) [102]. Hence SIRT4 downregulation during CR is linked to the changes in energy metabolism. SIRT7 was also negatively correlated with increasing levels of CR in our study. SIRT7 is mainly linked to maintenance of genome integrity and is associated with RNA polymerase I [103,104]. SIRT7 is highly expressed in tissues with dividing cells [104] and it was suggested that SIRT7 activity may be decreased during CR to restrain ribosome biogenesis and cell growth when energy is limited [105]. Short term 40%

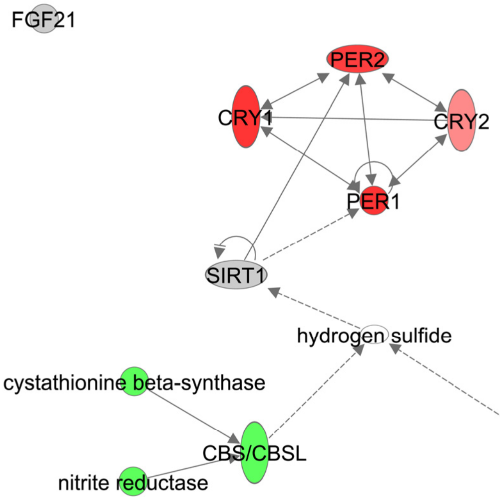

Figure 12. Hydrogen Sulfide production constructed in Ingenuity Pathway Analysis (IPA, www.qiagen.com/ingenuity) program. The normalized counts for each gene were correlated with the increase in calorie restriction (CR) level by Pearson correlation method. The pathway is colored based on a cut-off of an absolute correlation coefficient higher than 0.3. Red indicates a positive correlation with increasing CR level while green indicates a negative correlation.

CR (30 days) had no impact on expression levels (both mRNA and protein) of hepatic SIRT7 of 4 months old and 24 months old Wistar rats [106]. However, after 3 months of CR we did found lower expression levels of SIRT7 with increasing levels of CR.

Insulin/IGF-1 and NF-κB pathways were strongly down-regulated at the transcriptional level in relation to CR. For mTOR there was some evidence of down-regulation. Although SIRT4 and SIRT7 was negatively correlated with the increase in CR, their role regulating lifespan are limited. Hence we postulate that SIRT signaling is not necessary for the benefical effects of CR on longevity.

CR altered fuel utilization that may reduce ROS production, and antioxidant defenses

When mice were exposed to long-term CR (28 months) changes were found in the TCA cycle intermediates which might reflect an important adaptation to create available substrates for gluconeogenesis [107]. Levels of citrate, glutamate and alpha-ketoglutarate were decreased and levels of malate were increased [107]. Here we showed gluconeogenesis was increased under graded CR, which is in agreement with previous studies [108]. We found strong transcriptional upregulation of genes linked to glycolysis, the TCA cycle and the electron transport chain. This would indicate adaptation

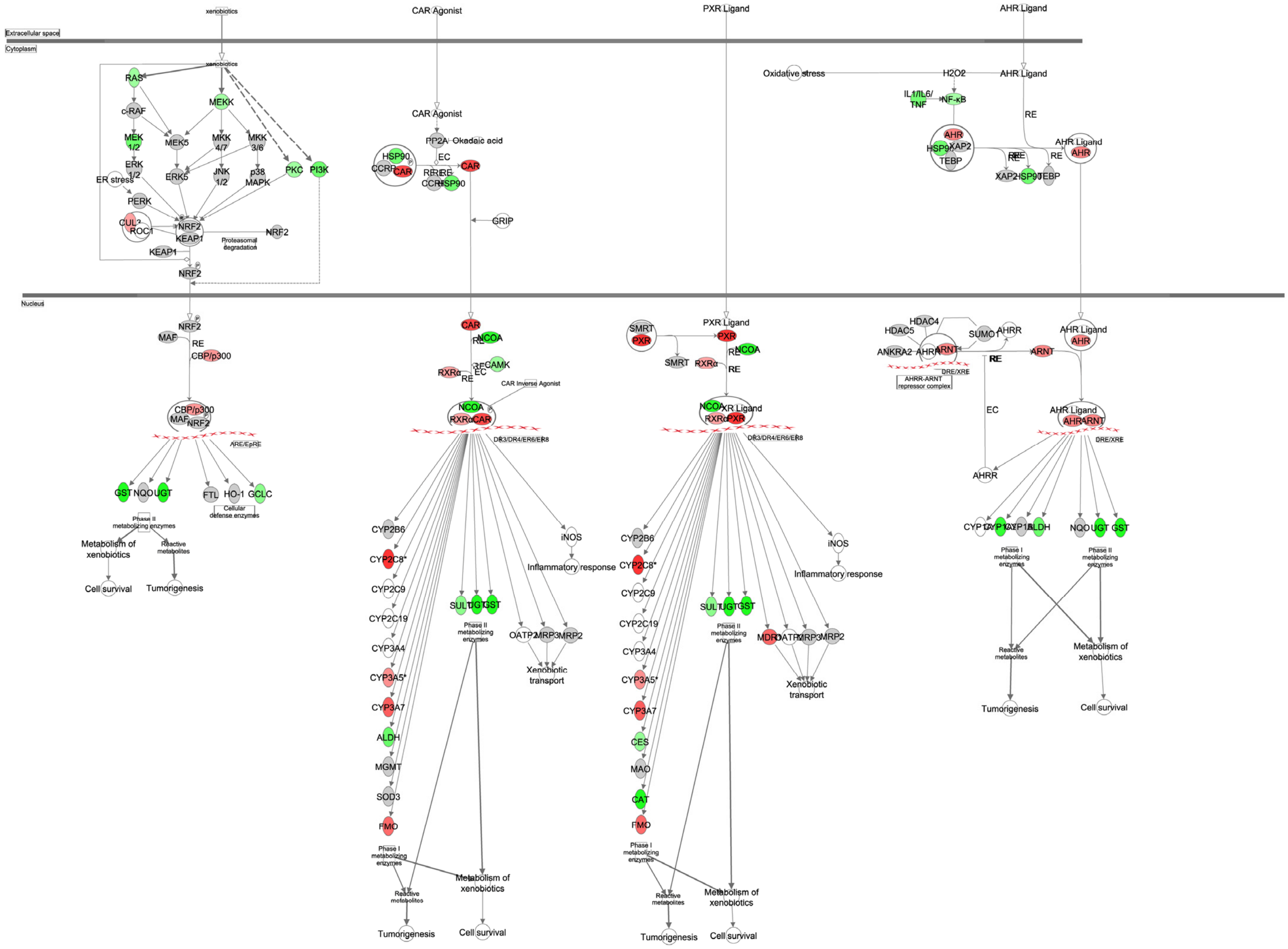

Figure 13. Xenobiotic metabolism obtained from the Ingenuity Pathway Analysis (IPA, www.qiagen.com/ingenuity) program. The normalized counts for each gene were correlated with the increase in calorie restriction (CR) level by Pearson correlation method. The pathway is colored based on a cut-off of an absolute correlation coefficient higher than 0.3. Red indicates a positive correlation with increasing CR level while green indicates a negative correlation.

for an increased level of metabolism at the tissue level. This response is paradoxical because at the whole animal level there is less energy being supplied when mice are under restriction and hence there is a need to reduce energy expenditure at the whole animal level. These observations can be reconciled if the animal under CR disproportionately reduces the amount of tissues in its body to more than compensate for the reduced energy intake, providing scope to elevate the tissue level of expenditure [109,110]. For the same individual mice studied in the present paper we have shown that the level of basal metabolic rate [21] is consistent with the measured changes in body composition at the end of the restriction period [15]. In fact, the increased gene expression in the glycolysis/ TCA cycle/ETC was negatively correlated with the measured BMR and average body temperature (Figure 11). The reported transcriptional changes in glycolysis/ TCA cycle/ETC may then be more important to support changes in physical activity patterns. Supporting this view, in these same individual mice there was an intense period of physical activity prior to food being delivered each day (food anticipatory activity) [18], and transcriptional changes in the glycolysis/TCA cycle/ETC cycle were strongly positively correlated with the levels of FAA in the same individual mice (Figure 11).

One of the earliest theories of aging is that the accumulation of damage caused by ROS, via electron leakage from the ETC, leads to a gradual decline in cellular function [34]. We also found a shift toward fatty acid β-oxidation, which produces FADH thereby potentially mitigating ROS production [33]. After only 6 weeks of CR, H_2O_2 production (i.e. a component of the ROS) in hepatic mitochondria of rats significantly decreased. Although ROS production was decreased at complex I in CR rats, this was not significant compared to complex II [111]. Long term CR significantly decreased H_2O_2 production by 46% in hepatic mitochondria of rats at complex I [112]. In the present analysis transcription of elements of both complex II and complex IV were positively correlated with increasing CR. A decrease in the capacity of the later enzymes in the ETC can theoretically lead to accumulation of electrons in the upstream complexes

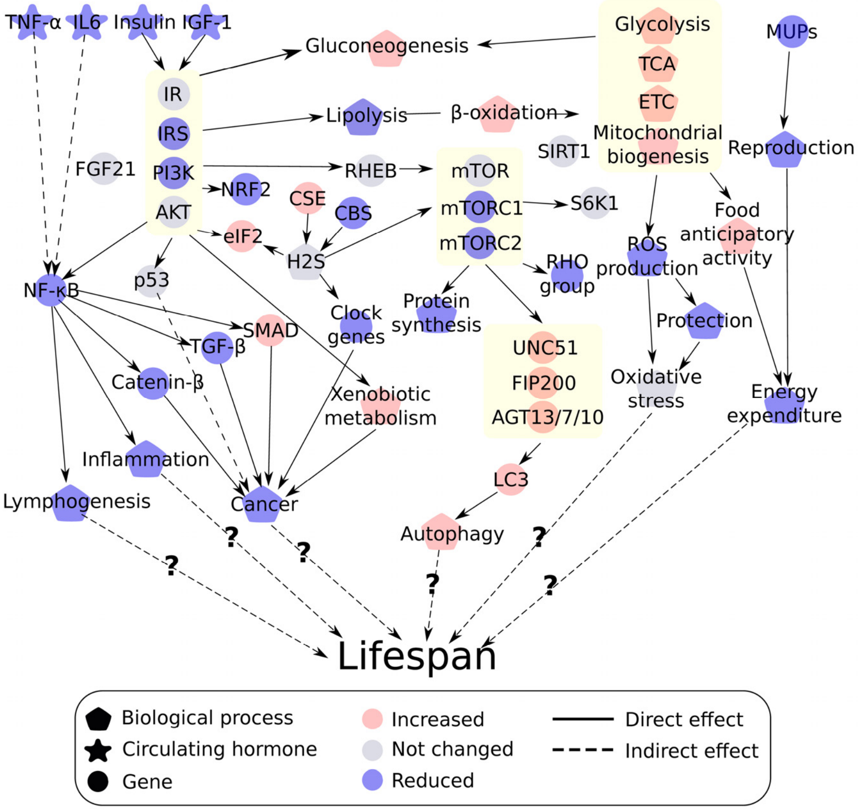

Figure 14. Integrated overview of the different theories of ageing affected by graded calorie restriction (CR). Red indicates a positive correlation with increasing CR while blue indicates a negative correlation. Grey indicates no linear changes with the increase in CR level. Genes or processes biologically related are grouped together indicated by a yellow box including the insulin/insulin like growth factor (IGF-1) signaling pathway, mechanistic target of rapamycin (mTOR) pathway, fuel utilization and autophagy.

increasing ROS production [113]. In mammalian brain and synaptic mitochondria of rats, decreased activity of complex IV was found with age [113,114]. In agreement with our results, previous studies have reported an increase in complex IV levels under CR in brain [115].

To further elaborate on the ROS theory, we previously measured the hepatic activity levels of enzymatic antioxidants (i.e. superoxide dismutase (SOD), glutathione peroxidase and catalase) [15] in livers of the same mice used in the present study. With increasing CR these three antioxidants had lower activity levels, which is potentially an adaptive response to the suggested reduction in ROS production under CR. This is also consistent with the fact that oxidative damage was unchanged in the same mice [15]. These data are consistent with the mice modulating their oxidative defense under CR, potentially to save energy, while maintaining damage levels constant.

We also investigated other pathways related to ROS and found eIF2 signaling was positively correlated and NRF2 negatively correlated with the level of CR. In response to cell stress eIF2 is phosphorylated and reduces formation of the eIF2-GTP complex. This lowers general translation and allows the cell to selectively enhance gene-specific translation [116]. Reduced translation of target genes by phosphorylated eIF2 can lower IκB, which as noted above is an inhibitor of NF-κB [117]. The upregulation of eIF2 signaling is inconsistent with the reduced ROS production and decreased levels of NF-κB observed here. However, phosphorylation of eIF2 may be a direct effect of CR. Western blots showed that eIF2 is phosphorylated to signal nutrient deficiency in the anterior piriform cortex of the brains of rats to induce a behavior response [118]. Although, eIF2 was up-regulated in liver, it may reflect the response to state of decreased nutrient availably and not a response to cellular oxidative stress. NRF2 signaling, the second ROS-associated pathway in our data, induces expression of genes related to the anti-oxidant response (reviewed in [119]). This pathway is activated as a cellular defense mechanism against oxidative stress [120] and its observed downregulation in relation to graded CR would be consistent with reduced ROS production. Hence, the changes in NRF2 but not eIF2 signaling induced by graded CR are in agreement with the previously measured reduced activity levels of the enzymatic anti-oxidants.

Overall, the changes we observed in genes related to fuel utilization may contribute to reduced ROS production. However, the responses to this reduction including reduced defense, resulted in minimal impact on oxidative damage. Hence, these changes are unlikely to contribute significantly to the observed increased lifespan by CR. However, recent work has highlighted a role for solute carrier family 13 (sodium-dependent citrate transporter), member 5 (SLC13A5) in whole body lipid and glucose metabolism during ageing [121]. Liver specific knockdown of SLC13A5 in rats improves insulin sensitivity, reduces plasma insulin, lipid and amino acid levels, and mediates a trend towards decreased basal metabolic rates [121]. Hence SLC13A5 may be an interesting focus for future longevity studies.

CR impacted MUPs genes and suggested a reduced reproductive investment

The disposable soma theory postulating a trade-off between investment in somatic maintenance and reproduction closes the gap between mechanistic and evolutionary theories of aging. In a natural environment, too high investment in somatic maintenance is not beneficial if the organism dies from extrinsic mortality before it can breed, while too low protection might result in premature death. The disposable soma theory argues that during CR organisms need to reallocate the limited energy sources to maintain the soma and this requires diversion of resources away from reproduction [31,32]. MUPs are used in scent marking, and can bind molecules that are pheromonally active but are also used as signaling molecules. Male mice produce on average three to four times more urinary MUPs than female mice [62]. More than 99% of urinary proteins are MUPs. MUPs are primarily produced in the liver and about 20-30% of all the proteins produced by the liver in male mice are MUPs [122]. Hence production of MUPs is likely to be energetically costly and reducing their production may conserve energy for allocation to somatic protection [31,62,63]. Gene expression for 16 different MUPs were all down-regulated at 20CR, 30CR and 40CR compared to 12AL consistent with previous data showing decreased levels of urinary MUPs under CR in the same individual mice [15] and another study of mice under CR [63]. We have also shown that gene expression of MUPs in adipose tissue of the same individuals studied here was also reduced [123]

CR had a positive impact on autophagy

During CR autophagy improves cellular survival and prevents cell death [124]. Previous work in humans has suggested that long-term CR leads to increased expression levels of autophagy related genes in skeletal muscle [125]. CR-induced autophagy leads to mice being more tolerant against chemotherapy induced cell damage [126]. Hence the beneficial effects of autophagy under CR seems to come in part from its ability to reduce the accumulation of damaged proteins. In addition, aging leads to damaged mitochondrial DNA (potentially ROS induced) and autophagy may remove these dysfunctional mitochondria [127]. In the present study, expression levels of 8 genes involved in autophagy were positively associated with the level of CR. When ATG7 is repressed in livers of lean mice, they develop severe insulin resistance [128], which also suggests a role for autophagy in insulin action. Circulating levels of insulin of the same mice indeed correlated with expression levels of genes involved in autophagy but not with *Atg7*. Hence increased autophagy may contribute to the improved insulin sensitivity we observed in these animals [15].

Graded CR had a graded protective effect against cancer

A large impact of short-term CR was found on cancer-related pathways. The beneficial effects of CR on cancer are well known and has been reported extensively (reviewed in [53]). We observed reduced signaling of Hedgehog, TGF-β and CTNN-β with increasing CR. Hedgehog signaling plays a role in differentiation and determination of cell fate [129]. Inhibition of Hedgehog proteins in mice leads to decreased propagation of chronic myelogenous leukemia [130] and Hedgehog proteins are known to co-express with other oncogenetic pathways such as TGF-β and WNT signaling [131]. It has been proposed that leptin (strongly reduced in our mice with increasing CR levels [15]) plays an important role as a cell fate modulator via Hedgehog signaling in liver fibrosis and obesity-associated cancer metastasis [132]. TNF-α is known to stimulate TGF-β gene expression, and TGF-β is released by adipocytes [133]. TNF-α also had progressively reduced circulating levels as severity of CR increased [15]. Previous analysis of putative signaling proteins secreted by adipose tissue in the same mice included those related to TGF-β signaling [123]. Hence this may result in reduced TGF-β signaling to other tissues, which was in agreement with our hepatic results. Excess adipose tissue leads to increased secretion of IGF-1, IL6, leptin and TGF-α which can promote tumor growth [134,135]. Fat mass and circulating levels of IGF-1, IL6 and leptin were all reduced in the same mice in a linear manner to the level of CR [15].

The altered hepatic gene expression indicated a progressively increased protective effect of graded CR on cancer development, which is in agreement with a graded decrease in factors promoting tumor growth such as circulating leptin levels and fat mass in the same mice. Hence, the protective effect of graded CR on cancer development may result from a system-wide adaptation.

CR had no impact on FGF21 and had a positive impact on H_2S

FGF21 is a hormone secreted by liver during fasting, and can induce hepatic fatty acid β-oxidation and ketogenesis. In mice, overexpression of FGF21 leads to an increased lifespan without reducing food intake [54]. Zhang et al. postulated that FGF21 primarily acts by blunting the growth factor/IGF-1 signaling pathway [54]. Although fatty acid β–oxidation and ketogenesis were increased and IGF-1 signaling decreased, we did not observe any increase in gene expression of *Fgf21* in relation to restriction level. This is in stark contrast with protein and methionine restriction (PR and MR) studies where *Fgf21* expression was significantly increased compared to controls [136–138]. Our CR diet protocol involved simultaneous reductions in both calorie and protein intake [14]. Nevertheless, our diets maximally involved 40% protein restriction, while previous PR and MR studies that impacted *Fgf21* gene expression involved restrictions of around 80%. Hence if *Fgf21* is induced by extremely low protein intake rather than reduced calories this may explain the absence of a significant upregulation of *Fgf21* in our CR study. Since CR studies seldom exceed 40% restriction (reviewed in [139]) and at this level there is a highly significant impact on lifespan, these data suggest *Fgf21* is unlikely to be a significant mediator of the CR effect on lifespan. H_2S is responsive to physiological stimuli and plays a signaling role in neural transmission, smooth muscle relaxation and can regulate release of insulin (reviewed in [140]). H_2S activity is also related to oxidative stress and may play a protective role against oxidative damage [141–143]. The two enzymes CSE and CBS are necessary for the synthesis of H_2S [144] and *Cth* was upregulated under CR but *Cbs* downregulated. H_2S production via CBS is dependent on S-adenosyl-methionine [145] and CSE produces H_2S via cysteine or homocysteine [146]. Cysteine and homocysteine were both upregulated in the liver metabolomics data of the same mice [22]. This might suggest more H_2S production via CSE. Increased H_2S production during CR induces signaling cascades leading to an activation of eIF2a (i.e. phosphorylated eIF2) and repression of mTOR [147,148]. This is in concordance with our results as we found an increase in eIF2 signaling and a decrease in mTORC1 and mTORC2 expression with increasing CR levels.

In hepatocytes, H_2S may regulate expression of circadian clock genes and *Sirt1* [66]. We found an increased gene expression of the clock genes *Cry1*, *Per1* and *Per2,* which was in agreement with the expression levels we found in hypothalamus of the same mice [19]. Although the circadian rhythms in older mice remain, they lose the ability to synchronize with the environment which has a negative effect on longevity [149,150]. CR synchronizes these rhythms and may protect against the loss of circadian rhythm synchronization [151]. Although circadian rhythms are mainly established in the suprachiasmatic nucleus clock, the central pacemaker in the hypothalamus, studies have suggested that expression of circadian clock genes in the liver could be established independent of the hypothalamus [152–154]. *Per1* and *Per2* have tumor suppression activity [155], which may tie in with the anti-cancer mechanism under CR [53]. Overall our data are consistent with H_2S signaling playing a key role in the impact of CR.

CR leads to up regulation of the xenobiotic metabolism

Genes in this pathway play an important role in protection against environmental toxins and furthermore interact with phase II conjugation enzymes, which enhance hydrophilicity and excretion rate of environmental toxins [156]. These toxins are then excreted into bile via downstream phase III transporters [156]. Interestingly, long-lived 'Little' mice show resistance to oxidative toxins, and xenobiotic metabolism is upregulated, specifically xenobiotic detoxification genes [157,158]. With age, genes involved in xenobiotic metabolism are decreased in expression [159] and therefore preserved xenobiotic metabolism is believed to contribute to the increase in lifespan observed in long-lived mice. Similar to Ames dwarf and Little mice, our data showed upregulation of genes involved in xenobiotic metabolism under graded CR relative to 12AL which corresponded with previous research focused at single levels of restriction [101,160]. The decreased ability of the liver to metabolize drugs is believed to be mainly due by loss of expression of cytochrome P450 family 2B and 2C, which were among the genes significantly upregulated in our dataset [161]. Furthermore our data also showed genes involved in the 'FXR/RXR activation' pathway were upregulated as a response to CR, which are primary regulators of xenobiotic metabolism [162]. The bile acid receptor FXR could potentially mediate the upregulation of xenobiotic genes in the long-lived Little mice [158]. Although no causal link has been found between increased xenobiotic metabolism activity and pro-longevity, a study in *C. elegans* supports such a hypothesis [56]. It is still unclear how xenobiotic metabolism can increase lifespan but potentially it could be as simple as the reduction in damage caused by toxic compounds. The beneficial effects of xenobiotic metabolism may be signaled via reduced insulin/IGF-1 signaling under CR. Genes regulated by the insulin/IGF-1 pathway in *C. elegans* include the xeno-biotic detoxification genes [56]. Microarray analysis in long-lived Ames dwarf mice and Little mice suggest a similar role for insulin and IGF-1 in regulating xenobiotic metabolism [157]. It has been postulated that xenobiotic metabolism may be a key modulator of aging, separate from oxidative stress [56].

MATERIALS AND METHODS

Animals and experimental manipulations

All procedures were approved by the University of Aberdeen ethical approval committee and carried out under the Animals (Scientific Procedures) Act 1986 Home Office license (PPL 60/3706 held by JRS). Forty eight male C57BL/6 mice (*Mus musculus*) purchased from Charles River (Ormiston, UK) were individually housed with free access to water. Mice were exposed to 12 hour dark/light cycle (lights on at 0630h) and body mass and food intake were recorded daily, immediately prior to nocturnal feeding. At 20 weeks of age (resembling early adulthood in human), mice were randomly allocated into 6 different treatment groups: (12AL n=8, 24AL n=8, 10CR n=8, 20CR n=8, 30CR n=7, 40CR n=9). Mice in 24AL and 12AL group were fed *ad libitum* for 24h or 12h during the dark period respectively. 10CR, 20CR, 30CR and 40CR indicates 10 %, 20 %, 30 % and 40 % lower calories respectively than their own individual intakes measured over a baseline period of 14 days prior to introducing CR.

Animals fed completely *ad libitum* (i.e., having 24 hours access to food) may over feed and become obese. CR associated changes compared to 24AL are therefore most likely to reflect the anti-obesity effect of CR [4,163]. In addition, CR-restricted mice generally consume food during the first few hours of food provided. The 24AL animals can by definition eat at any time throughout a 24h period. Hence, when CR-restricted mice were culled they may have been starving for 10h-16h while 24AL may have eaten in the hour prior to culling. To address this issue, 12AL was set as a reference to avoid the "time since last meal effect" and graded levels of CR were introduced to investigate a potential graded response. Information on overall study design, diet composition and detailed rationale are described elsewhere [14].

RNA isolation, cDNA synthesis and RNA sequencing

After culling by a terminal CO_2 overdose the liver was removed as part of the overall dissection [14], weighed, divided into 7 pieces which were immediately snap frozen in liquid nitrogen and stored in -80°C until one piece was used for RNA isolation. RNA was isolated by homogenizing in Tri-Reagent (Sigma Aldrich, UK) according to manufacturer's instructions. Prior to RNA quantification by Agilent RNA 6000 Nano Kit samples were denatured at 65 °C. RNA of 37 individual mice was successfully isolated and sent to Beijing Genomic Institute (BGI, Hong Kong) for RNA sequencing.

Library preparation was conducted by enriching total RNA by using oligo(dT) magnetic beads. The fragmentation buffer was added to obtain short fragments from the RNA. The mRNA was used as template for the random hexamer primers which synthesizes the first strand of cDNA. The second strand was synthesized by adding buffer dNTPs, RNase and DNA polymerase. QiaQuick PCR extraction kit was used to purify the double stranded cDNA and washed with an elution buffer for end repair and single nucleotide A addition. The fragments were ligated with sequencing adaptors and purified by agarose gel-electrophoresis to obtain the correct fragments. These were enriched by PCR amplification. During the quality control step, Agilent 2100 Bioanalyser and ABI StepOnePlus Real-Time PCR System are used to qualify and quantify of the sample library. The library products were sequenced using an Illumina Hi-seq 2000 resulting in 50 bp single ended reads (standard protocol BGI, Hong Kong). Standard primers and barcodes developed by BGI were used.

Alignment to the reference genome

Prior to alignment to the reference genome, FASTQ files were quality controlled to identify the presence of adaptors or low quality sequences using fastQC (http://www.bioinformatics.bbsrc.ac.uk/projects/fastqc/) . To ensure high sequencing quality, the reads were trimmed with a cut-off phred score of 28 using Trimmomatic [164]. Reads were aligned to the reference genome obtained from the National Center for Biotechnology Information (NCBI) database (Mus musculus, version MGSCv37, 2010/09/23, http://www.ncbi.nlm.nih.gov/assembly/165668/). The reference genome was indexed using Bowtie2 [165] and reads aligned with Tophat2 [166] using default settings. Of the 492,199,393 reads 482,311,031 (97.99%) were successfully aligned to the reference genome. 15.6 % contained multi mapped reads which were removed using the Sequence Alignment/Map (SAM) tool [167] before proceeding to quantification of the reads. Aligned sequencing reads were counted with HTSeq-count [168] by identification of how many reads mapped onto a single feature (genes containing exons).

Analytical procedure

To remove any genes that exhibited no or a very low number of mapped reads, only genes that had more than 1 count per million in at least 4 samples across all treatments were retained for further analysis. This resulted in a total of 12,183 unique genes. Read counts were normalized using the trimmed mean of M values (TMM normalization) [169] to account for highly expressed genes consuming a substantial proportion of the total library size. This composition effect would cause remaining genes to be under sampled [170]. Differential gene expression was modeled using the edgeR package [170] in R (version 3.1.2) [171] and pairwise comparisons were conducted between 12AL and 24AL and between 12AL and each level of CR. Significant genes were identified based on a cut off p-value < 0.05 and an absolute log fold change (log FC) of 1. We identified differentially expressed genes (DEGs) relative to 12AL based on the adjusted p-value (FDR < 0.05). At 24AL, 10CR and 20CR none of the genes were differently expressed relative to 12AL. At 30CR only four genes had a FDR lower than 0.05 and at 40CR this massively increased to 855. We therefore used a cut-off value of absolute $\log_2$ fold changes (log FC) > 1.00 and p-value < 0.05. The amount of DEGs relative to 12AL responded to CR in a graded manner (24AL, 10CR, 20CR, 30CR and 40CR): 88, 138, 533, 316 and 608 respectively.

Biological interpretation

The normalized counts for each gene were correlated with the increase in CR level by Pearson correlation method in the statistical environment R (version 3.1.2) [171]. The correlation coefficient for all genes (n=12,183) and their associated logFC relative to 12AL was then loaded into the IPA program (version 2000-2016, Ingenuity® Systems, www.ingenuity.com) to visualize the associated changes with CR in the aging pathways. The insulin/IGF-1 signaling pathway was constructed by merging the "Insulin Receptor Signaling" and "IGF-1 signaling". For the mTOR signaling pathway, the "mTOR signaling" was used. The pathways "NF-κB Signaling" and "NF-κB Activation by Viruses" were merged to obtain the NF-κB signaling pathway. IPA did not have a prebuilt sirtuin signaling pathway. We therefore manually constructed this pathway based on the summarized data by Nakagawa and Guarente (2011) [61]. The sirtuin signaling pathway was manually constructed by using the built-in Path Designer function. For the oxidative stress pathway, pathways classified as "Cellular Stress and Injury" were merged with the pathway "Production of Nitric Oxide and Reactive Oxygen Species in Macrophages". The reproduction pathway was built by merging "Germ Cell-Sertoli Cell Junction Signaling", "Sertoli Cell-Sertoli Cell Junction Signaling", MUP genes and the function reproduction. For the cancer signaling, autophagy pathway and xenobiotic metabolism, the "Molecular Mechanism of Cancer", "Autophagy", "Xenobiotic Metabolism Signaling" were used. For the changes in fuel utilization, the pathways "Glycolysis I", "TCA cycle II (Eukaryotic)", "Fatty Acid β-oxidation I" and "Gluconeogenesis I" were used. Mitochondrial biogenesis was obtained by merging "Mitochondrial Dysfunction" and the function mito-chondrial biogenesis. Lastly the H_2S pathways were manually constructed. The p-value is calculated using the right-tailed Fisher Exact Test. The z-score predicts the activation state (i.e. increased or decreased) of a pathway based on the significant patterns that match the curated knowledge of gene expression levels and the causal relations with the pathway. Hence a pathway may have a significant p-value but lack a z-score if the expression levels of genes does not match the pre-defined associated regulation in that particular pathway. The custom built pathways do not have a z-score and hence we do not have a prediction of their down or upregulation calculated by IPA. Physiological data and behavior al data (methods and data described in [15,16,18,21]) were correlated with each gene and each individual using Pearson correlations conducted in the statistical environment R (version 3.2.5) [171].

AUTHOR CONTRIBUTIONS

JRS conceptualized and designed the original graded CR experiment, raised the funding to execute it and was the HO project license holder. SEM performed all experimental procedures related to the study. AD and DD performed the bio-informatic and statistical analysis. DD and JRS interpreted the results. DD wrote the manuscript and AD, DL, SEM and JRS revised it. All authors discussed the results at joint meetings and gave suggestions.

ACKNOWLEDGEMENTS

We would like to acknowledge the BSU staff for their invaluable help with caring for the animals.

CONFLICTS OF INTEREST

Authors declare no conflict of interest.

FUNDING

The work was supported by the UK Biotechnology and Biological Sciences Research Council BBSRC (grants BB/G009953/1 and BB/J020028/1 to JRS and SEM) and a studentship of DD supported by the Centre for Genome Enabled Biology and Medicine, Aberdeen, UK. DL was supported by Office of Naval Research (ONR) grant N000141512377.

REFERENCES

1. Tereshina EV. Metabolic abnormalities as a basis for age-dependent diseases and aging? State of the art. Adv Gerontol. 2009; 22:129–38.
2. McCay C, Crowell M, Maynard L. The effect of retarded growth upon the length of life span and upon the ultimate body size. J Nutr. 1935; 10:63–79.
3. Speakman JR, Hambly C. Starving for life: what animal studies can and cannot tell us about the use of caloric restriction to prolong human lifespan. J Nutr. 2007; 137:1078–86.
4. Speakman JR, Mitchell SE. Caloric restriction. Mol Aspects Med. 2011; 32:159–221. https://doi.org/10.1016/j.mam.2011.07.001
5. Fabrizio P, Longo VD. The chronological life span of Saccharomyces cerevisiae. Aging Cell. 2003; 2:73–81. https://doi.org/10.1046/j.1474-9728.2003.00033.x
6. Bross TG, Rogina B, Helfand SL. Behavioral, physical, and demographic changes in Drosophila populations through dietary restriction. Aging Cell. 2005; 4:309–17. https://doi.org/10.1111/j.1474-9726.2005.00181.x
7. Burger JM, Buechel SD, Kawecki TJ. Dietary restriction affects lifespan but not cognitive aging in Drosophila melanogaster. Aging Cell. 2010; 9:327–35. https://doi.org/10.1111/j.1474-9726.2010.00560.x
8. Colman RJ, Beasley TM, Kemnitz JW, Johnson SC, Weindruch R, Anderson RM. Caloric restriction reduces age-related and all-cause mortality in rhesus monkeys. Nat Commun. 2014; 5:3557. https://doi.org/10.1038/ncomms4557
9. Mattison JA, Colman RJ, Beasley TM, Allison DB, Kemnitz JW, Roth GS, Ingram DK, Weindruch R, de Cabo R, Anderson RM, Gibbs RA, Zimin AV, Bowden DM, et al. Caloric restriction improves health and survival of rhesus monkeys. Nat Commun. 2017; 8:14063. https://doi.org/10.1038/ncomms14063
10. Mercken EM, Crosby SD, Lamming DW, JeBailey L, Krzysik-Walker S, Villareal DT, Capri M, Franceschi C, Zhang Y, Becker K, Sabatini DM, de Cabo R, Fontana L. Calorie restriction in humans inhibits the PI3K/AKT pathway and induces a younger transcription profile. Aging Cell. 2013; 12:645–51. https://doi.org/10.1111/acel.12088
11. Fontana L, Meyer TE, Klein S, Holloszy JO. Long-term calorie restriction is highly effective in reducing the risk for atherosclerosis in humans. Proc Natl Acad Sci USA. 2004; 101:6659–63. https://doi.org/10.1073/pnas.0308291101
12. Fontana L, Klein S, Holloszy JO. Effects of long-term calorie restriction and endurance exercise on glucose

tolerance, insulin action, and adipokine production. Age (Dordr). 2010; 32:97–108. https://doi.org/10.1007/s11357-009-9118-z

13. Koopman JJ, van Heemst D, van Bodegom D, Bonkowski MS, Sun LY, Bartke A. Measuring ageing rates of mice subjected to caloric restriction and genetic disruption of growth hormone signaling. Aging (Albany NY). 2016; 8:539–46. https://doi.org/10.18632/aging.100919
14. Mitchell SE, Tang Z, Kerbois C, Delville C, Konstantopedos P, Bruel A, Derous D, Green C, Aspden RM, Goodyear SR, Chen L, Han JJ, Wang Y, et al. The effects of graded levels of calorie restriction: I. impact of short term calorie and protein restriction on body composition in the C57BL/6 mouse. Oncotarget. 2015; 6:15902–30. https://doi.org/10.18632/oncotarget.4142
15. Mitchell SE, Delville C, Konstantopedos P, Hurst J, Derous D, Green C, Chen L, Han JJ, Wang Y, Promislow DE, Lusseau D, Douglas A, Speakman JR. The effects of graded levels of calorie restriction: II. Impact of short term calorie and protein restriction on circulating hormone levels, glucose homeostasis and oxidative stress in male C57BL/6 mice. Oncotarget. 2015; 6:23213–37. https://doi.org/10.18632/oncotarget.4003
16. Mitchell SE, Delville C, Konstantopedos P, Derous D, Green CL, Chen L, Han JD, Wang Y, Promislow DE, Douglas A, Lusseau D, Speakman JR. The effects of graded levels of calorie restriction: III. Impact of short term calorie and protein restriction on mean daily body temperature and torpor use in the C57BL/6 mouse. Oncotarget. 2015; 6:18314–37. https://doi.org/10.18632/oncotarget.4506
17. Lusseau D, Mitchell SE, Barros C, Derous D, Green C, Chen L, Han JD, Wang Y, Promislow DE, Douglas A, Speakman JR. The effects of graded levels of calorie restriction: IV. Non-linear change in behavioural phenotype of mice in response to short-term calorie restriction. Sci Rep. 2015; 5:13198. https://doi.org/10.1038/srep13198
18. Mitchell SE, Delville C, Konstantopedos P, Derous D, Green CL, Wang Y, Han JD, Promislow DE, Douglas A, Chen L, Lusseau D, Speakman JR. The effects of graded levels of calorie restriction: V. Impact of short term calorie and protein restriction on physical activity in the C57BL/6 mouse. Oncotarget. 2016; 7:19147–70. https://doi.org/10.18632/oncotarget.8158
19. Derous D, Mitchell SE, Green CL, Chen L, Han JD, Wang Y, Promislow DE, Lusseau D, Speakman JR, Douglas A. The effects of graded levels of calorie restriction: VI. Impact of short-term graded calorie restriction on transcriptomic responses of the hypothalamic hunger and circadian signaling pathways. Aging (Albany NY). 2016; 8:642–63. https://doi.org/10.18632/aging.100895
20. Derous D, Mitchell SE, Green CL, Wang Y, Han JD, Chen L, Promislow DE, Lusseau D, Speakman JR, Douglas A. The effects of graded levels of calorie restriction: VII. Topological rearrangement of hypothalamic aging networks. Aging (Albany NY). 2016; 8:917–32. https://doi.org/10.18632/aging.100944
21. Mitchell SE, Tang Z, Kerbois C, Delville C, Derous D, Green CL, Wang Y, Han JJ, Chen L, Douglas A, Lusseau D, Promislow DE, Speakman JR. The effects of graded levels of calorie restriction: VIII. Impact of short term calorie and protein restriction on basal metabolic rate in the C57BL/6 mouse. Oncotarget. 2017; 8:17453–74. https://doi.org/10.18632/oncotarget.15294
22. Green CL, Mitchell SE, Derous D, Wang Y, Chen L, Han JJ, Promislow DE, Lusseau D, Douglas A, Speakman JR. The effects of graded levels of calorie restriction: IX. Global metabolomic screen reveals modulation of carnitines, sphingolipids and bile acids in the liver of C57BL/6 mice. Aging Cell. 2017; 16:529–40. https://doi.org/10.1111/acel.12570
23. Schmucker DL. Aging and the liver: an update. J Gerontol A Biol Sci Med Sci. 1998; 53:B315–20. https://doi.org/10.1093/gerona/53A.5.B315
24. Cao SX, Dhahbi JM, Mote PL, Spindler SR. Genomic profiling of short- and long-term caloric restriction effects in the liver of aging mice. Proc Natl Acad Sci USA. 2001; 98:10630–35. https://doi.org/10.1073/pnas.191313598
25. Medvedev ZA. An attempt at a rational classification of theories of ageing. Biol Rev Camb Philos Soc. 1990; 65:375–98. https://doi.org/10.1111/j.1469-185X.1990.tb01428.x
26. Kuhla A, Hahn S, Butschkau A, Lange S, Wree A, Vollmar B. Lifelong caloric restriction reprograms hepatic fat metabolism in mice. J Gerontol A Biol Sci Med Sci. 2014; 69:915–22. https://doi.org/10.1093/gerona/glt160
27. Kuhla A, Blei T, Jaster R, Vollmar B. Aging is associated with a shift of fatty metabolism toward lipogenesis. J Gerontol A Biol Sci Med Sci. 2011; 66:1192–200. https://doi.org/10.1093/gerona/glr124
28. Badman MK, Pissios P, Kennedy AR, Koukos G, Flier JS, Maratos-Flier E. Hepatic fibroblast growth factor 21 is regulated by PPARalpha and is a key mediator of hepatic lipid metabolism in ketotic states. Cell Metab. 2007; 5:426–37. https://doi.org/10.1016/j.cmet.2007.05.002

29. Gerhart-Hines Z, Rodgers JT, Bare O, Lerin C, Kim SH, Mostoslavsky R, Alt FW, Wu Z, Puigserver P. Metabolic control of muscle mitochondrial function and fatty acid oxidation through SIRT1/PGC-1alpha. EMBO J. 2007; 26:1913–23. https://doi.org/10.1038/sj.emboj.7601633
30. Takemori K, Kimura T, Shirasaka N, Inoue T, Masuno K, Ito H. Food restriction improves glucose and lipid metabolism through Sirt1 expression: a study using a new rat model with obesity and severe hypertension. Life Sci. 2011; 88:1088–94. https://doi.org/10.1016/j.lfs.2011.04.002
31. Kirkwood TB. Evolution of ageing. Nature. 1977; 270:301–04. https://doi.org/10.1038/270301a0
32. Kowald A, Kirkwood TB. Evolutionary significance of ageing in the wild. Exp Gerontol. 2015; 71:89–94. https://doi.org/10.1016/j.exger.2015.08.006
33. Hirst J, King MS, Pryde KR. The production of reactive oxygen species by complex I. Biochem Soc Trans. 2008; 36:976–80. https://doi.org/10.1042/BST0360976
34. Harman D. Aging: a theory based on free radical and radiation chemistry. J Gerontol. 1956; 11:298–300. https://doi.org/10.1093/geronj/11.3.298
35. Argentino DP, Dominici FP, Al-Regaiey K, Bonkowski MS, Bartke A, Turyn D. Effects of long-term caloric restriction on early steps of the insulin-signaling system in mouse skeletal muscle. J Gerontol A Biol Sci Med Sci. 2005; 60:28–34. https://doi.org/10.1093/gerona/60.1.28
36. Breese CR, Ingram RL, Sonntag WE. Influence of age and long-term dietary restriction on plasma insulin-like growth factor-1 (IGF-1), IGF-1 gene expression, and IGF-1 binding proteins. J Gerontol. 1991; 46:B180–87. https://doi.org/10.1093/geronj/46.5.B180
37. Johnson SC, Rabinovitch PS, Kaeberlein M. mTOR is a key modulator of ageing and age-related disease. Nature. 2013; 493:338–45. https://doi.org/10.1038/nature11861
38. Tilstra JS, Clauson CL, Niedernhofer LJ, Robbins PD. NF-κB in Aging and Disease. Aging Dis. 2011; 2:449–65.
39. Houtkooper RH, Pirinen E, Auwerx J. Sirtuins as regulators of metabolism and healthspan. Nat Rev Mol Cell Biol. 2012; 13:225–38. https://doi.org/10.1038/nrm3293
40. Wolkow CA, Kimura KD, Lee MS, Ruvkun G. Regulation of C. elegans life-span by insulinlike signaling in the nervous system. Science. 2000; 290:147–50. https://doi.org/10.1126/science.290.5489.147
41. Kimura KD, Tissenbaum HA, Liu Y, Ruvkun G. daf-2, an insulin receptor-like gene that regulates longevity and diapause in Caenorhabditis elegans. Science. 1997; 277:942–46. https://doi.org/10.1126/science.277.5328.942
42. Blüher M, Michael MD, Peroni OD, Ueki K, Carter N, Kahn BB, Kahn CR. Adipose tissue selective insulin receptor knockout protects against obesity and obesity-related glucose intolerance. Dev Cell. 2002; 3:25–38. https://doi.org/10.1016/S1534-5807(02)00199-5
43. Selman C, Partridge L, Withers DJ. Replication of extended lifespan phenotype in mice with deletion of insulin receptor substrate 1. PLoS One. 2011; 6:e16144. https://doi.org/10.1371/journal.pone.0016144
44. Selman C, Lingard S, Choudhury AI, Batterham RL, Claret M, Clements M, Ramadani F, Okkenhaug K, Schuster E, Blanc E, Piper MD, Al-Qassab H, Speakman JR, et al. Evidence for lifespan extension and delayed age-related biomarkers in insulin receptor substrate 1 null mice. FASEB J. 2008; 22:807–18. https://doi.org/10.1096/fj.07-9261com
45. Stanfel MN, Shamieh LS, Kaeberlein M, Kennedy BK. The TOR pathway comes of age. Biochimica et Biophysica Acta - General Subjects. 2009. p. 1067–74.
46. Kanfi Y, Naiman S, Amir G, Peshti V, Zinman G, Nahum L, Bar-Joseph Z, Cohen HY. The sirtuin SIRT6 regulates lifespan in male mice. Nature. 2012; 483:218–21. https://doi.org/10.1038/nature10815
47. Giannakou ME, Goss M, Jünger MA, Hafen E, Leevers SJ, Partridge L. Long-lived Drosophila with overexpressed dFOXO in adult fat body. Science. 2004; 305:361. https://doi.org/10.1126/science.1098219
48. Kaeberlein M, McVey M, Guarente L. The SIR2/3/4 complex and SIR2 alone promote longevity in Saccharomyces cerevisiae by two different mechanisms. Genes Dev. 1999; 13:2570–80. https://doi.org/10.1101/gad.13.19.2570
49. Tissenbaum HA, Guarente L. Increased dosage of a sir-2 gene extends lifespan in Caenorhabditis elegans. Nature. 2001; 410:227–30. https://doi.org/10.1038/35065638
50. Kenyon C, Chang J, Gensch E, Rudner A, Tabtiang R. A C. elegans mutant that lives twice as long as wild type. Nature. 1993; 366:461–64. https://doi.org/10.1038/366461a0
51. Giannakou ME, Partridge L. The interaction between FOXO and SIRT1: tipping the balance towards survival. Trends Cell Biol. 2004; 14:408–12. https://doi.org/10.1016/j.tcb.2004.07.006

52. Morselli E, Maiuri MC, Markaki M, Megalou E, Pasparaki A, Palikaras K, Criollo A, Galluzzi L, Malik SA, Vitale I, Michaud M, Madeo F, Tavernarakis N, Kroemer G. Caloric restriction and resveratrol promote longevity through the Sirtuin-1-dependent induction of autophagy. Cell Death Dis. 2010; 1:e10. https://doi.org/10.1038/cddis.2009.8

53. Longo VD, Fontana L. Calorie restriction and cancer prevention: metabolic and molecular mechanisms. Trends Pharmacol Sci. 2010; 31:89–98. https://doi.org/10.1016/j.tips.2009.11.004

54. Zhang Y, Xie Y, Berglund ED, Coate KC, He TT, Katafuchi T, Xiao G, Potthoff MJ, Wei W, Wan Y, Yu RT, Evans RM, Kliewer SA, Mangelsdorf DJ. The starvation hormone, fibroblast growth factor-21, extends lifespan in mice. eLife. 2012; 1:e00065. https://doi.org/10.7554/eLife.00065

55. Zhang Y, Tang ZH, Ren Z, Qu SL, Liu MH, Liu LS, Jiang ZS. Hydrogen sulfide, the next potent preventive and therapeutic agent in aging and age-associated diseases. Mol Cell Biol. 2013; 33:1104–13. https://doi.org/10.1128/MCB.01215-12

56. McElwee JJ, Schuster E, Blanc E, Thomas JH, Gems D. Shared transcriptional signature in Caenorhabditis elegans Dauer larvae and long-lived daf-2 mutants implicates detoxification system in longevity assurance. J Biol Chem. 2004; 279:44533–43. https://doi.org/10.1074/jbc.M406207200

57. Merry BJ. Molecular mechanisms linking calorie restriction and longevity. Int J Biochem Cell Biol. 2002; 34:1340–54. https://doi.org/10.1016/S1357-2725(02)00038-9

58. Duffy PH, Lewis SM, Mayhugh MA, Trotter RW, Latendresse JR, Thorn BT, Feuers RJ. The effects of different levels of dietary restriction on neoplastic pathology in the male Sprague-Dawley rat. Aging Clin Exp Res. 2004; 16:448–56. https://doi.org/10.1007/BF03327400

59. Nogueira LM, Lavigne JA, Chandramouli GV, Lui H, Barrett JC, Hursting SD. Dose-dependent effects of calorie restriction on gene expression, metabolism, and tumor progression are partially mediated by insulin-like growth factor-1. Cancer Med. 2012; 1:275–88. https://doi.org/10.1002/cam4.23

60. Kim SS, Choi KM, Kim S, Park T, Cho IC, Lee JW, Lee CK. Whole-transcriptome analysis of mouse adipose tissue in response to short-term caloric restriction. Mol Genet Genomics. 2016; 291:831–47. https://doi.org/10.1007/s00438-015-1150-3

61. Nakagawa T, Guarente L. Sirtuins at a glance. J Cell Sci. 2011; 124:833–38. https://doi.org/10.1242/jcs.081067

62. Beynon RJ, Hurst JL. Urinary proteins and the modulation of chemical scents in mice and rats. Peptides. 2004; 25:1553–63. https://doi.org/10.1016/j.peptides.2003.12.025

63. Mitchell SJ, Madrigal-Matute J, Scheibye-Knudsen M, Fang E, Aon M, González-Reyes JA, Cortassa S, Kaushik S, Gonzalez-Freire M, Patel B, Wahl D, Ali A, Calvo-Rubio M, et al. Effects of Sex, Strain, and Energy Intake on Hallmarks of Aging in Mice. Cell Metab. 2016; 23:1093–112. https://doi.org/10.1016/j.cmet.2016.05.027

64. Hu W, Feng Z, Teresky AK, Levine AJ. p53 regulates maternal reproduction through LIF. Nature. 2007; 450:721–24. https://doi.org/10.1038/nature05993

65. Levine AJ, Tomasini R, McKeon FD, Mak TW, Melino G. The p53 family: guardians of maternal reproduction. Nat Rev Mol Cell Biol. 2011; 12:259–65. https://doi.org/10.1038/nrm3086

66. Shang Z, Lu C, Chen S, Hua L, Qian R. Effect of H2S on the circadian rhythm of mouse hepatocytes. Lipids Health Dis. 2012; 11:23. https://doi.org/10.1186/1476-511X-11-23

67. Turturro A, Duffy P, Hass B, Kodell R, Hart R. Survival characteristics and age-adjusted disease incidences in C57BL/6 mice fed a commonly used cereal-based diet modulated by dietary restriction. J Gerontol A Biol Sci Med Sci. 2002; 57:B379–89. https://doi.org/10.1093/gerona/57.11.B379

68. Paradis S, Ruvkun G. Caenorhabditis elegans Akt/PKB transduces insulin receptor-like signals from AGE-1 PI3 kinase to the DAF-16 transcription factor. Genes Dev. 1998; 12:2488–98. https://doi.org/10.1101/gad.12.16.2488

69. Holland R, Hardie DG. Both insulin and epidermal growth factor stimulate fatty acid synthesis and increase phosphorylation of acetyl-CoA carboxylase and ATP-citrate lyase in isolated hepatocytes. FEBS Lett. 1985; 181:308–12. https://doi.org/10.1016/0014-5793(85)80282-9

70. Fromenty B, Robin MA, Igoudjil A, Mansouri A, Pessayre D. The ins and outs of mitochondrial dysfunction in NASH. Diabetes Metab. 2004; 30:121–38. https://doi.org/10.1016/S1262-3636(07)70098-8

71. van Heemst D. Insulin, IGF-1 and longevity. Aging Dis. 2010; 1:147–57.

72. Lambert AJ, Portero-Otin M, Pamplona R, Merry BJ. Effect of ageing and caloric restriction on specific markers of protein oxidative damage and membrane peroxidizability in rat liver mitochondria. Mech Ageing Dev. 2004; 125:529–38. https://doi.org/10.1016/j.mad.2004.06.002

73. Lambert AJ, Wang B, Yardley J, Edwards J, Merry BJ. The effect of aging and caloric restriction on mitochondrial protein density and oxygen consumption. Exp Gerontol. 2004; 39:289–95. https://doi.org/10.1016/j.exger.2003.12.009

74. Tucci P. Caloric restriction: is mammalian life extension linked to p53? Aging (Albany NY). 2012; 4:525–34. https://doi.org/10.18632/aging.100481

75. Gems D. Long-lived dwarf mice: are bile acids a longevity signal? Aging Cell. 2007; 6:421–23. https://doi.org/10.1111/j.1474-9726.2007.00309.x

76. Burks DJ, Font de Mora J, Schubert M, Withers DJ, Myers MG, Towery HH, Altamuro SL, Flint CL, White MF. IRS-2 pathways integrate female reproduction and energy homeostasis. Nature. 2000; 407:377–82. https://doi.org/10.1038/35030105

77. Sliwowska JH, Fergani C, Gawałek M, Skowronska B, Fichna P, Lehman MN. Insulin: its role in the central control of reproduction. Physiol Behav. 2014; 133:197–206. https://doi.org/10.1016/j.physbeh.2014.05.021

78. Kaaks R, Lukanova A. Energy balance and cancer: the role of insulin and insulin-like growth factor-I. Proc Nutr Soc. 2001; 60:91–106. https://doi.org/10.1079/PNS200070

79. Jia K, Chen D, Riddle DL. The TOR pathway interacts with the insulin signaling pathway to regulate C. elegans larval development, metabolism and life span. Development. 2004; 131:3897–906. https://doi.org/10.1242/dev.01255

80. Vellai T, Takacs-Vellai K, Zhang Y, Kovacs AL, Orosz L, Müller F. Genetics: influence of TOR kinase on lifespan in C. elegans. Nature. 2003; 426:620. https://doi.org/10.1038/426620a

81. Katewa SD, Kapahi P. Role of TOR signaling in aging and related biological processes in Drosophila melanogaster. Exp Gerontol. 2011; 46:382–90. https://doi.org/10.1016/j.exger.2010.11.036

82. Bjedov I, Toivonen JM, Kerr F, Slack C, Jacobson J, Foley A, Partridge L. Mechanisms of life span extension by rapamycin in the fruit fly Drosophila melanogaster. Cell Metab. 2010; 11:35–46. https://doi.org/10.1016/j.cmet.2009.11.010

83. Harrison DE, Strong R, Sharp ZD, Nelson JF, Astle CM, Flurkey K, Nadon NL, Wilkinson JE, Frenkel K, Carter CS, Pahor M, Javors MA, Fernandez E, Miller RA. Rapamycin fed late in life extends lifespan in genetically heterogeneous mice. Nature. 2009; 460:392–95. https://doi.org/10.1038/nature08221

84. Miller RA, Harrison DE, Astle CM, Baur JA, Boyd AR, de Cabo R, Fernandez E, Flurkey K, Javors MA, Nelson JF, Orihuela CJ, Pletcher S, Sharp ZD, et al. Rapamycin, but not resveratrol or simvastatin, extends life span of genetically heterogeneous mice. J Gerontol A Biol Sci Med Sci. 2011; 66:191–201. https://doi.org/10.1093/gerona/glq178

85. Kenyon CJ. The genetics of ageing. Nature. 2010; 464:504–12. https://doi.org/10.1038/nature08980

86. Lamming DW, Ye L, Katajisto P, Goncalves MD, Saitoh M, Stevens DM, Davis JG, Salmon AB, Richardson A, Ahima RS, Guertin DA, Sabatini DM, Baur JA. Rapamycin-induced insulin resistance is mediated by mTORC2 loss and uncoupled from longevity. Science. 2012; 335:1638–43. https://doi.org/10.1126/science.1215135

87. Selman C, Tullet JM, Wieser D, Irvine E, Lingard SJ, Choudhury AI, Claret M, Al-Qassab H, Carmignac D, Ramadani F, Woods A, Robinson IC, Schuster E, et al. Ribosomal protein S6 kinase 1 signaling regulates mammalian life span. Science. 2009; 326:140–44. https://doi.org/10.1126/science.1177221

88. Sharp ZD, Strong R. The role of mTOR signaling in controlling mammalian life span: what a fungicide teaches us about longevity. J Gerontol A Biol Sci Med Sci. 2010; 65:580–89. https://doi.org/10.1093/gerona/glp212

89. Dufner A, Thomas G. Ribosomal S6 kinase signaling and the control of translation. Exp Cell Res. 1999; 253:100–09. https://doi.org/10.1006/excr.1999.4683

90. Tsai SY, Rodriguez AA, Dastidar SG, Del Greco E, Carr KL, Sitzmann JM, Academia EC, Viray CM, Martinez LL, Kaplowitz BS, Ashe TD, La Spada AR, Kennedy BK. Increased 4E-BP1 Expression Protects against Diet-Induced Obesity and Insulin Resistance in Male Mice. Cell Reports. 2016; 16:1903–14. https://doi.org/10.1016/j.celrep.2016.07.029

91. Adler AS, Sinha S, Kawahara TL, Zhang JY, Segal E, Chang HY. Motif module map reveals enforcement of aging by continual NF-kappaB activity. Genes Dev. 2007; 21:3244–57. https://doi.org/10.1101/gad.1588507

92. Ghosh S, May MJ, Kopp EB. NF-kappa B and Rel proteins: evolutionarily conserved mediators of immune responses. Annu Rev Immunol. 1998; 16:225–60. https://doi.org/10.1146/annurev.immunol.16.1.225

93. Kim HJ, Jung KJ, Yu BP, Cho CG, Choi JS, Chung HY. Modulation of redox-sensitive transcription factors by calorie restriction during aging. Mech Ageing Dev. 2002; 123:1589–95. https://doi.org/10.1016/S0047-6374(02)00094-5

94. Pahl HL. Activators and target genes of Rel/NF-kappaB

transcription factors. Oncogene. 1999; 18:6853–66. https://doi.org/10.1038/sj.onc.1203239

95. Mauro C, Leow SC, Anso E, Rocha S, Thotakura AK, Tornatore L, Moretti M, De Smaele E, Beg AA, Tergaonkar V, Chandel NS, Franzoso G. NF-κB controls energy homeostasis and metabolic adaptation by upregulating mitochondrial respiration. Nat Cell Biol. 2011; 13:1272–79. https://doi.org/10.1038/ncb2324

96. Kawauchi K, Araki K, Tobiume K, Tanaka N. p53 regulates glucose metabolism through an IKK-NF-kappaB pathway and inhibits cell transformation. Nat Cell Biol. 2008; 10:611–18. https://doi.org/10.1038/ncb1724

97. Johnson RF, Witzel II, Perkins ND. p53-dependent regulation of mitochondrial energy production by the RelA subunit of NF-κB. Cancer Res. 2011; 71:5588–97. https://doi.org/10.1158/0008-5472.CAN-10-4252

98. Frye RA. Phylogenetic classification of prokaryotic and eukaryotic Sir2-like proteins. Biochem Biophys Res Commun. 2000; 273:793–98. https://doi.org/10.1006/bbrc.2000.3000

99. Mostoslavsky R, Chua KF, Lombard DB, Pang WW, Fischer MR, Gellon L, Liu P, Mostoslavsky G, Franco S, Murphy MM, Mills KD, Patel P, Hsu JT, et al. Genomic instability and aging-like phenotype in the absence of mammalian SIRT6. Cell. 2006; 124:315–29. https://doi.org/10.1016/j.cell.2005.11.044

100. Haigis MC, Mostoslavsky R, Haigis KM, Fahie K, Christodoulou DC, Murphy AJ, Valenzuela DM, Yancopoulos GD, Karow M, Blander G, Wolberger C, Prolla TA, Weindruch R, et al. SIRT4 inhibits glutamate dehydrogenase and opposes the effects of calorie restriction in pancreatic beta cells. Cell. 2006; 126:941–54. https://doi.org/10.1016/j.cell.2006.06.057

101. Tsuchiya T, Dhahbi JM, Cui X, Mote PL, Bartke A, Spindler SR. Additive regulation of hepatic gene expression by dwarfism and caloric restriction. Physiol Genomics. 2004; 17:307–15. https://doi.org/10.1152/physiolgenomics.00039.2004

102. Laurent G, German NJ, Saha AK, de Boer VC, Davies M, Koves TR, Dephoure N, Fischer F, Boanca G, Vaitheesvaran B, Lovitch SB, Sharpe AH, Kurland IJ, et al. SIRT4 coordinates the balance between lipid synthesis and catabolism by repressing malonyl CoA decarboxylase. Mol Cell. 2013; 50:686–98. https://doi.org/10.1016/j.molcel.2013.05.012

103. Vazquez BN, Thackray JK, Serrano L. Sirtuins and DNA damage repair: SIRT7 comes to play. Nucleus. 2017; 8:107–15. https://doi.org/10.1080/19491034.2016.1264552

104. Ford E, Voit R, Liszt G, Magin C, Grummt I, Guarente L. Mammalian Sir2 homolog SIRT7 is an activator of RNA polymerase I transcription. Genes Dev. 2006; 20:1075–80. https://doi.org/10.1101/gad.1399706

105. Guarente L. Sirtuins as potential targets for metabolic syndrome. Nature. 2006; 444:868–74. https://doi.org/10.1038/nature05486

106. Wronska A, Lawniczak A, Wierzbicki PM, Kmiec Z. Age-Related Changes in Sirtuin 7 Expression in Calorie-Restricted and Refed Rats. Gerontology. 2016; 62:304–10. https://doi.org/10.1159/000441603

107. Hagopian K, Ramsey JJ, Weindruch R. Krebs cycle enzymes from livers of old mice are differentially regulated by caloric restriction. Exp Gerontol. 2004; 39:1145–54. https://doi.org/10.1016/j.exger.2004.04.009

108. Hagopian K, Ramsey JJ, Weindruch R. Caloric restriction increases gluconeogenic and transaminase enzyme activities in mouse liver. Exp Gerontol. 2003; 38:267–78. https://doi.org/10.1016/S0531-5565(02)00202-4

109. Speakman JR, Selman C, McLaren JS, Harper EJ. Living fast, dying when? The link between aging and energetics. J Nutr. 2002 (Suppl 2); 132:1583S–97S.

110. Selman C, Phillips T, Staib JL, Duncan JS, Leeuwenburgh C, Speakman JR. Energy expenditure of calorically restricted rats is higher than predicted from their altered body composition. Mech Ageing Dev. 2005; 126:783–93. https://doi.org/10.1016/j.mad.2005.02.004

111. Gredilla R, Barja G, López-Torres M. Effect of short-term caloric restriction on H2O2 production and oxidative DNA damage in rat liver mitochondria and location of the free radical source. J Bioenerg Biomembr. 2001; 33:279–87. https://doi.org/10.1023/A:1010603206190

112. López-Torres M, Gredilla R, Sanz A, Barja G, López-Torres M, Gredilla R, Sanz A, Barja G. Influence of aging and long-term caloric restriction on oxygen radical generation and oxidative DNA damage in rat liver mitochondria. Free Radic Biol Med. 2002; 32:882–89. https://doi.org/10.1016/S0891-5849(02)00773-6

113. Ames BN, Shigenaga MK, Hagen TM. Mitochondrial decay in aging. Biochim Biophys Acta. 1995; 1271:165–70. https://doi.org/10.1016/0925-4439(95)00024-X

114. Allen RG, Keogh BP, Tresini M, Gerhard GS, Volker C, Pignolo RJ, Horton J, Cristofalo VJ. Development and age-associated differences in electron transport potential and consequences for oxidant generation. J

Biol Chem. 1997; 272:24805–12.
https://doi.org/10.1074/jbc.272.40.24805

115. Olgun A, Akman S, Serdar MA, Kutluay T. Oxidative phosphorylation enzyme complexes in caloric restriction. Exp Gerontol. 2002; 37:639–45. https://doi.org/10.1016/S0531-5565(02)00009-8

116. Wek RC, Jiang HY, Anthony TG. Coping with stress: eIF2 kinases and translational control. Biochem Soc Trans. 2006; 34:7–11. https://doi.org/10.1042/BST0340007

117. Jiang HY, Wek SA, McGrath BC, Scheuner D, Kaufman RJ, Cavener DR, Wek RC. Phosphorylation of the alpha subunit of eukaryotic initiation factor 2 is required for activation of NF-kappaB in response to diverse cellular stresses. Mol Cell Biol. 2003; 23:5651–63. https://doi.org/10.1128/MCB.23.16.5651-5663.2003

118. Gietzen DW, Ross CM, Hao S, Sharp JW. Phosphorylation of eIF2alpha is involved in the signaling of indispensable amino acid deficiency in the anterior piriform cortex of the brain in rats. J Nutr. 2004; 134:717–23.

119. Ma Q. Role of nrf2 in oxidative stress and toxicity. Annu Rev Pharmacol Toxicol. 2013; 53:401–26. https://doi.org/10.1146/annurev-pharmtox-011112-140320

120. Nguyen T, Nioi P, Pickett CB. The Nrf2-antioxidant response element signaling pathway and its activation by oxidative stress. J Biol Chem. 2009; 284:13291–95. https://doi.org/10.1074/jbc.R900010200

121. Pesta DH, Perry RJ, Guebre-Egziabher F, Zhang D, Jurczak M, Fischer-Rosinsky A, Daniels MA, Willmes DM, Bhanot S, Bornstein SR, Knauf F, Samuel VT, Shulman GI, Birkenfeld AL. Prevention of diet-induced hepatic steatosis and hepatic insulin resistance by second generation antisense oligonucleotides targeted to the longevity gene mIndy (Slc13a5). Aging (Albany NY). 2015; 7:1086–93. https://doi.org/10.18632/aging.100854

122. Berger FG, Szoka P. Biosynthesis of the major urinary proteins in mouse liver: a biochemical genetic study. Biochem Genet. 1981; 19:1261–73. https://doi.org/10.1007/BF00484578

123. Derous D, Mitchell SE, Green CL, Wang Y, Han JD, Chen L, Promislow DE, Lusseau D, Douglas A, Speakman JR. The Effects of Graded Levels of Calorie Restriction: X. Transcriptomic Responses of Epididymal Adipose Tissue. J Gerontol A Biol Sci Med Sci. 2017. Epub ahead of print. https://doi.org/10.1093/gerona/glx101

124. Tasdemir E, Maiuri MC, Galluzzi L, Vitale I, Djavaheri-Mergny M, D'Amelio M, Criollo A, Morselli E, Zhu C, Harper F, Nannmark U, Samara C, Pinton P, et al. Regulation of autophagy by cytoplasmic p53. Nat Cell Biol. 2008; 10:676–87. https://doi.org/10.1038/ncb1730

125. Yang L, Licastro D, Cava E, Veronese N, Spelta F, Rizza W, Bertozzi B, Villareal DT, Hotamisligil GS, Holloszy JO, Fontana L. Long-Term Calorie Restriction Enhances Cellular Quality-Control Processes in Human Skeletal Muscle. Cell Reports. 2015.

126. Lee C, Safdie FM, Raffaghello L, Wei M, Madia F, Parrella E, Hwang D, Cohen P, Bianchi G, Longo VD. Reduced levels of IGF-I mediate differential protection of normal and cancer cells in response to fasting and improve chemotherapeutic index. Cancer Res. 2010; 70:1564–72. https://doi.org/10.1158/0008-5472.CAN-09-3228

127. Moreau K, Luo S, Rubinsztein DC. Cytoprotective roles for autophagy. Curr Opin Cell Biol. 2010; 22:206–11. https://doi.org/10.1016/j.ceb.2009.12.002

128. Yang L, Li P, Fu S, Calay ES, Hotamisligil GS. Defective hepatic autophagy in obesity promotes ER stress and causes insulin resistance. Cell Metab. 2010; 11:467–78. https://doi.org/10.1016/j.cmet.2010.04.005

129. King PJ, Guasti L, Laufer E. Hedgehog signalling in endocrine development and disease. J Endocrinol. 2008; 198:439–50. https://doi.org/10.1677/JOE-08-0161

130. Zhao C, Chen A, Jamieson CH, Fereshteh M, Abrahamsson A, Blum J, Kwon HY, Kim J, Chute JP, Rizzieri D, Munchhof M, VanArsdale T, Beachy PA, Reya T. Hedgehog signalling is essential for maintenance of cancer stem cells in myeloid leukaemia. Nature. 2009; 458:776–79. https://doi.org/10.1038/nature07737

131. Rubin LL, de Sauvage FJ. Targeting the Hedgehog pathway in cancer. Nat Rev Drug Discov. 2006; 5:1026–33. https://doi.org/10.1038/nrd2086

132. Choi SS, Syn WK, Karaca GF, Omenetti A, Moylan CA, Witek RP, Agboola KM, Jung Y, Michelotti GA, Diehl AM. Leptin promotes the myofibroblastic phenotype in hepatic stellate cells by activating the hedgehog pathway. J Biol Chem. 2010; 285:36551–60. https://doi.org/10.1074/jbc.M110.168542

133. Samad F, Yamamoto K, Pandey M, Loskutoff DJ. Elevated expression of transforming growth factor-beta in adipose tissue from obese mice. Mol Med. 1997; 3:37–48.

134. Musi N, Guardado-Mendoza R. Adipose Tissue as an Endocrine Organ. Cellular Endocrinology in Health and Disease. 2014. p. 229–37.

135. Park J, Scherer PE. Leptin and cancer: from cancer stem cells to metastasis. Endocr Relat Cancer. 2011; 18:C25–29. https://doi.org/10.1530/ERC-11-0163

136. Laeger T, Henagan TM, Albarado DC, Redman LM, Bray GA, Noland RC, Münzberg H, Hutson SM, Gettys TW, Schwartz MW, Morrison CD. FGF21 is an endocrine signal of protein restriction. J Clin Invest. 2014; 124:3913–22. https://doi.org/10.1172/JCI74915

137. Lees EK, Król E, Grant L, Shearer K, Wyse C, Moncur E, Bykowska AS, Mody N, Gettys TW, Delibegovic M. Methionine restriction restores a younger metabolic phenotype in adult mice with alterations in fibroblast growth factor 21. Aging Cell. 2014; 13:817–27. https://doi.org/10.1111/acel.12238

138. Stone KP, Wanders D, Orgeron M, Cortez CC, Gettys TW. Mechanisms of increased in vivo insulin sensitivity by dietary methionine restriction in mice. Diabetes. 2014; 63:3721–33. https://doi.org/10.2337/db14-0464

139. Speakman JR, Mitchell SE, Mazidi M. Calories or protein? The effect of dietary restriction on lifespan in rodents is explained by calories alone. Exp Gerontol. 2016; 86:28–38. https://doi.org/10.1016/j.exger.2016.03.011

140. Kimura H. Hydrogen sulfide: its production, release and functions. Amino Acids. 2011; 41:113–21. https://doi.org/10.1007/s00726-010-0510-x

141. Whiteman M, Armstrong JS, Chu SH, Jia-Ling S, Wong BS, Cheung NS, Halliwell B, Moore PK. The novel neuromodulator hydrogen sulfide: an endogenous peroxynitrite 'scavenger'? J Neurochem. 2004; 90:765–68. https://doi.org/10.1111/j.1471-4159.2004.02617.x

142. Whiteman M, Li L, Kostetski I, Chu SH, Siau JL, Bhatia M, Moore PK. Evidence for the formation of a novel nitrosothiol from the gaseous mediators nitric oxide and hydrogen sulphide. Biochem Biophys Res Commun. 2006; 343:303–10. https://doi.org/10.1016/j.bbrc.2006.02.154

143. Kimura Y, Goto Y, Kimura H. Hydrogen sulfide increases glutathione production and suppresses oxidative stress in mitochondria. Antioxid Redox Signal. 2010; 12:1–13. https://doi.org/10.1089/ars.2008.2282

144. Patel P, Vatish M, Heptinstall J, Wang R, Carson RJ. The endogenous production of hydrogen sulphide in intrauterine tissues. Reprod Biol Endocrinol. 2009; 7:10. https://doi.org/10.1186/1477-7827-7-10

145. Singh S, Padovani D, Leslie RA, Chiku T, Banerjee R. Relative contributions of cystathionine beta-synthase and gamma-cystathionase to H2S biogenesis via alternative trans-sulfuration reactions. J Biol Chem. 2009; 284:22457–66. https://doi.org/10.1074/jbc.M109.010868

146. Chiku T, Padovani D, Zhu W, Singh S, Vitvitsky V, Banerjee R. H2S biogenesis by human cystathionine gamma-lyase leads to the novel sulfur metabolites lanthionine and homolanthionine and is responsive to the grade of hyperhomocysteinemia. J Biol Chem. 2009; 284:11601–12. https://doi.org/10.1074/jbc.M808026200

147. Hine C, Harputlugil E, Zhang Y, Ruckenstuhl C, Lee BC, Brace L, Longchamp A, Treviño-Villarreal JH, Mejia P, Ozaki CK, Wang R, Gladyshev VN, Madeo F, et al. Endogenous hydrogen sulfide production is essential for dietary restriction benefits. Cell. 2015; 160:132–44. https://doi.org/10.1016/j.cell.2014.11.048

148. Robertson LT, Treviño-Villarreal JH, Mejia P, Grondin Y, Harputlugil E, Hine C, Vargas D, Zheng H, Ozaki CK, Kristal BS, Simpson SJ, Mitchell JR. Protein and Calorie Restriction Contribute Additively to Protection from Renal Ischemia Reperfusion Injury Partly via Leptin Reduction in Male Mice. J Nutr. 2015; 145:1717–27. https://doi.org/10.3945/jn.114.199380

149. Taylor P, Weinert H, Weinert D, Waterhouse J. The Circadian Activity and Body Temperature Rhythms of Mice During Their Last Days of Life. Biol Rhythm Res. 2010; 33:37–41.

150. Wyse CA, Coogan AN, Selman C, Hazlerigg DG, Speakman JR. Association between mammalian lifespan and circadian free-running period: the circadian resonance hypothesis revisited. Biol Lett. 2010; 6:696–98. https://doi.org/10.1098/rsbl.2010.0152

151. Froy O, Chapnik N, Miskin R. Relationship between calorie restriction and the biological clock: lessons from long-lived transgenic mice. Rejuvenation Res. 2008; 11:467–71. https://doi.org/10.1089/rej.2008.0669

152. Hara R, Wan K, Wakamatsu H, Aida R, Moriya T, Akiyama M, Shibata S. Restricted feeding entrains liver clock without participation of the suprachiasmatic nucleus. Genes Cells. 2001; 6:269–78. https://doi.org/10.1046/j.1365-2443.2001.00419.x

153. Stokkan KA, Yamazaki S, Tei H, Sakaki Y, Menaker M. Entrainment of the circadian clock in the liver by feeding. Science. 2001; 291:490–93. https://doi.org/10.1126/science.291.5503.490

154. Vollmers C, Gill S, DiTacchio L, Pulivarthy SR, Le HD, Panda S. Time of feeding and the intrinsic circadian clock drive rhythms in hepatic gene expression. Proc Natl Acad Sci USA. 2009; 106:21453–58.

https://doi.org/10.1073/pnas.0909591106

155. Lee CC. Tumor suppression by the mammalian Period genes. Cancer Causes Control. 2006; 17:525–30. https://doi.org/10.1007/s10552-005-9003-8

156. Omiecinski CJ, Vanden Heuvel JP, Perdew GH, Peters JM. Xenobiotic metabolism, disposition, and regulation by receptors: from biochemical phenomenon to predictors of major toxicities. Toxicol Sci. 2011 (Suppl 1); 120:S49–75. https://doi.org/10.1093/toxsci/kfq338

157. Amador-Noguez D, Yagi K, Venable S, Darlington G. Gene expression profile of long-lived Ames dwarf mice and Little mice. Aging Cell. 2004; 3:423–41. https://doi.org/10.1111/j.1474-9728.2004.00125.x

158. Amador-Noguez D, Dean A, Huang W, Setchell K, Moore D, Darlington G. Alterations in xenobiotic metabolism in the long-lived Little mice. Aging Cell. 2007; 6:453–70. https://doi.org/10.1111/j.1474-9726.2007.00300.x

159. Mori K, Blackshear PE, Lobenhofer EK, Parker JS, Orzech DP, Roycroft JH, Walker KL, Johnson KA, Marsh TA, Irwin RD, Boorman GA. Hepatic transcript levels for genes coding for enzymes associated with xenobiotic metabolism are altered with age. Toxicol Pathol. 2007; 35:242–51. https://doi.org/10.1080/01926230601156286

160. Steinbaugh MJ, Sun LY, Bartke A, Miller RA. Activation of genes involved in xenobiotic metabolism is a shared signature of mouse models with extended lifespan. Am J Physiol Endocrinol Metab. 2012; 303:E488–95. https://doi.org/10.1152/ajpendo.00110.2012

161. Woodhouse K, Wynne HA. Age-related changes in hepatic function. Implications for drug therapy. Drugs Aging. 1992; 2:243–55. https://doi.org/10.2165/00002512-199202030-00007

162. Meyer UA. Endo-xenobiotic crosstalk and the regulation of cytochromes P450. Drug Metab Rev. 2007; 39:639–46. https://doi.org/10.1080/03602530701498737

163. Sohal RS, Forster MJ. Caloric restriction and the aging process: a critique. Free Radic Biol Med. 2014; 73:366–82. https://doi.org/10.1016/j.freeradbiomed.2014.05.015

164. Bolger AM, Lohse M, Usadel B. Trimmomatic: a flexible trimmer for Illumina sequence data. Bioinformatics. 2014; 30:2114–20. https://doi.org/10.1093/bioinformatics/btu170

165. Langmead B, Trapnell C, Pop M, Salzberg SL. Ultrafast and memory-efficient alignment of short DNA sequences to the human genome. Genome Biol. 2009; 10:R25. https://doi.org/10.1186/gb-2009-10-3-r25

166. Trapnell C, Pachter L, Salzberg SL. TopHat: discovering splice junctions with RNA-Seq. Bioinformatics. 2009; 25:1105–11. https://doi.org/10.1093/bioinformatics/btp120

167. Li H, Handsaker B, Wysoker A, Fennell T, Ruan J, Homer N, Marth G, Abecasis G, Durbin R, and 1000 Genome Project Data Processing Subgroup. The Sequence Alignment/Map format and SAMtools. Bioinformatics. 2009; 25:2078–79. https://doi.org/10.1093/bioinformatics/btp352

168. Anders S, Pyl PT, Huber W. HTSeq--a Python framework to work with high-throughput sequencing data. Bioinformatics. 2015; 31:166–69. https://doi.org/10.1093/bioinformatics/btu638

169. Robinson MD, Oshlack A. A scaling normalization method for differential expression analysis of RNA-seq data. Genome Biol. 2010; 11:R25. https://doi.org/10.1186/gb-2010-11-3-r25

170. Robinson MD, McCarthy DJ, Smyth GK. edgeR: a Bioconductor package for differential expression analysis of digital gene expression data. Bioinformatics. 2010; 26:139–40. https://doi.org/10.1093/bioinformatics/btp616

171. R Core Team. R: a language and environment for statistical computing. Vienna, Austria. R Foundation for Statistical Computing. Vienna, Austria; 2014. Available from: http://www.r-project.org/

SUPPLEMENTARY MATERIAL

Table S1. Expression levels of genes involved in insulin/IGF-1 signaling pathway correlated with the increase in calorie restriction (CR) and their gene expression at each level of CR relative to 12h ad libitum intake.

			10CR		**20CR**		**30CR**		**40CR**	
Symbol	**Gene Symbol**	***r***	***Log FC***	***p***	**Log FC**	**p**	**Log FC**	**p**	**Log FC**	**p**
4E-BP1	*Eif4ebp1*	-0.227	*-0.055*	*0.711*	0.056	0.689	-0.305	0.043	-0.295	0.026
ACLY	*Acly*	-0.339	*-1.654*	*0.002*	-1.324	0.007	-0.787	0.124	-1.310	0.003
AFX	*Foxo4*	-0.308	*-0.115*	*0.519*	-0.305	0.073	-0.185	0.301	-0.261	0.098
BAD	*Bad*	0.476	*-0.024*	*0.925*	0.089	0.711	0.240	0.339	0.415	0.062
c-FOS	*Fos*	0.121	*-1.152*	*0.104*	0.271	0.656	-0.193	0.770	0.217	0.705
c-JUN	*Jun*	-0.025	*-0.027*	*0.943*	0.834	0.017	-0.052	0.891	-0.014	0.966
c-RAF	*Raf1*	-0.299	*-0.165*	*0.253*	-0.215	0.116	-0.278	0.055	-0.247	0.052
C3G	*Rapgef1*	0.321	*0.178*	*0.169*	0.258	0.036	0.109	0.400	0.215	0.062
CASP9	*Casp9*	-0.257	*-0.279*	*0.109*	-0.157	0.336	-0.164	0.344	-0.471	0.002
CBL	*Cbl*	0.217	*-0.226*	*0.512*	0.034	0.916	0.044	0.897	0.089	0.766
CIP4	*Trip10*	0.217	*0.211*	*0.281*	0.383	0.037	0.256	0.190	0.281	0.107
eIF4E	*Eif4e*	-0.131	*-0.018*	*0.898*	-0.044	0.746	0.139	0.325	0.069	0.582
ELK-1	*Elk1*	-0.377	*-0.063*	*0.808*	0.045	0.852	-0.388	0.142	-0.412	0.077
FAK	*Ptk2*	-0.093	*0.133*	*0.357*	0.032	0.819	-0.038	0.797	0.021	0.873
FKHRL1	*Foxo3*	0.168	*-0.019*	*0.924*	-0.241	0.220	-0.120	0.562	0.015	0.933
FYN	*Fyn*	-0.297	*0.002*	*0.993*	0.118	0.519	0.012	0.953	-0.240	0.171
GAB1	*Gab1*	0.370	*0.234*	*0.149*	0.187	0.227	0.188	0.248	0.200	0.169
GLUT4	*Slc2a4*	0.168	*-1.636*	*0.013*	-0.688	0.244	0.257	0.671	-0.059	0.913
GRB10	*Grb10*	-0.142	*0.242*	*0.536*	0.444	0.231	-0.550	0.178	-0.432	0.224
GRB2	*Grb2*	-0.346	*-0.098*	*0.434*	0.003	0.982	-0.104	0.405	-0.123	0.266
IGF-1	*Igf1*	0.160	*0.284*	*0.223*	-0.005	0.983	0.321	0.169	0.053	0.800
IGF1R	*Igf1r*	0.293	*0.371*	*0.297*	0.573	0.088	0.257	0.476	0.693	0.029
INSR	*Insr*	0.507	*0.106*	*0.572*	-0.076	0.670	0.153	0.414	0.245	0.141
IRS1	*Irs1*	0.120	*-0.229*	*0.408*	-0.191	0.466	-0.129	0.639	0.412	0.089
JNK1	*Mapk8*	0.392	*0.183*	*0.239*	0.051	0.730	0.211	0.173	0.312	0.023
LAR	*Ptprf*	-0.623	*-0.293*	*0.176*	-0.325	0.113	-0.615	0.005	-0.594	0.002
LIPE	*Lipe*	-0.141	*-0.183*	*0.446*	-0.270	0.235	-0.265	0.271	-0.431	0.043
mTOR	*Mtor*	-0.119	*0.060*	*0.704*	0.159	0.289	0.043	0.787	-0.122	0.384
NCK	*Nck1*	-0.176	*-0.094*	*0.564*	-0.169	0.274	-0.205	0.212	-0.137	0.343
PDE3B	*Pde3b*	0.488	*0.236*	*0.276*	0.162	0.432	0.418	0.053	0.415	0.031
PDK1	*Pdpk1*	0.279	*0.092*	*0.564*	0.054	0.723	-0.018	0.910	0.220	0.120
PTEN	*Pten*	0.131	*0.001*	*0.995*	-0.097	0.595	0.069	0.717	0.041	0.807
PTP1B	*Ptpn1*	0.112	*0.040*	*0.799*	0.261	0.075	0.112	0.472	0.153	0.266
PXN	*Pxn*	0.248	*-0.126*	*0.367*	0.059	0.652	-0.112	0.424	0.054	0.661
RAPTOR	*Rptor*	-0.214	*-0.063*	*0.667*	-0.104	0.450	-0.167	0.254	-0.175	0.176
RAS GAP	*Rasa1*	0.001	*0.057*	*0.695*	-0.090	0.516	-0.034	0.818	-0.048	0.710
SGK	*Sgk1*	0.108	*0.275*	*0.330*	0.580	0.030	0.500	0.075	0.479	0.057
SHC	*Shc1*	-0.180	*-0.091*	*0.512*	0.026	0.845	-0.072	0.607	-0.258	0.036
SHP2	*Ptpn11*	0.124	*0.155*	*0.295*	0.114	0.418	0.045	0.764	0.179	0.173
SOCS3	*Socs3*	-0.221	*-0.655*	*0.148*	-0.046	0.913	-0.919	0.045	-0.677	0.086
SRF	*Srf*	-0.308	*-0.259*	*0.175*	-0.140	0.434	-0.432	0.026	-0.155	0.353
STAT3	*Stat3*	0.227	*-0.364*	*0.151*	0.348	0.142	0.043	0.862	0.271	0.223
STX4	*Stx4a*	-0.442	*-0.455*	*0.021*	-0.771	0.000	-0.361	0.065	-0.572	0.001
SYNIP	*Stxbp4*	-0.129	*-0.026*	*0.941*	-0.099	0.763	-0.295	0.406	-0.473	0.134

TC10	*Rhoq*	0.483	*0.240*	*0.171*	0.245	0.143	0.319	0.068	0.428	0.006
TSC1	*Tsc1*	0.205	*-0.028*	*0.846*	-0.272	0.047	0.014	0.922	0.046	0.713
TSC2	*Tsc2*	0.011	*0.078*	*0.581*	0.119	0.371	0.094	0.503	0.058	0.643
VAMP2	*Vamp2*	0.381	*-0.001*	*0.992*	-0.017	0.882	0.035	0.774	0.032	0.770

Table S2. Expression levels of genes involved in mTOR signaling pathway correlated with the increase in calorie restriction (CR) and their gene expression at each level of CR relative to 12h ad libitum intake.

			10CR		**20CR**		**30CR**		**40CR**	
Symbol	**Gene Symbol**	**r**	**logFC**	**p**	**logFC**	**p**	**logFC**	**p**	**logFC**	**p**
4EBP	*Eif4ebp1*	-0.227	-0.055	0.711	0.056	0.689	-0.305	0.043	-0.295	0.026
ATG13	*Atg13*	-0.003	-0.132	0.372	-0.241	0.088	-0.143	0.335	-0.097	0.458
DGKζ	*Dgkz*	0.070	0.067	0.655	0.249	0.080	0.041	0.784	0.090	0.499
eIF4B	*Eif4b*	-0.188	-0.026	0.882	-0.097	0.566	-0.054	0.761	-0.245	0.120
eIF4E	*Eif4e*	-0.131	-0.018	0.898	-0.044	0.746	0.139	0.325	0.069	0.582
FKBP1	*Fkbp1a*	-0.007	0.028	0.861	0.289	0.054	0.119	0.454	0.089	0.528
GBL	*Mlst8*	-0.440	0.244	0.367	0.231	0.369	-0.230	0.413	-0.196	0.428
HIF1α	*Hif1a*	0.060	0.008	0.954	-0.089	0.502	-0.113	0.421	-0.054	0.661
INSR	*Insr*	0.507	0.106	0.572	-0.076	0.670	0.153	0.414	0.245	0.141
IRS1	*Irs1*	0.120	-0.229	0.408	-0.191	0.466	-0.129	0.639	0.412	0.089
LKB1	*Stk11*	-0.353	0.037	0.776	-0.073	0.558	-0.158	0.232	-0.165	0.159
mTOR	*Mtor*	-0.119	0.060	0.704	0.159	0.289	0.043	0.787	-0.122	0.384
p70S6K	*Rps6kb1*	0.112	0.098	0.566	-0.043	0.791	0.022	0.899	0.131	0.384
PDK1	*Pdpk1*	0.279	0.092	0.564	0.054	0.723	-0.018	0.910	0.220	0.120
PKCα	*Prkca*	0.269	0.134	0.509	0.079	0.681	0.151	0.455	0.296	0.099
PRAS40	*Akt1s1*	-0.256	-0.189	0.199	-0.139	0.315	-0.208	0.159	-0.257	0.048
RAC	*Rac1*	-0.077	-0.032	0.801	-0.003	0.981	-0.037	0.773	-0.059	0.604
RAPTOR	*Rptor*	-0.214	-0.063	0.667	-0.104	0.450	-0.167	0.254	-0.175	0.176
REDD1	*Ddit4*	0.446	0.176	0.752	0.840	0.106	0.954	0.078	1.777	0.000
RHEB	*Rheb*	0.222	0.117	0.447	0.184	0.205	0.092	0.548	0.222	0.103
RICTOR	*Rictor*	0.328	0.312	0.161	0.231	0.276	0.270	0.226	0.332	0.094
RPS6	*Rps6*	0.487	-0.032	0.858	0.035	0.839	0.163	0.364	0.268	0.093
SIN1	*Mapkap1*	-0.318	-0.018	0.889	-0.119	0.345	-0.118	0.375	-0.131	0.267
TSC1	*Tsc1*	0.205	-0.028	0.846	-0.272	0.047	0.014	0.922	0.046	0.713
TSC2	*Tsc2*	0.011	0.078	0.581	0.119	0.371	0.094	0.503	0.058	0.643
ULK1	*Ulk1*	-0.040	-0.384	0.029	-0.214	0.197	-0.290	0.098	-0.103	0.504

Table S3. Expression levels of genes involved in NF-κB signaling pathway correlated with the increase in calorie restriction (CR) and their gene expression at each level of CR relative to 12h ad libitum intake.

			10CR		**20CR**		**30CR**		**40CR**	
Symbol	**Gene Symbol**	**r**	**logFC**	**p**	**logFC**	**p**	**logFC**	**p**	**logFC**	**p**
β-TrCP	*Btrc*	-0.112	-0.003	0.986	0.009	0.958	0.020	0.913	-0.157	0.337
A20	*Tnfaip3*	-0.100	0.218	0.582	0.351	0.349	-0.399	0.334	-0.311	0.389
ABIN-1	*Tnip1*	-0.219	-0.115	0.764	0.330	0.358	-0.569	0.146	-0.645	0.059
Bcl10	*Bcl10*	0.106	-0.238	0.314	0.110	0.616	0.101	0.663	0.007	0.975
BIMP1	*Card10*	0.062	0.207	0.354	0.318	0.132	0.231	0.302	0.120	0.548
c-RAF	*Raf1*	-0.299	-0.165	0.253	-0.215	0.116	-0.278	0.055	-0.247	0.052

CARD11	*Card11*	-0.294	-0.096	0.883	-0.445	0.479	-0.963	0.166	-1.573	0.013
Caspase8	*Casp8*	0.075	0.093	0.508	0.039	0.770	0.047	0.737	-0.072	0.568
CCR5	*Ccr5*	-0.087	0.160	0.608	0.536	0.065	0.350	0.258	0.112	0.687
CD4	*Cd4*	-0.550	-0.161	0.797	-0.779	0.204	-2.064	0.005	-1.509	0.011
Cot	*Map3k8*	0.125	-0.422	0.256	-0.131	0.703	-0.368	0.321	-0.050	0.877
FADD	*Fadd*	-0.480	-0.293	0.095	-0.301	0.070	-0.415	0.019	-0.565	0.000
GSK-3β	*Gsk3b*	0.117	0.144	0.273	0.063	0.614	0.006	0.966	0.095	0.416
HVEM	*Tnfrsf14*	-0.030	0.162	0.622	0.339	0.270	0.186	0.572	-0.191	0.528
IKKα	*Chuk*	0.065	0.152	0.458	-0.183	0.349	0.035	0.865	-0.021	0.908
IKKβ	*Ikbkb*	-0.137	-0.011	0.926	-0.068	0.535	-0.054	0.646	-0.124	0.230
IKKγ	*Ikbkg*	-0.099	0.213	0.163	0.202	0.165	-0.021	0.892	0.072	0.599
IRAK-M	*Irak3*	0.031	-0.275	0.389	-0.126	0.671	-0.430	0.187	0.047	0.865
JNK1	*Mapk8*	0.392	0.183	0.239	0.051	0.730	0.211	0.173	0.312	0.023
LTBR	*Ltbr*	-0.028	-0.067	0.630	0.041	0.755	-0.107	0.442	-0.024	0.844
MALT1	*Malt1*	-0.026	0.070	0.704	-0.135	0.446	-0.024	0.899	-0.040	0.808
MEKK1	*Map3k1*	-0.017	0.233	0.317	0.167	0.452	-0.016	0.946	0.145	0.486
MYD88	*Myd88*	0.040	-0.245	0.162	-0.095	0.564	-0.174	0.318	0.009	0.954
NAK	*Tbk1*	0.311	-0.048	0.771	-0.089	0.570	-0.024	0.883	0.254	0.079
NAP1	*Azi2*	0.566	0.166	0.283	-0.040	0.784	0.281	0.067	0.236	0.085
NF-κB1 p50	*Nfkb1*	-0.133	0.105	0.571	-0.092	0.605	-0.161	0.396	-0.100	0.548
NF-κB2 p100	*Nfkb2*	-0.234	0.203	0.592	0.479	0.182	-0.394	0.313	-0.734	0.034
NGF	*Ngf*	-0.225	0.430	0.558	0.679	0.333	-0.142	0.850	-0.245	0.711
NIK	*Map3k14*	0.156	0.511	0.241	1.164	0.004	0.402	0.361	0.667	0.088
p65/RelA	*Rela*	-0.300	-0.150	0.371	-0.134	0.396	-0.409	0.016	-0.292	0.049
PELI1	*Peli1*	0.206	0.022	0.896	-0.185	0.247	-0.106	0.527	0.025	0.866
PKCζ	*Prkcz*	-0.322	-0.132	0.538	-0.358	0.081	-0.368	0.089	-0.566	0.003
PKR	*Eif2ak2*	-0.007	0.058	0.719	-0.039	0.801	0.057	0.727	0.084	0.559
PLCγ2	*Plcg2*	-0.289	0.043	0.917	0.196	0.619	-0.318	0.454	-1.239	0.001
RelB	*Relb*	-0.255	0.435	0.434	0.567	0.283	-0.477	0.414	-1.635	0.003
RIP	*Ripk1*	0.125	0.025	0.864	0.012	0.927	-0.139	0.336	0.063	0.619
TAB1	*Tab1*	0.100	0.458	0.179	0.301	0.358	0.341	0.323	0.388	0.207
TANK	*Tank*	-0.150	0.138	0.360	-0.049	0.734	-0.178	0.250	0.035	0.793
TBP	*Tbp*	0.368	0.146	0.476	0.122	0.531	0.052	0.803	0.443	0.014
TGF-α	*Tgfa*	-0.169	-0.020	0.907	-0.033	0.844	-0.340	0.057	-0.297	0.058
TIRAP	*Tirap*	-0.481	-0.091	0.608	-0.187	0.267	-0.044	0.804	-0.222	0.157
TRADD	*Tradd*	-0.114	-0.526	0.016	-0.135	0.494	-0.100	0.631	-0.240	0.198
TRAF2	*Traf2*	-0.004	0.326	0.163	0.400	0.071	0.112	0.638	0.206	0.330
TRAF6	*Traf6*	0.420	0.135	0.414	0.082	0.601	0.150	0.365	0.383	0.009
TTRAP	*Tdp2*	0.498	0.012	0.949	0.050	0.787	0.382	0.047	0.288	0.094
UBE2N	*Ube2n*	-0.386	-0.143	0.276	-0.157	0.209	-0.223	0.092	-0.120	0.302
UBE2V1	*Ube2v1*	-0.301	-0.096	0.446	0.027	0.818	-0.069	0.584	-0.080	0.472
Zap70	*Zap70*	-0.169	0.242	0.441	0.624	0.034	0.314	0.316	-0.250	0.381

Table S4. Expression levels of genes involved in sirtuin signaling pathway correlated with the increase in calorie restriction (CR) and their gene expression at each level of CR relative to 12h ad libitum intake.

			10CR		20CR		30CR		40CR	
Symbol	Gene symbol	r	logFC	p	logFC	p	logFC	p	logFC	p
ACADL	*Acadl*	0.763	0.111	0.612	0.263	0.208	0.468	0.032	0.557	0.005
ARNTL	*Arntl*	-0.105	-1.581	0.038	-1.588	0.026	-1.808	0.020	0.261	0.674

BIRC5	*Birc5*	-0.039	0.321	0.580	1.432	0.008	-0.403	0.507	0.053	0.920
CDKN1A	*Cdkn1a*	0.055	0.775	0.288	1.702	0.016	-0.253	0.736	1.225	0.066
CPS1	*Cps1*	0.476	-0.279	0.234	-0.222	0.317	0.030	0.899	0.177	0.392
CRTC2	*Crtc2*	0.626	0.135	0.439	0.130	0.432	0.220	0.204	0.463	0.003
CTNNB1	*Ctnnb1*	-0.363	-0.100	0.550	-0.083	0.601	-0.220	0.190	-0.268	0.069
CYC1	*Cyc1*	0.617	-0.086	0.611	0.020	0.898	0.157	0.349	0.309	0.039
CYCS	*Cycs*	0.572	0.064	0.782	-0.084	0.702	0.231	0.313	0.523	0.011
E2F1	*E2f1*	-0.296	0.182	0.629	0.681	0.050	-0.128	0.741	-0.441	0.210
EPAS1	*Epas1*	0.343	-0.396	0.183	-0.125	0.655	0.108	0.714	0.108	0.678
FOXO1	*Foxo1*	0.603	0.236	0.302	0.322	0.139	0.382	0.094	0.681	0.001
FOXO3	*Foxo3*	0.168	-0.019	0.924	-0.241	0.220	-0.120	0.562	0.015	0.933
FOXO4	*Foxo4*	-0.308	-0.115	0.519	-0.305	0.073	-0.185	0.301	-0.261	0.098
GLUD1	*Glud1*	0.655	-0.123	0.559	0.047	0.815	0.230	0.271	0.460	0.014
HIF1A	*Hif1a*	0.060	0.008	0.954	-0.089	0.502	-0.113	0.421	-0.054	0.661
HNF4A	*Hnf4a*	0.338	-0.104	0.665	0.075	0.744	-0.060	0.802	0.316	0.139
HSF1	*Hsf1*	0.015	-0.047	0.744	-0.059	0.666	-0.040	0.782	0.012	0.925
IDE	*Ide*	-0.662	-0.125	0.442	-0.345	0.026	-0.422	0.010	-0.371	0.010
IDH2	*Idh2*	0.556	0.443	0.099	0.740	0.004	0.818	0.002	0.850	<0.001
MRPL10	*Mrpl10*	-0.223	-0.127	0.302	0.007	0.949	-0.188	0.131	-0.035	0.747
NDUFA9	*Ndufa9*	0.506	-0.136	0.385	-0.142	0.340	0.097	0.535	0.240	0.082
NFKB1	*Nfkb1*	-0.133	0.105	0.571	-0.092	0.605	-0.161	0.396	-0.100	0.548
NFKB2	*Nfkb2*	-0.234	0.203	0.592	0.479	0.182	-0.394	0.313	-0.734	0.034
NR1H2	*Nr1h2*	0.381	-0.140	0.341	0.037	0.787	0.101	0.485	0.232	0.069
NR1H3	*Nr1h3*	-0.540	-0.134	0.458	-0.134	0.432	-0.152	0.397	-0.344	0.030
PARP1	*Parp1*	-0.363	-0.176	0.288	-0.179	0.252	-0.208	0.209	-0.418	0.004
PER2	*Per2*	0.724	0.671	0.039	0.828	0.008	1.028	0.002	0.950	0.001
PIP5K1A	*Pip5k1a*	0.105	-0.069	0.723	0.277	0.121	-0.003	0.988	-0.009	0.960
PIP5K1C	*Pip5k1c*	-0.120	-0.027	0.840	0.135	0.282	-0.001	0.995	0.049	0.676
PPARA	*Ppara*	0.257	-0.004	0.987	-0.055	0.811	0.114	0.637	-0.037	0.864
PPARG	*Pparg*	-0.012	0.249	0.483	0.534	0.113	0.024	0.947	-0.111	0.729
PPARGC1A	*Ppargc1a*	0.806	-0.172	0.624	0.249	0.452	0.623	0.071	1.064	0.001
PPID	*Ppid*	-0.654	-0.037	0.856	-0.242	0.208	-0.380	0.063	-0.319	0.074
RARA	*Rara*	-0.358	0.048	0.765	0.051	0.739	-0.203	0.217	-0.363	0.013
RARB	*Rarb*	0.370	0.166	0.594	0.802	0.005	0.631	0.037	0.646	0.017
RB1	*Rb1*	-0.315	0.052	0.757	-0.338	0.039	-0.251	0.146	-0.217	0.153
RBL1	*Rbl1*	-0.021	0.645	0.161	0.934	0.032	0.086	0.858	-0.011	0.980
RBL2	*Rbl2*	0.562	0.004	0.983	-0.245	0.127	0.051	0.762	0.252	0.090
RELA	*Rela*	-0.300	-0.150	0.371	-0.134	0.396	-0.409	0.016	-0.292	0.049
SDHA	*Sdha*	0.185	-0.084	0.658	-0.239	0.185	0.027	0.886	0.013	0.937
SDHB	*Sdhb*	0.462	0.127	0.474	-0.026	0.876	0.195	0.271	0.193	0.220
SIRT1	*Sirt1*	0.214	0.016	0.938	0.066	0.732	-0.119	0.560	0.299	0.092
SIRT2	*Sirt2*	-0.080	-0.038	0.754	-0.037	0.749	-0.131	0.282	-0.098	0.361
SIRT3	*Sirt3*	-0.032	0.028	0.890	-0.262	0.174	-0.003	0.988	-0.233	0.192
SIRT4	*Sirt4*	-0.653	0.037	0.882	-0.299	0.216	-0.638	0.017	-0.499	0.030
SIRT5	*Sirt5*	-0.297	-0.066	0.770	-0.172	0.422	-0.033	0.884	-0.523	0.010
SIRT6	*Sirt6*	0.051	0.203	0.561	0.142	0.669	-0.145	0.687	0.035	0.911
SIRT7	*Sirt7*	-0.501	-0.184	0.248	-0.317	0.037	-0.286	0.074	-0.304	0.031
SLC25A5	*Slc25a5*	0.732	0.046	0.803	0.165	0.344	0.368	0.044	0.478	0.003
SMAD7	*Smad7*	0.052	0.229	0.338	0.123	0.588	0.431	0.069	-0.247	0.254
SREBF1	*Srebf1*	-0.463	-0.260	0.435	-0.102	0.745	-0.343	0.304	-0.914	0.002
SREBF2	*Srebf2*	0.257	-0.236	0.226	0.115	0.529	0.035	0.855	0.094	0.583
TLE1	*Tle1*	-0.153	-0.255	0.141	-0.284	0.083	-0.443	0.011	-0.049	0.746
TP53	*Trp53*	-0.159	0.136	0.551	0.326	0.131	-0.272	0.245	-0.076	0.711

TSC2	*Tsc2*	0.011	0.078	0.581	0.119	0.371	0.094	0.503	0.058	0.643
TUBA1A	*Tuba1a*	-0.226	-0.288	0.545	0.102	0.818	-0.756	0.124	-0.799	0.062
TUBA1B	*Tuba1b*	-0.307	-0.171	0.565	0.169	0.541	-0.311	0.301	-0.530	0.047
TUBA1C	*Tuba1c*	-0.377	-0.283	0.481	0.108	0.774	-0.693	0.090	-0.688	0.053
TUBA4A	*Tuba4a*	-0.595	-0.502	0.077	-0.665	0.014	-0.803	0.005	-0.597	0.016
TUBA8	*Tuba8*	0.525	1.004	0.123	1.542	0.014	1.050	0.108	2.228	<0.001
UCP2	*Ucp2*	-0.133	0.204	0.479	0.582	0.033	0.177	0.540	-0.190	0.458
WRN	*Wrn*	-0.057	0.014	0.930	-0.190	0.222	-0.129	0.430	-0.135	0.351
XRCC6	*Xrcc6*	-0.321	-0.083	0.677	0.210	0.256	-0.045	0.820	-0.238	0.179

Table S5. Expression levels of genes involved in oxidative stress signaling pathway correlated with the increase in calorie restriction (CR) and their gene expression at each level of CR relative to 12h ad libitum intake.

			10CR		**20CR**		**30CR**		**40CR**	
Symbol	**Gene Symbol**	**r**	**logFC**	**p**	**logFC**	**p**	**logFC**	**p**	**logFC**	**p**
53BP1	*Trp53bp1*	-0.455	0.142	0.346	-0.124	0.392	-0.160	0.297	-0.182	0.181
AKR	*Akr1a1*	-0.214	-0.013	0.939	0.062	0.704	-0.016	0.926	-0.083	0.587
AKT	*Akt1*	0.072	0.049	0.710	0.258	0.038	0.109	0.405	0.046	0.695
AOX1	*Aox1*	-0.316	0.156	0.476	0.159	0.446	-0.046	0.835	-0.185	0.343
ARD1	*Naa10*	0.052	-0.251	0.082	-0.064	0.633	-0.025	0.861	0.004	0.977
ARNT	*Arnt*	0.457	0.085	0.566	0.091	0.519	0.273	0.063	0.201	0.126
ASK1	*Map3k5*	0.525	0.195	0.382	0.019	0.928	0.152	0.494	0.294	0.137
ATF2	*Atf2*	0.414	0.014	0.922	-0.053	0.690	0.046	0.745	0.208	0.093
ATF4	*Atf4*	-0.141	-0.061	0.700	-0.055	0.714	-0.034	0.830	-0.161	0.253
ATF6	*Atf6*	-0.227	-0.058	0.724	-0.022	0.889	-0.318	0.055	-0.090	0.538
ATM	*Atm*	0.005	0.105	0.576	-0.050	0.780	0.011	0.954	-0.078	0.646
BACH1	*Bach1*	0.070	0.365	0.051	0.088	0.625	0.096	0.610	-0.094	0.573
BID	*Bid*	-0.364	-0.040	0.835	-0.201	0.275	-0.184	0.345	-0.408	0.019
BIP	*Hspa5*	-0.431	-0.164	0.571	-0.197	0.473	-0.519	0.076	-0.500	0.050
BLM	*Blm*	-0.066	-0.193	0.591	-0.702	0.044	-0.239	0.507	-0.460	0.150
BRCA1	*Brca1*	0.463	0.008	0.985	0.734	0.055	0.903	0.024	1.072	0.003
c-Abl	*Abl1*	0.245	0.189	0.215	0.260	0.071	0.246	0.105	0.122	0.371
c-Jun	*Jun*	-0.025	-0.027	0.943	0.834	0.017	-0.052	0.891	-0.014	0.966
c-MAF	*Maf*	0.259	0.052	0.748	0.210	0.175	0.236	0.146	0.176	0.223
c-RAF	*Raf1*	-0.299	-0.165	0.253	-0.215	0.116	-0.278	0.055	-0.247	0.052
CALR	*Calr*	-0.616	-0.562	0.065	-0.444	0.122	-0.902	0.003	-0.638	0.016
CASP3	*Casp3*	-0.315	-0.439	0.038	-0.312	0.115	-0.059	0.774	-0.472	0.011
CASP7	*Casp7*	0.158	-0.014	0.941	-0.025	0.887	0.268	0.142	-0.086	0.600
CASP9	*Casp9*	-0.257	-0.279	0.109	-0.157	0.336	-0.164	0.344	-0.471	0.002
CAT	*Cat*	-0.805	-0.091	0.700	-0.470	0.039	-0.487	0.043	-0.668	0.001
CBP	*Crebbp*	0.395	0.196	0.375	0.185	0.379	0.138	0.533	0.399	0.042
CBR1	*Cbr1*	0.712	0.505	0.221	1.316	0.001	1.314	0.001	1.858	0.000
CCT7	*Cct7*	0.068	-0.152	0.253	0.049	0.697	-0.010	0.937	0.005	0.968
CDC25A	*Cdc25a*	0.175	0.154	0.598	0.426	0.116	0.273	0.348	0.376	0.144
CDK1	*Cdk1*	-0.132	0.564	0.430	1.514	0.025	0.445	0.538	-0.742	0.267
CDK2	*Cdk2*	0.027	0.145	0.420	-0.176	0.315	0.068	0.709	-0.078	0.631
Chk2	*Chek2*	-0.238	0.188	0.623	0.426	0.234	0.330	0.386	-0.226	0.524
CHOP	*Ddit3*	-0.200	0.635	0.174	0.784	0.079	0.146	0.759	-0.136	0.749
CLPP	*Clpp*	-0.026	-0.128	0.359	-0.074	0.574	-0.092	0.511	-0.004	0.977
CSF2Rα	*Csf2ra*	-0.123	0.121	0.738	0.439	0.197	-0.017	0.962	-0.735	0.026
CSF2Rβ	*Csf2rb2*	-0.032	0.382	0.327	0.706	0.056	0.191	0.554	-0.029	0.921

CUL2	*Cul2*	-0.524	0.027	0.848	-0.253	0.061	-0.094	0.508	-0.186	0.137
EIF2S1	*Eif2s1*	-0.195	0.050	0.740	0.101	0.480	-0.117	0.440	-0.105	0.433
eIF4E	*Eif4e*	-0.131	-0.018	0.898	-0.044	0.746	0.139	0.325	0.069	0.582
elF2α	*Eif2a*	0.502	0.059	0.628	0.019	0.873	0.161	0.188	0.185	0.089
elF2γ	*Eif2s3x*	0.426	0.109	0.460	-0.003	0.985	0.159	0.280	0.253	0.054
elF4C	*Eif1a*	0.038	-0.028	0.906	0.159	0.483	-0.019	0.938	0.221	0.296
ELK-1	*Elk1*	-0.377	-0.063	0.808	0.045	0.852	-0.388	0.142	-0.412	0.077
EPHX1	*Ephx1*	0.042	0.282	0.421	0.846	0.011	0.418	0.232	0.633	0.044
ERK5	*Mapk7*	-0.087	0.035	0.909	0.106	0.709	-0.127	0.682	-0.082	0.765
ERP29	*Erp29*	-0.508	-0.227	0.173	-0.084	0.593	-0.293	0.080	-0.313	0.033
FKBP5	*Fkbp5*	0.780	0.438	0.411	1.267	0.013	1.575	0.003	2.180	0.000
FMO1	*Fmo1*	0.818	0.439	0.149	0.724	0.012	1.206	0.000	1.099	0.000
FTH1	*Fth1*	0.532	0.184	0.319	0.283	0.108	0.326	0.077	0.409	0.013
GADD34	*Ppp1r15a*	0.191	0.049	0.799	0.170	0.348	-0.004	0.984	0.139	0.416
GCLC	*Gclc*	-0.388	0.246	0.368	0.017	0.948	-0.571	0.041	-0.504	0.038
GCLM	*Gclm*	0.003	0.221	0.152	0.332	0.024	0.131	0.396	0.160	0.245
GCN2	*Eif2ak4*	0.387	-0.003	0.989	0.084	0.635	0.139	0.454	0.300	0.067
gp91	*Cybb*	-0.071	0.217	0.534	0.732	0.027	0.021	0.951	-0.483	0.120
GRB2	*Grb2*	-0.346	-0.098	0.434	0.003	0.982	-0.104	0.405	-0.123	0.266
GRP94	*Hsp90b1*	-0.486	-0.287	0.160	-0.337	0.082	-0.370	0.071	-0.302	0.092
GSK3β	*Gsk3b*	0.117	0.144	0.273	0.063	0.614	0.006	0.966	0.095	0.416
GSR	*Gsr*	-0.153	0.054	0.710	0.121	0.376	-0.187	0.198	-0.034	0.788
H2AX	*H2afx*	-0.111	0.212	0.396	0.289	0.220	-0.184	0.479	0.144	0.523
HERPUD1	*Herpud1*	0.184	-0.120	0.645	0.004	0.987	-0.025	0.922	0.216	0.347
HIF1α	*Hif1a*	0.060	0.008	0.954	-0.089	0.502	-0.113	0.421	-0.054	0.661
HIP2	*Ube2k*	0.058	-0.050	0.678	-0.039	0.730	-0.006	0.963	0.124	0.245
HO-1	*Hmox1*	0.117	-0.006	0.985	0.739	0.020	-0.080	0.813	0.241	0.418
HP1	*Cbx5*	0.205	0.255	0.067	0.183	0.167	0.177	0.204	0.062	0.620
HRI	*Eif2ak1*	0.151	-0.016	0.903	-0.161	0.192	-0.118	0.363	-0.002	0.989
HSP90	*Hsp90aa1*	-0.423	0.055	0.820	0.124	0.588	-0.203	0.404	-0.150	0.483
IκBα	*Nfkbia*	0.575	0.116	0.557	0.074	0.695	0.160	0.418	0.462	0.008
ICAM1	*Icam1*	-0.056	-0.036	0.914	0.411	0.194	0.081	0.809	-0.085	0.775
ICSBP	*Irf8*	-0.080	0.320	0.324	0.472	0.125	0.093	0.776	-0.458	0.121
INSR	*Insr*	0.507	0.106	0.572	-0.076	0.670	0.153	0.414	0.245	0.141
IRE1	*Ern1*	-0.184	-0.033	0.895	-0.344	0.154	-0.466	0.069	-0.009	0.969
IRF-1	*Irf1*	-0.132	-0.040	0.851	-0.090	0.656	-0.261	0.225	-0.208	0.269
JAB1	*Cops5*	0.151	-0.080	0.547	-0.069	0.583	0.044	0.739	-0.008	0.945
JAK2	*Jak2*	-0.138	0.054	0.707	-0.132	0.337	-0.130	0.368	-0.177	0.167
JIK	*Taok3*	0.580	0.045	0.804	0.040	0.813	0.101	0.571	0.349	0.028
JNK1	*Mapk8*	0.392	0.183	0.239	0.051	0.730	0.211	0.173	0.312	0.023
KAP-1	*Trim28*	0.142	-0.072	0.661	0.024	0.880	0.007	0.965	0.005	0.974
MDC1	*Mdc1*	0.099	-0.010	0.960	0.079	0.672	0.082	0.680	0.117	0.506
MDM2	*Mdm2*	0.001	0.116	0.521	0.217	0.203	0.048	0.791	0.120	0.456
MDMX	*Mdm4*	0.309	0.298	0.281	0.279	0.289	0.337	0.222	0.311	0.207
MEK1	*Map2k1*	-0.493	-0.174	0.283	-0.122	0.426	-0.182	0.262	-0.359	0.012
MEK5	*Map2k5*	0.099	-0.098	0.545	0.004	0.978	-0.200	0.220	-0.058	0.687
MEKK	*Map3k1*	-0.017	0.233	0.317	0.167	0.452	-0.016	0.946	0.145	0.486
MRE11	*Mre11a*	0.072	0.142	0.625	0.123	0.657	-0.236	0.435	0.075	0.773
MRP1	*Abcc1*	-0.030	0.317	0.441	0.360	0.357	-0.148	0.727	-0.369	0.329
MRP2	*Abcc2*	0.241	0.209	0.333	0.190	0.355	0.132	0.543	0.139	0.470
MRP4	*Abcc4*	0.073	1.657	0.007	2.157	0.000	0.988	0.108	1.217	0.030
NBS1	*Nbn*	0.141	0.014	0.925	-0.089	0.534	-0.079	0.604	0.024	0.857
NRF2	*Nfe2l2*	-0.139	-0.035	0.828	-0.105	0.491	-0.146	0.365	-0.057	0.687

NRPB	*Enc1*	0.455	0.275	0.558	1.004	0.024	0.988	0.033	1.406	0.001
p21CIP1	*Cdkn1a*	0.055	0.775	0.288	1.702	0.016	-0.253	0.736	1.225	0.066
p22phox	*Cyba*	-0.101	0.115	0.767	0.647	0.075	0.062	0.874	-0.394	0.258
p38MAPK	*Mapk14*	0.614	0.219	0.157	0.243	0.099	0.306	0.048	0.436	0.002
p40phox	*Ncf4*	-0.231	-0.210	0.679	0.161	0.733	-0.169	0.739	-1.054	0.025
p47phox	*Ncf1*	-0.150	0.301	0.338	0.621	0.036	-0.082	0.799	-0.444	0.123
p53	*Trp53*	-0.159	0.136	0.551	0.326	0.131	-0.272	0.245	-0.076	0.711
P58IPK	*Dnajc3*	-0.105	-0.070	0.703	-0.144	0.409	-0.119	0.518	0.083	0.609
p67phox	*Ncf2*	-0.112	-0.069	0.857	0.271	0.447	-0.019	0.960	-0.427	0.210
PABP	*Pabpc1*	-0.272	0.045	0.775	0.011	0.944	-0.191	0.230	-0.180	0.200
PAI-1	*Serpine1*	0.039	-0.037	0.954	0.875	0.140	0.254	0.687	-0.365	0.521
PDK1	*Pdpk1*	0.279	0.092	0.564	0.054	0.723	-0.018	0.910	0.220	0.120
PERK	*Eif2ak3*	-0.206	0.109	0.663	-0.187	0.438	-0.587	0.024	-0.329	0.145
PKCβ	*Prkcb*	-0.177	-0.169	0.508	0.129	0.589	-0.223	0.385	-0.648	0.005
PKR	*Eif2ak2*	-0.007	0.058	0.719	-0.039	0.801	0.057	0.727	0.084	0.559
PMF-1	*Pmf1*	0.453	-0.372	0.063	-0.128	0.491	0.074	0.702	0.211	0.221
PPARα	*Ppara*	0.257	-0.004	0.987	-0.055	0.811	0.114	0.637	-0.037	0.864
PPIB	*Ppib*	-0.602	-0.394	0.099	-0.258	0.252	-0.507	0.034	-0.526	0.012
PRDX1	*Prdx1*	-0.201	-0.130	0.457	-0.079	0.632	-0.058	0.738	-0.078	0.610
Rac1	*Rac1*	-0.077	-0.032	0.801	-0.003	0.981	-0.037	0.773	-0.059	0.604
Rad50	*Rad50*	0.066	0.028	0.870	0.108	0.508	0.063	0.714	-0.009	0.956
RAD9	*Rad9a*	0.112	0.093	0.512	0.175	0.191	0.048	0.735	0.033	0.792
REF1	*Apex1*	-0.363	-0.469	0.021	-0.188	0.323	-0.298	0.140	-0.469	0.009
SHC	*Shc1*	-0.180	-0.091	0.512	0.026	0.845	-0.072	0.607	-0.258	0.036
SIRPα	*Sirpa*	-0.184	0.119	0.738	0.451	0.180	-0.253	0.481	-0.597	0.059
SP1	*Sp1*	-0.145	-0.081	0.528	-0.179	0.146	-0.215	0.100	-0.138	0.228
SQSTM1	*Sqstm1*	-0.287	0.000	0.999	0.200	0.481	-0.483	0.110	-0.475	0.072
SR-BI	*Scarb1*	0.155	-0.154	0.397	0.015	0.930	-0.146	0.422	0.125	0.438
SRC-1	*Ncoa1*	0.269	-0.018	0.903	-0.090	0.507	0.104	0.465	0.194	0.123
STAT1	*Stat1*	-0.217	0.044	0.866	0.120	0.631	-0.417	0.116	-0.336	0.148
STIP1	*Stip1*	-0.520	-0.131	0.496	-0.084	0.646	-0.361	0.064	-0.289	0.089
TCEB1	*Tceb1*	-0.252	0.119	0.519	0.005	0.978	0.076	0.682	-0.016	0.922
TDP1	*Tdp1*	-0.089	-0.083	0.827	0.200	0.569	0.005	0.990	-0.327	0.339
TLR4	*Tlr4*	-0.006	-0.007	0.979	0.146	0.576	0.044	0.875	0.005	0.986
TPA	*Plat*	-0.148	0.369	0.658	0.767	0.334	-1.024	0.248	-1.440	0.064
TRAF2	*Traf2*	-0.004	0.326	0.163	0.400	0.071	0.112	0.638	0.206	0.330
TRXR1	*Txnrd1*	-0.057	0.190	0.296	0.174	0.314	-0.053	0.773	0.134	0.405
TXN	*Txn1*	-0.298	-0.127	0.418	-0.351	0.019	-0.176	0.265	-0.196	0.157
UB2R1	*Cdc34*	-0.111	0.082	0.607	0.241	0.108	-0.105	0.512	0.053	0.707
UbcM2	*Ube2e3*	0.477	-0.026	0.855	0.063	0.640	0.154	0.275	0.241	0.054
USP14	*Usp14*	-0.191	-0.044	0.732	-0.114	0.352	-0.041	0.750	-0.039	0.734
VCAM1	*Vcam1*	0.456	0.122	0.711	0.847	0.007	0.542	0.097	0.639	0.029
VCP	*Vcp*	-0.549	-0.369	0.088	-0.321	0.116	-0.538	0.013	-0.542	0.004
VHL	*Vhl*	-0.256	0.052	0.835	0.116	0.621	-0.004	0.986	-0.045	0.838
XBP1	*Xbp1*	-0.571	-0.085	0.732	-0.283	0.230	-0.429	0.087	-0.659	0.003

Table S6. Expression levels of genes involved in reproduction signaling pathway correlated with the increase in calorie restriction (CR) and their gene expression at each level of CR relative to 12h ad libitum intake.

			10CR		20CR		30CR		40CR	
Symbol	**Gene Symbol**	**r**	**logFC**	**p**	**logFC**	**p**	**logFC**	**p**	**logFC**	**p**
β-catenin	*Ctnnb1*	-0.363	-0.100	0.550	-0.083	0.601	-0.220	0.190	-0.268	0.069
ACOX1	*Acox1*	0.368	0.052	0.793	0.115	0.541	0.242	0.221	0.079	0.653
AHR	*Ahr*	0.468	-0.012	0.957	0.117	0.564	0.293	0.166	0.422	0.025
AKT1	*Akt1*	0.072	0.049	0.710	0.258	0.038	0.109	0.405	0.046	0.695
Apaf1	*Apaf1*	0.020	0.141	0.693	0.775	0.018	0.373	0.290	0.037	0.908
ASPH	*Asph*	-0.207	0.026	0.858	-0.093	0.499	-0.155	0.287	-0.043	0.737
ATF2	*Atf2*	0.414	0.014	0.922	-0.053	0.690	0.046	0.745	0.208	0.093
ATM	*Atm*	0.005	0.105	0.576	-0.050	0.780	0.011	0.954	-0.078	0.646
ATR	*Atr*	0.422	0.237	0.206	0.302	0.089	0.340	0.068	0.422	0.011
AXIN	*Axin1*	0.117	-0.146	0.373	-0.029	0.851	-0.154	0.349	0.088	0.540
BAX	*Bax*	-0.138	-0.095	0.696	0.118	0.604	-0.205	0.403	-0.219	0.312
Bcl-2	*Bcl2*	-0.221	0.665	0.077	0.396	0.274	-0.449	0.265	-0.401	0.256
Bcl-xL	*Bcl2l1*	-0.005	0.134	0.473	0.224	0.205	-0.077	0.684	0.065	0.695
Brca1	*Brca1*	0.463	0.008	0.985	0.734	0.055	0.903	0.024	1.072	0.003
c-Jun	*Jun*	-0.025	-0.027	0.943	0.834	0.017	-0.052	0.891	-0.014	0.966
c-Raf	*Raf1*	-0.299	-0.165	0.253	-0.215	0.116	-0.278	0.055	-0.247	0.052
CABC1	*Adck3*	-0.158	-0.780	0.025	-0.975	0.003	-0.615	0.075	-0.145	0.628
Caspase 6	*Casp6*	0.263	-0.210	0.243	-0.154	0.366	0.177	0.315	0.024	0.881
CDK2	*Cdk2*	0.027	0.145	0.420	-0.176	0.315	0.068	0.709	-0.078	0.631
CDK4	*Cdk4*	-0.195	-0.021	0.904	0.111	0.508	-0.094	0.595	-0.288	0.068
CEBPA	*Cebpa*	-0.650	-0.363	0.155	-0.441	0.069	-0.512	0.046	-0.817	0.000
CGN	*Cgn*	-0.260	-0.382	0.041	-0.284	0.105	-0.443	0.018	-0.246	0.133
Chk2	*Chek2*	-0.238	0.188	0.623	0.426	0.234	0.330	0.386	-0.226	0.524
CK1δ	*Csnk1d*	0.154	-0.057	0.648	0.067	0.570	-0.100	0.426	0.148	0.179
CTNNγ	*Jup*	0.163	-0.203	0.247	0.307	0.062	0.136	0.433	0.171	0.266
CyclinG	*Ccng1*	-0.121	0.068	0.665	0.035	0.813	0.079	0.616	-0.107	0.447
CyclinK	*Ccnk*	0.409	-0.082	0.576	0.076	0.579	0.004	0.976	0.138	0.282
Cyclin D1	*Ccnd1*	0.103	0.588	0.224	1.520	0.001	1.324	0.006	0.226	0.601
Cyclin D2	*Ccnd2*	-	0.264	0.353	0.128	0.637	-	0.555	-	0.026

		0.259					0.170		0.571	
DLG1	*Dlg1*	-0.413	-0.076	0.588	-0.139	0.300	-0.238	0.093	-0.373	0.003
DNA-PK	*Prkdc*	-0.237	-0.157	0.479	-0.085	0.682	-0.346	0.126	-0.229	0.246
DRAM	*Dram1*	0.084	-0.729	0.187	0.178	0.718	0.064	0.903	-0.332	0.482
E-Cadherin	*Cdh1*	-0.251	0.025	0.945	0.151	0.656	-0.722	0.048	-0.405	0.200
E2F1	*E2f1*	-0.296	0.182	0.629	0.681	0.050	-0.128	0.741	-0.441	0.210
Elk-1	*Elk1*	-0.377	-0.063	0.808	-0.045	0.852	-0.388	0.142	-0.412	0.077
FAK	*Ptk2*	-0.093	0.133	0.357	0.032	0.819	-0.038	0.797	0.021	0.873
FAS	*Fas*	0.107	0.015	0.932	0.319	0.043	0.096	0.570	0.187	0.212
FASN	*Fasn*	-0.367	-1.511	0.008	-1.297	0.014	-0.592	0.280	-1.562	0.001
FST	*Fst*	-0.524	-1.391	0.008	-1.190	0.015	-1.540	0.004	-1.968	0.000
G6PC	*G6pc*	0.183	-0.646	0.195	-0.285	0.543	0.167	0.733	0.657	0.133
GPD1	*Gpd1*	-0.415	-0.191	0.434	-0.330	0.155	-0.473	0.055	-0.071	0.740
Gsk3β	*Gsk3b*	0.117	0.144	0.273	0.063	0.614	0.006	0.966	0.095	0.416
HDAC	*Hdac1*	-0.330	-0.097	0.537	-0.041	0.785	0.024	0.878	-0.379	0.007
HDAC9	*Hdac9*	-0.109	-0.090	0.845	0.113	0.790	0.030	0.948	-0.550	0.200
HIF1A	*Hif1a*	0.060	0.008	0.954	-0.089	0.502	-0.113	0.421	-0.054	0.661
HIPK2	*Hipk2*	0.317	0.359	0.141	-0.016	0.945	0.068	0.782	0.299	0.172
HMGN1	*Hmgn1*	0.202	-0.053	0.698	-0.013	0.920	0.185	0.170	0.029	0.810
HTT	*Htt*	-0.338	-0.107	0.582	-0.185	0.315	-0.267	0.174	-0.313	0.070
IGF2	*Igf2*	-0.067	0.383	0.800	7.505	0.000	0.764	0.613	0.486	0.720
IGFBP1	*Igfbp1*	0.377	0.089	0.878	1.118	0.042	0.318	0.581	1.199	0.022
ILK	*Ilk*	-0.121	0.016	0.904	-0.076	0.539	-0.169	0.197	-0.152	0.188
INSR	*Insr*	0.507	0.106	0.572	-0.076	0.670	0.153	0.414	0.245	0.141
JMY	*Jmy*	0.286	0.096	0.554	-0.006	0.968	-0.056	0.731	0.257	0.072
JNK1	*Mapk8*	0.392	0.183	0.239	0.051	0.730	0.211	0.173	0.312	0.023
LEPR	*Lepr*	0.686	0.201	0.680	0.594	0.199	1.115	0.021	1.526	0.001
MDM2	*Mdm2*	0.001	0.116	0.521	0.217	0.203	0.048	0.791	0.120	0.456
MDM4	*Mdm4*	0.309	0.298	0.281	0.279	0.289	0.337	0.222	0.311	0.207
MKK3	*Map2k3*	0.044	0.262	0.106	0.221	0.152	0.193	0.233	-0.038	0.792
MLXIPL	*Mlxipl*	-0.493	-0.236	0.412	-0.743	0.007	-0.638	0.028	-0.520	0.040
Mup20	*Mup20*	-0.884	-1.845	0.255	-6.244	0.001	-6.679	0.001	-7.905	0.000
NFE2L2	*Nfe2l2*	-0.139	-0.035	0.828	-0.105	0.491	-0.146	0.365	-0.057	0.687

NR1I2	*Nr1i2*	0.805	0.306	0.204	0.498	0.030	0.782	0.001	0.783	0.000
NR2C2	*Nr2c2*	0.443	0.051	0.775	-0.013	0.937	0.082	0.641	0.216	0.166
NRF1	*Nrf1*	-0.120	-0.128	0.471	-0.168	0.317	-0.152	0.394	-0.087	0.581
OCLN	*Ocln*	0.248	-0.402	0.104	-0.181	0.434	-0.173	0.478	0.224	0.295
p130CAS	*Bcar1*	-0.613	-0.188	0.434	-0.271	0.235	-0.570	0.020	-0.893	0.000
p21Cip1	*Cdkn1a*	0.055	0.775	0.288	1.702	0.016	-0.253	0.736	1.225	0.066
p300	*Ep300*	0.476	0.129	0.501	0.097	0.593	0.087	0.650	0.432	0.011
p38 MAPK	*Mapk14*	0.614	0.219	0.157	0.243	0.099	0.306	0.048	0.436	0.002
p48	*St13*	-0.267	-0.042	0.777	-0.071	0.614	-0.130	0.384	-0.103	0.432
p53	*Trp53*	-0.159	0.136	0.551	0.326	0.131	-0.272	0.245	-0.076	0.711
p53R2	*Rrm2b*	0.386	0.497	0.054	0.215	0.390	0.496	0.055	0.556	0.016
PAI-1	*Serpine2*	-0.614	-0.181	0.579	-0.932	0.003	-1.420	0.000	-0.789	0.007
PALS2	*Mpp6*	0.277	0.094	0.606	-0.002	0.991	0.192	0.289	0.221	0.169
PCAF	*Kat2b*	0.424	0.184	0.354	-0.120	0.527	0.198	0.319	0.240	0.174
PCK1	*Pck1*	0.677	0.004	0.990	0.424	0.199	0.514	0.137	0.943	0.003
PCNA	*Pcna*	0.228	0.037	0.808	0.208	0.143	0.245	0.102	0.207	0.122
PDK1	*Pdpk1*	0.279	0.092	0.564	0.054	0.723	-0.018	0.910	0.220	0.120
PERP	*Perp*	0.317	-0.055	0.761	-0.129	0.450	0.106	0.551	0.236	0.136
PIAS1	*Pias1*	0.270	-0.171	0.269	-0.129	0.375	-0.044	0.774	0.151	0.259
PILT	*Tjap1*	-0.084	0.299	0.309	0.358	0.197	-0.289	0.352	0.097	0.715
PML	*Pml*	-0.243	-0.181	0.390	-0.134	0.500	-0.160	0.448	-0.263	0.157
PPARA	*Ppara*	0.257	-0.004	0.987	-0.055	0.811	0.114	0.637	-0.037	0.864
PPARG	*Pparg*	-0.012	0.249	0.483	0.534	0.113	0.024	0.947	-0.111	0.729
PPARGC1A	*Ppargc1a*	0.806	-0.172	0.624	0.249	0.452	0.623	0.071	1.064	0.001
PTEN	*Pten*	0.131	0.001	0.995	-0.097	0.595	0.069	0.717	0.041	0.807
PUMA	*Bbc3*	-0.311	-0.894	0.013	-0.599	0.071	-0.364	0.293	-0.659	0.033
PXN	*Pxn*	0.248	-0.126	0.367	0.059	0.652	-0.112	0.424	0.054	0.661
Rac	*Rac1*	-0.077	-0.032	0.801	-0.003	0.981	-0.037	0.773	-0.059	0.604
Rb	*Rb1*	-0.315	0.052	0.757	0.338	0.039	-0.251	0.146	-0.217	0.153
RORA	*Rora*	0.240	0.063	0.759	-0.141	0.470	0.063	0.758	-0.054	0.768
RORC	*Rorc*	0.817	0.610	0.053	0.696	0.021	1.162	0.000	1.088	0.000
SCD	*Scd1*	-0.123	-0.561	0.125	-0.670	0.053	-0.278	0.444	-0.438	0.169
SCO2	*Sco2*	0.082	-	0.714	0.026	0.942	0.427	0.251	0.310	0.354

			0.142							
SEPP1	*Sepp1*	0.386	0.167	0.376	0.116	0.521	0.284	0.133	0.247	0.141
SIRT	*Sirt1*	0.214	0.016	0.938	0.066	0.732	-0.119	0.560	0.299	0.092
Slug	*Snai2*	0.429	-0.004	0.988	0.037	0.889	0.139	0.617	0.319	0.194
SMARCB1	*Smarcb1*	-0.320	-0.075	0.759	0.152	0.507	-0.226	0.358	-0.477	0.029
STAG1	*Stag1*	0.180	0.023	0.880	-0.157	0.274	0.048	0.750	0.153	0.247
STAT3	*Stat3*	0.227	-0.364	0.151	0.348	0.142	0.043	0.862	0.271	0.223
Survivin	*Birc5*	-0.039	0.321	0.580	1.432	0.008	-0.403	0.507	0.053	0.920
SYMPK	*Sympk*	0.080	-0.071	0.652	0.061	0.681	-0.018	0.910	0.115	0.408
Teap	*Trp53inp1*	0.171	0.270	0.336	0.427	0.110	0.359	0.200	0.659	0.009
TGF-β	*Tgfb3*	-0.224	0.037	0.953	0.029	0.961	-0.691	0.296	-1.709	0.004
TGFBR3	*Tgfbr3*	0.436	0.114	0.564	-0.108	0.570	0.104	0.600	0.170	0.332
THRA	*Thra*	0.214	0.118	0.561	0.259	0.173	0.088	0.664	0.215	0.230
TNFR	*Tnfrsf1a*	-0.049	-0.297	0.103	0.063	0.712	-0.135	0.458	-0.168	0.293
TOPBP1	*Topbp1*	0.303	-0.238	0.201	0.137	0.424	0.097	0.592	0.133	0.406
TRAP220	*Med1*	0.350	0.083	0.572	0.036	0.798	-0.017	0.907	0.153	0.241
TSP1	*Thbs1*	-0.121	-0.291	0.683	0.505	0.447	-0.995	0.176	-1.492	0.021
VINCULIN	*Vcl*	-0.378	-0.070	0.692	-0.189	0.265	-0.408	0.024	-0.476	0.003
WASP	*Was*	-0.118	-0.151	0.704	0.245	0.503	-0.322	0.426	-0.585	0.107
WT1	*Wt1*	-0.140	0.136	0.846	0.389	0.555	-0.419	0.559	-1.344	0.040
ZAC1	*Plagl1*	-0.209	0.437	0.499	0.368	0.551	-0.597	0.377	-0.771	0.194
ZO2	*Tjp2*	-0.264	-0.261	0.199	-0.102	0.593	-0.227	0.264	-0.433	0.016
ZO3	*Tjp3*	-0.613	-0.435	0.112	-0.557	0.032	-0.795	0.004	-0.734	0.002

Table S7. Expression levels of genes involved in cancer signaling pathway correlated with the increase in calorie restriction (CR) and their gene expression at each level of CR relative to 12h ad libitum intake.

			10CR		20CR		30CR		40CR	
Symbol	**Gene Symbol**	**r**	**logFC**	**p**	**logFC**	**p**	**logFC**	**p**	**logFC**	**p**
APAF1	*Apaf1*	0.020	0.141	0.693	0.775	0.018	0.373	0.290	0.037	0.908
APC	*Apc*	0.413	0.334	0.112	0.247	0.219	0.332	0.115	0.452	0.016
ASK1	*Map3k5*	0.525	0.195	0.382	0.019	0.928	0.152	0.494	0.294	0.137
ATM	*Atm*	0.005	0.105	0.576	-0.050	0.780	0.011	0.954	-0.078	0.646
ATR	*Atr*	0.422	0.237	0.206	0.302	0.089	0.340	0.068	0.422	0.011
AXIN	*Axin1*	0.117	-0.146	0.373	-0.029	0.851	-0.154	0.349	0.088	0.540
B-RAF	*Braf*	0.417	-0.058	0.768	-0.284	0.132	0.114	0.560	0.303	0.080

BAD	*Bad*	0.476	-0.024	0.925	0.089	0.711	0.240	0.339	0.415	0.062
BAK	*Bak1*	-0.276	0.001	0.996	0.172	0.541	-0.274	0.363	-0.446	0.093
BAX	*Bax*	-0.138	-0.095	0.696	0.118	0.604	-0.205	0.403	-0.219	0.312
BCL2	*Bcl2*	-0.221	0.665	0.077	0.396	0.274	-0.449	0.265	-0.401	0.256
BclXL	*Bcl2l1*	-0.005	0.134	0.473	0.224	0.205	-0.077	0.684	0.065	0.695
BIM	*Bcl2l11*	0.546	0.078	0.774	0.328	0.199	0.371	0.167	0.574	0.016
BMPR2	*Bmpr2*	0.334	0.618	0.038	0.610	0.032	0.562	0.060	0.606	0.024
BRCA1	*Brca1*	0.463	0.008	0.985	0.734	0.055	0.903	0.024	1.072	0.003
c-Fos	*Fos*	0.121	-1.152	0.104	0.271	0.656	-0.193	0.770	0.217	0.705
c-Jun	*Jun*	-0.025	-0.027	0.943	0.834	0.017	-0.052	0.891	-0.014	0.966
c-RAF	*Raf1*	-0.299	-0.165	0.253	-0.215	0.116	-0.278	0.055	-0.247	0.052
C3G	*Rapgef1*	0.321	0.178	0.169	0.258	0.036	0.109	0.400	0.215	0.062
Caspase9	*Casp9*	-0.257	-0.279	0.109	-0.157	0.336	-0.164	0.344	-0.471	0.002
CBL	*Cbl*	0.217	-0.226	0.512	0.034	0.916	0.044	0.897	0.089	0.766
CBP	*Crebbp*	0.395	0.196	0.375	0.185	0.379	0.138	0.533	0.399	0.042
CCND1	*Ccnd1*	0.103	0.588	0.224	1.520	0.001	1.324	0.006	0.226	0.601
CDHE	*Cdh1*	-0.251	0.025	0.945	0.151	0.656	-0.722	0.048	-0.405	0.200
CDK2	*Cdk2*	0.027	0.145	0.420	-0.176	0.315	0.068	0.709	-0.078	0.631
CHK2	*Chek2*	-0.238	0.188	0.623	0.426	0.234	0.330	0.386	-0.226	0.524
CRK	*Crk*	0.303	0.242	0.138	0.011	0.943	0.190	0.245	0.274	0.060
CTNNβ	*Ctnnb1*	-0.363	-0.100	0.550	-0.083	0.601	-0.220	0.190	-0.268	0.069
CTNNδ	*Ctnnd1*	-0.070	-0.185	0.187	-0.089	0.502	-0.154	0.274	-0.124	0.314
DAXX	*Daxx*	-0.147	-0.233	0.212	-0.204	0.247	-0.389	0.040	-0.237	0.152
DNAPK	*Prkdc*	-0.237	-0.157	0.479	-0.085	0.682	-0.346	0.126	-0.229	0.246
DSH	*Dvl1*	0.490	-0.054	0.744	0.094	0.547	0.168	0.306	0.288	0.047
ELK-1	*Elk1*	-0.377	-0.063	0.808	0.045	0.852	-0.388	0.142	-0.412	0.077
EPAC1	*Rapgef3*	-0.192	0.200	0.525	0.094	0.754	-0.223	0.498	-0.083	0.774
FADD	*Fadd*	-0.480	-0.293	0.095	-0.301	0.070	-0.415	0.019	-0.565	0.000
FAK	*Ptk2*	-0.093	0.133	0.357	0.032	0.819	-0.038	0.797	0.021	0.873
FAS	*Fas*	0.107	0.015	0.932	0.319	0.043	0.096	0.570	0.187	0.212
FLIP	*Cflar*	0.329	0.243	0.163	0.046	0.782	0.211	0.225	0.278	0.072
FOXO1	*Foxo1*	0.603	0.236	0.302	0.322	0.139	0.382	0.094	0.681	0.001
FYN	*Fyn*	-0.297	0.002	0.993	0.118	0.519	0.012	0.953	-0.240	0.171
GRB2	*Grb2*	-0.346	-0.098	0.434	0.003	0.982	-0.104	0.405	-0.123	0.266
GSK3β	*Gsk3b*	0.117	0.144	0.273	0.063	0.614	0.006	0.966	0.095	0.416
HAT1	*Hat1*	-0.099	0.082	0.702	0.107	0.596	0.106	0.620	-0.017	0.929
HIF1α	*Hif1a*	0.060	0.008	0.954	-0.089	0.502	-0.113	0.421	-0.054	0.661
HIPK2	*Hipk2*	0.317	0.359	0.141	-0.016	0.945	0.068	0.782	0.299	0.172
IRS1	*Irs1*	0.120	-0.229	0.408	-0.191	0.466	-0.129	0.639	0.412	0.089
MAX	*Max*	-0.149	0.166	0.250	0.098	0.476	-0.038	0.795	-0.022	0.866
MDM2	*Mdm2*	0.001	0.116	0.521	0.217	0.203	0.048	0.791	0.120	0.456
MIZ1	*Zbtb17*	-0.167	-0.035	0.846	-0.020	0.907	-0.122	0.500	-0.181	0.262
MYC	*Myc*	-0.042	0.872	0.151	0.459	0.431	0.226	0.713	-0.618	0.261
NBS1	*Nbn*	0.141	0.014	0.925	-0.089	0.534	-0.079	0.604	0.024	0.857
NCSTN	*Ncstn*	0.043	-0.233	0.123	0.029	0.840	-0.005	0.972	-0.009	0.944
NF1	*Nf1*	0.031	0.026	0.875	-0.134	0.388	-0.085	0.603	0.005	0.972
NICD	*Notch1*	0.150	-0.173	0.398	0.081	0.675	0.095	0.640	0.226	0.207
NLK	*Nlk*	-0.352	0.120	0.533	-0.227	0.224	-0.041	0.834	-0.212	0.226
p18INK4C	*Cdkn2c*	0.118	0.474	0.161	0.528	0.101	0.653	0.052	0.545	0.073
p21CIP1	*Cdkn1a*	0.055	0.775	0.288	1.702	0.016	-0.253	0.736	1.225	0.066
p27KIP1	*Cdkn1b*	-0.152	0.054	0.745	-0.047	0.766	-0.197	0.243	-0.047	0.748
p300	*Ep300*	0.476	0.129	0.501	0.097	0.593	0.087	0.650	0.432	0.011
p53	*Trp53*	-0.159	0.136	0.551	0.326	0.131	-0.272	0.245	-0.076	0.711

PTCH	*Ptch1*	0.204	-0.103	0.684	-0.136	0.572	-0.397	0.125	0.184	0.410
PUMA	*Bbc3*	-0.311	-0.894	0.013	-0.599	0.071	-0.364	0.293	-0.659	0.033
RalGAP	*Ralbp1*	-0.357	0.061	0.689	0.004	0.980	-0.136	0.373	-0.318	0.019
RALGEF	*Ralgds*	-0.171	0.225	0.595	0.514	0.198	0.222	0.602	-0.368	0.345
RASGAP	*Rasa1*	0.001	0.057	0.695	-0.090	0.516	-0.034	0.818	-0.048	0.710
RASGRP	*Rasgrp1*	-0.187	-0.031	0.932	0.175	0.608	0.029	0.936	-0.592	0.077
Rb	*Rb1*	-0.315	0.052	0.757	-0.338	0.039	-0.251	0.146	-0.217	0.153
RBL1	*Rbl1*	-0.021	0.645	0.161	0.934	0.032	0.086	0.858	-0.011	0.980
RBPJK	*Rbpj*	-0.100	0.052	0.722	-0.083	0.554	-0.033	0.825	-0.110	0.402
SHC	*Shc1*	-0.180	-0.091	0.512	0.026	0.845	-0.072	0.607	-0.258	0.036
SHP2	*Ptpn11*	0.124	0.155	0.295	0.114	0.418	0.045	0.764	0.179	0.173
SMAC	*Diablo*	-0.164	-0.006	0.968	0.107	0.482	-0.172	0.298	-0.090	0.533
SMAD4	*Smad4*	0.360	0.133	0.407	-0.007	0.962	0.110	0.493	0.229	0.106
SMAD6	*Smad6*	0.041	-0.118	0.627	0.074	0.744	-0.081	0.740	-0.183	0.399
SMAD7	*Smad7*	0.052	0.229	0.338	0.123	0.588	0.431	0.069	-0.247	0.254
SMO	*Smo*	-0.431	-0.320	0.397	-0.254	0.477	-0.951	0.015	-1.234	0.000
SRC	*Src*	-0.082	0.633	0.301	1.359	0.020	-0.224	0.724	0.037	0.947
STK6	*Aurka*	-0.053	-0.194	0.695	0.913	0.040	-0.333	0.507	0.189	0.661
SUFU	*Sufu*	0.011	-0.010	0.978	0.343	0.298	0.214	0.547	0.094	0.768
TAB1	*Tab2*	0.270	-0.086	0.639	-0.147	0.397	-0.244	0.183	0.322	0.046
tBID	*Bid*	-0.364	-0.040	0.835	-0.201	0.275	-0.184	0.345	-0.408	0.019
TGFβR1	*Tgfbr1*	0.221	0.328	0.077	0.288	0.103	0.280	0.132	0.358	0.031
TGFβR2	*Tgfbr2*	0.066	0.076	0.665	0.151	0.363	0.055	0.755	0.032	0.835
WNT5A	*Wnt5a*	0.004	0.322	0.584	0.458	0.413	-0.300	0.628	-0.209	0.700

Table S8. Expression levels of genes involved in autophagy pathway correlated with the increase in calorie restriction (CR) and their gene expression at each level of CR relative to 12h ad libitum intake.

			10CR		**20CR**		**30CR**		**40CR**	
Symbol	**Gene Symbol**	**r**	**logFC**	**p**	**logFC**	**p**	**logFC**	**p**	**logFC**	**p**
ATG10	*Atg10*	-0.125	0.083	0.725	-0.177	0.441	0.043	0.856	-0.163	0.448
ATG12	*Atg12*	-0.095	0.089	0.566	0.096	0.513	-0.052	0.738	-0.007	0.960
ATG13	*Atg13*	-0.003	-0.132	0.372	-0.241	0.088	-0.143	0.335	-0.097	0.458
ATG16L1	*Atg16l1*	0.651	0.036	0.842	0.033	0.848	0.144	0.427	0.466	0.004
ATG3	*Atg3*	0.411	0.006	0.972	-0.094	0.553	0.188	0.256	0.160	0.278
ATG5	*Atg5*	0.319	0.052	0.731	0.087	0.546	0.167	0.269	0.163	0.226
ATG7	*Atg7*	-0.403	-0.189	0.229	-0.108	0.465	-0.277	0.080	-0.358	0.010
BCL2	*Bcl2*	-0.221	0.665	0.077	0.396	0.274	-0.449	0.265	-0.401	0.256
BECN1	*Becn1*	-0.366	0.115	0.361	-0.052	0.665	-0.123	0.333	-0.024	0.831
FIP200	*Rb1cc1*	0.399	0.184	0.299	0.049	0.773	0.171	0.335	0.273	0.083
LAMP1	*Lamp1*	-0.301	-0.006	0.973	0.007	0.963	-0.116	0.472	-0.100	0.478
LAMP2	*Lamp2*	-0.611	-0.130	0.494	-0.260	0.152	-0.272	0.155	-0.192	0.253
LC3-II	*Map1lc3a*	0.450	-0.003	0.986	0.106	0.572	0.183	0.353	0.497	0.004
LC3-II	*Map1lc3b*	0.486	-0.009	0.956	0.133	0.369	0.109	0.485	0.238	0.085
mTOR	*Mtor*	-0.119	0.060	0.704	0.159	0.289	0.043	0.787	-0.122	0.384
NBR1	*Nbr1*	0.080	-0.032	0.843	-0.176	0.249	-0.051	0.752	-0.015	0.915
SQSTM1	*Sqstm1*	-0.287	0.000	0.999	0.200	0.481	-0.483	0.110	-0.475	0.072
STX17	*Stx17*	0.403	0.117	0.464	-0.034	0.824	0.199	0.210	0.160	0.257
ULK1	*Ulk1*	-0.040	-0.384	0.029	-0.214	0.197	-0.290	0.098	-0.103	0.504
WDFY3	*Wdfy3*	0.471	0.120	0.531	0.106	0.561	0.198	0.302	0.309	0.070
WIPI1	*Wipi1*	0.054	-0.500	0.019	-0.287	0.148	-0.371	0.079	-0.174	0.344

Table S9. Expression levels of genes involved in fuel utilization correlated with the increase in calorie restriction (CR) and their gene expression at each level of CR relative to 12h ad libitum intake.

			10CR		20CR		30CR		40CR	
Symbol	**Gene Symbol**	**r**	**logFC**	**p**	**logFC**	**p**	**logFC**	**p**	**logFC**	**p**
ABAD	*Hsd17b10*	0.523	-0.002	0.991	-0.016	0.930	0.165	0.382	0.322	0.055
ACAA1	*Acaa1a*	0.364	0.098	0.609	0.178	0.323	0.286	0.129	0.158	0.346
Acaa1b	*Acaa1b*	0.340	0.334	0.329	0.184	0.574	0.655	0.055	0.551	0.072
ACAA2	*Acaa2*	0.309	0.054	0.780	-0.024	0.896	0.132	0.493	0.205	0.230
ACADM	*Acadm*	0.561	0.138	0.510	0.243	0.222	0.384	0.065	0.601	0.001
ACO1	*Aco1*	0.057	-0.037	0.829	-0.085	0.606	-0.056	0.746	-0.013	0.932
ACO2	*Aco2*	0.698	0.123	0.600	0.349	0.117	0.513	0.028	0.652	0.002
ACSL1	*Acsl1*	0.247	0.390	0.179	-0.073	0.794	0.234	0.422	0.143	0.581
ACSL3	*Acsl3*	0.024	-0.361	0.132	-0.082	0.715	0.088	0.711	-0.402	0.056
ACSL4	*Acsl4*	-0.161	0.140	0.550	0.298	0.179	0.062	0.792	-0.162	0.434
ACSL5	*Acsl5*	-0.021	-0.622	0.011	-0.484	0.035	-0.320	0.185	-0.242	0.254
ADRB3	*Adrb3*	-0.524	-0.341	0.498	-1.337	0.007	-0.883	0.087	-1.689	0.000
AIF	*Aifm1*	0.086	-0.143	0.341	-0.080	0.574	-0.018	0.902	0.062	0.640
ALDOA	*Aldoa*	0.291	-0.060	0.753	0.237	0.191	0.093	0.625	0.226	0.181
ALDOB	*Aldob*	0.504	-0.169	0.509	-0.091	0.705	0.174	0.494	0.452	0.046
ALDOC	*Aldoc*	0.152	-0.490	0.215	0.132	0.721	0.167	0.665	-0.176	0.608
APP	*App*	-0.016	0.306	0.340	0.670	0.028	0.244	0.448	0.269	0.347
ATP5A1	*Atp5a1*	0.575	-0.066	0.715	-0.075	0.660	0.141	0.431	0.222	0.163
ATP5B	*Atp5b*	0.608	0.007	0.968	0.061	0.725	0.211	0.244	0.352	0.029
ATP5C1	*Atp5c1*	0.683	0.085	0.650	0.090	0.615	0.302	0.106	0.362	0.030
ATP5D	*Atp5d*	0.348	-0.031	0.846	0.056	0.708	0.065	0.679	0.176	0.205
ATP5F1	*Atp5f1*	0.662	0.036	0.831	0.033	0.838	0.280	0.099	0.316	0.037
ATP5G3	*Atp5g3*	0.520	0.163	0.313	0.005	0.972	0.301	0.061	0.313	0.029
ATP5H	*Atp5h*	0.687	-0.067	0.717	-0.014	0.937	0.266	0.149	0.381	0.020
ATP5J	*Atp5j*	0.267	0.038	0.814	-0.120	0.436	0.138	0.393	0.099	0.489
ATP5J2	*Atp5j2*	0.360	0.175	0.317	-0.007	0.966	0.267	0.125	0.255	0.100
AUH	*Auh*	0.032	0.079	0.611	-0.119	0.422	0.004	0.978	0.001	0.995
BCL2	*Bcl2*	-0.221	0.665	0.077	0.396	0.274	-0.449	0.265	-0.401	0.256
BECN1	*Becn1*	-0.366	0.115	0.361	-0.052	0.665	-0.123	0.333	-0.024	0.831
BPGM	*Bpgm*	-0.142	-0.084	0.666	0.123	0.500	-0.226	0.251	0.207	0.226
CAMK4	*Camk4*	0.023	0.409	0.340	0.055	0.896	-0.389	0.397	0.076	0.845
Caspase 3	*Casp3*	-0.315	-0.439	0.038	-0.312	0.115	-0.059	0.774	-0.472	0.011
Caspase 8	*Casp8*	0.075	0.093	0.508	0.039	0.770	0.047	0.737	-0.072	0.568
Caspase 9	*Casp9*	-0.257	-0.279	0.109	-0.157	0.336	-0.164	0.344	-0.471	0.002
CAT	*Cat*	-0.805	-0.091	0.700	-0.470	0.039	-0.487	0.043	-0.668	0.001
CHUK	*Chuk*	0.065	0.152	0.458	-0.183	0.349	0.035	0.865	-0.021	0.908
COX4I1	*Cox4i1*	0.429	-0.070	0.693	0.002	0.993	0.155	0.381	0.202	0.199
COX5A	*Cox5a*	0.576	-0.010	0.952	-0.054	0.740	0.230	0.176	0.293	0.053

COX6A1	*Cox6a1*	0.406	0.082	0.596	-0.055	0.706	0.049	0.752	0.205	0.135
COX6B1	*Cox6b1*	0.367	0.100	0.548	-0.003	0.987	0.158	0.344	0.229	0.122
COX7A1	*Cox7a1*	0.820	0.405	0.386	0.721	0.099	1.188	0.008	1.585	0.000
COX7A2	*Cox7a2*	-0.035	0.050	0.751	-0.173	0.300	-0.024	0.893	-0.017	0.911
COX7B	*Cox7b*	0.545	0.179	0.410	-0.066	0.752	0.400	0.065	0.404	0.037
COX8A	*Cox8a*	0.627	0.119	0.465	-0.027	0.863	0.247	0.130	0.298	0.040
CRTC3	*Crtc3*	-0.027	-0.254	0.137	-0.181	0.258	-0.286	0.096	-0.041	0.780
CS	*Cs*	-0.012	-0.604	0.005	-0.502	0.014	-0.238	0.266	-0.259	0.170
DHOH	*Dhodh*	-0.254	-0.337	0.151	0.007	0.972	-0.111	0.627	-0.262	0.204
DHTKD1	*Dhtkd1*	0.515	0.213	0.316	0.040	0.842	0.355	0.094	0.333	0.078
DJ - 1	*Park7*	0.310	0.002	0.986	-0.045	0.741	0.115	0.416	0.181	0.149
DLD	*Dld*	0.453	0.035	0.817	-0.081	0.570	0.093	0.534	0.243	0.067
DLST	*Dlst*	0.479	0.107	0.519	0.124	0.433	0.242	0.144	0.311	0.035
ECHS1	*Echs1*	0.632	-0.040	0.833	-0.011	0.950	0.319	0.092	0.289	0.086
ECI1	*Eci1*	0.315	0.098	0.596	0.029	0.870	0.364	0.048	0.136	0.408
ECI2	*Eci2*	0.519	0.378	0.164	0.191	0.461	0.501	0.065	0.425	0.080
EHHADH	*Ehhadh*	0.721	0.463	0.318	1.047	0.019	1.570	0.001	1.803	0.000
ENO1	*Eno1*	0.524	-0.496	0.113	-0.147	0.615	0.086	0.778	0.433	0.108
ENO3	*Eno3*	0.077	0.256	0.361	-0.183	0.507	-0.074	0.798	-0.012	0.962
FBP1	*Fbp1*	0.117	-0.036	0.851	-0.076	0.681	0.079	0.682	0.065	0.702
FH	*Fh1*	0.161	-0.215	0.233	-0.012	0.946	-0.067	0.709	0.071	0.653
FIS1	*Fis1*	0.128	-0.052	0.752	0.094	0.545	0.045	0.784	0.071	0.624
FURIN	*Furin*	0.598	-0.163	0.353	-0.128	0.441	-0.020	0.908	0.205	0.186
GAPDH	*Gapdh*	0.360	-0.139	0.484	-0.112	0.552	-0.076	0.701	0.262	0.134
GNAS	*Gnas*	-0.311	0.014	0.928	-0.036	0.811	-0.116	0.459	-0.069	0.620
GPD2	*Gpd2*	0.235	-0.267	0.329	-0.510	0.050	-0.056	0.837	0.147	0.541
GPI	*Gpi1*	0.571	-0.176	0.505	0.023	0.926	0.187	0.474	0.625	0.007
GPX4	*Gpx4*	0.057	0.208	0.384	0.575	0.011	0.274	0.251	0.284	0.182
GPX7	*Gpx7*	0.074	0.809	0.208	1.710	0.005	0.803	0.215	0.573	0.329
GRX2	*Glrx2*	0.014	0.050	0.737	-0.113	0.423	0.041	0.784	0.070	0.592
GSR	*Gsr*	-0.153	0.054	0.710	0.121	0.376	-0.187	0.198	-0.034	0.788
HADH	*Hadh*	0.620	0.147	0.475	0.343	0.080	0.565	0.006	0.511	0.005
HADHA	*Hadha*	0.377	0.038	0.833	0.067	0.693	0.044	0.805	0.178	0.262
HSD17B10	*Hsd17b10*	0.523	-0.002	0.991	-0.016	0.930	0.165	0.382	0.322	0.055
HSD17B4	*Hsd17b4*	0.149	-0.001	0.997	-0.060	0.723	0.055	0.758	0.166	0.295
HSD17B8	*H2-Ke6*	-0.084	-0.332	0.043	-0.167	0.281	-0.228	0.163	-0.099	0.489
HtrA2	*Htra2*	0.193	-0.097	0.668	0.174	0.408	0.151	0.497	-0.007	0.970
HTT	*Htt*	-0.338	-0.107	0.582	-0.185	0.315	-0.267	0.174	-0.313	0.070
IDH3A	*Idh3a*	0.806	0.181	0.412	0.233	0.266	0.541	0.013	0.850	0.000
IDH3B	*Idh3b*	0.631	0.148	0.324	0.073	0.611	0.256	0.088	0.300	0.024
IDH3G	*Idh3g*	0.371	0.054	0.668	-0.030	0.805	0.104	0.413	0.178	0.113
IL15	*Il15*	0.392	0.490	0.203	0.285	0.446	0.576	0.133	0.482	0.165
IVD	*Ivd*	0.083	0.075	0.626	0.006	0.969	0.091	0.551	0.057	0.675
KGDH	*Ogdh*	0.350	-0.016	0.923	0.030	0.849	0.021	0.900	0.117	0.428
LETM1	*Letm1*	-0.130	-0.091	0.533	-0.139	0.315	-0.284	0.054	0.067	0.603

LRRK2	*Lrrk2*	0.014	0.417	0.191	0.147	0.636	0.226	0.488	-0.107	0.721
MAOA	*Maoa*	0.678	0.006	0.974	0.224	0.203	0.559	0.002	0.559	0.001
MAOB	*Maob*	0.756	0.141	0.522	0.283	0.177	0.603	0.006	0.680	0.001
MDH1	*Mdh1*	0.205	-0.074	0.681	-0.112	0.514	0.035	0.848	0.028	0.862
MDH2	*Mdh2*	0.482	-0.093	0.652	0.258	0.185	0.204	0.320	0.518	0.005
ME1	*Me1*	0.029	-0.743	0.073	-0.928	0.018	-0.228	0.577	-0.288	0.423
ME2	*Me2*	-0.006	0.269	0.424	0.461	0.146	0.228	0.502	-0.076	0.803
MIRO2	*Rhot2*	0.348	0.116	0.416	0.148	0.274	0.171	0.231	0.300	0.018
MKK4	*Map2k4*	0.197	0.077	0.479	0.047	0.645	0.102	0.344	0.109	0.258
mtSOD	*Sod2*	0.568	0.162	0.327	0.034	0.827	0.255	0.122	0.320	0.029
NCT	*Ncstn*	0.043	-0.233	0.123	0.029	0.840	-0.005	0.972	-0.009	0.944
NDUFA1	*Ndufa11*	0.343	-0.008	0.966	-0.061	0.720	0.043	0.813	0.309	0.052
NDUFA10	*Ndufa10*	0.380	-0.059	0.689	-0.060	0.667	0.067	0.650	0.178	0.171
NDUFA12	*Ndufa12*	0.621	0.163	0.382	-0.044	0.803	0.238	0.199	0.529	0.001
NDUFA13	*Ndufa13*	-0.200	-0.008	0.956	-0.104	0.471	-0.102	0.503	-0.041	0.761
NDUFA2	*Ndufa2*	0.152	0.046	0.808	-0.218	0.231	0.171	0.363	0.176	0.293
NDUFA3	*Ndufa3*	0.193	0.062	0.725	-0.118	0.487	0.091	0.609	0.205	0.192
NDUFA4	*Ndufa4*	0.235	0.008	0.967	-0.215	0.256	0.023	0.906	0.173	0.326
NDUFA5	*Ndufa5*	0.543	0.156	0.443	-0.052	0.790	0.459	0.022	0.396	0.027
NDUFA6	*Ndufa6*	0.263	0.007	0.975	-0.353	0.084	0.022	0.917	0.174	0.357
NDUFA7	*Ndufa7*	0.634	0.083	0.645	0.182	0.286	0.388	0.029	0.509	0.001
NDUFA8	*Ndufa8*	0.619	-0.072	0.665	0.003	0.986	0.108	0.514	0.355	0.016
NDUFA9	*Ndufa9*	0.506	-0.136	0.385	-0.142	0.340	0.097	0.535	0.240	0.082
NDUFAF1	*Ndufaf1*	-0.610	-0.265	0.184	-0.352	0.064	-0.390	0.053	-0.460	0.009
NDUFB10	*Ndufb10*	0.543	-0.001	0.995	0.011	0.939	0.205	0.185	0.300	0.029
NDUFB11	*Ndufb11*	0.296	-0.105	0.560	-0.182	0.289	0.071	0.694	0.170	0.287
NDUFB2	*Ndufb2*	0.001	0.182	0.328	0.054	0.759	0.065	0.728	0.111	0.503
NDUFB3	*Ndufb3*	0.139	0.030	0.867	-0.329	0.059	0.021	0.906	-0.005	0.975
NDUFB4	*Ndufb4*	0.336	0.126	0.486	0.133	0.437	0.234	0.194	0.306	0.056
NDUFB5	*Ndufb5*	0.524	0.028	0.859	-0.107	0.474	0.202	0.194	0.242	0.080
NDUFB6	*Ndufb6*	0.463	-0.075	0.683	-0.129	0.460	0.235	0.195	0.313	0.053
NDUFB7	*Ndufb7*	0.210	-0.112	0.460	-0.112	0.436	0.094	0.533	0.100	0.454
NDUFB8	*Ndufb8*	0.569	0.000	0.998	-0.160	0.404	0.328	0.102	0.320	0.074
NDUFB9	*Ndufb9*	0.534	0.048	0.799	0.000	0.999	0.231	0.216	0.264	0.112
NDUFS1	*Ndufs1*	0.478	-0.006	0.967	-0.111	0.427	0.180	0.219	0.164	0.208
NDUFS2	*Ndufs2*	0.625	0.013	0.932	0.036	0.798	0.119	0.423	0.305	0.021
NDUFS4	*Ndufs4*	0.355	-0.007	0.966	-0.166	0.300	0.263	0.113	0.105	0.477
NDUFS6	*Ndufs6*	-0.050	0.121	0.547	-0.091	0.555	0.001	0.994	0.065	0.648
NDUFS7	*Ndufs7*	0.219	-0.141	0.391	-0.140	0.371	-0.018	0.914	0.065	0.652
NDUFS8	*Ndufs8*	0.027	-0.019	0.899	0.063	0.651	0.065	0.654	-0.011	0.935
NDUFV1	*Ndufv1*	0.572	-0.139	0.404	-0.064	0.686	0.002	0.988	0.280	0.057
NDUFV2	*Ndufv2*	0.592	0.097	0.572	0.012	0.942	0.273	0.112	0.405	0.008
NDUFV3	*Ndufv3*	0.374	0.102	0.491	0.025	0.858	0.089	0.548	0.223	0.088
NOS3	*Nos3*	-0.093	-0.404	0.219	0.012	0.968	-0.140	0.663	-0.345	0.232
NR1D1	*Nr1d1*	-0.724	-0.966	0.028	-1.327	0.002	-1.619	0.000	-1.734	0.000

OGDH	*Ogdh*	0.350	-0.016	0.923	0.030	0.849	0.021	0.900	0.117	0.428
Parkin	*Park2*	0.012	0.161	0.636	-0.111	0.734	0.515	0.121	-0.210	0.496
PDHA	*Pdha1*	0.650	0.140	0.497	-0.122	0.533	0.296	0.148	0.367	0.045
PFKL	*Pfkl*	-0.327	-0.080	0.672	0.056	0.753	-0.087	0.648	-0.128	0.448
PFKM	*Pfkm*	0.407	-0.325	0.099	-0.114	0.536	0.205	0.282	-0.001	0.993
PFKP	*Pfkp*	0.187	0.393	0.179	0.529	0.057	0.238	0.419	0.323	0.217
PGAM1	*Pgam1*	0.383	0.018	0.911	0.009	0.953	0.039	0.803	0.328	0.018
PGK1	*Pgk1*	0.756	-0.019	0.925	0.161	0.407	0.353	0.083	0.616	0.001
PINK1	*Pink1*	0.640	-0.059	0.736	0.072	0.663	0.211	0.224	0.305	0.049
PKLR	*Pklr*	-0.281	-0.556	0.146	-0.928	0.011	-0.253	0.505	-0.495	0.137
PKM	*Pkm*	-0.155	-0.011	0.971	0.418	0.148	-0.176	0.569	-0.358	0.188
PPARGC1A	*Ppargc1a*	0.806	-0.172	0.624	0.249	0.452	0.623	0.071	1.064	0.001
PPARGC1B	*Ppargc1b*	0.189	0.051	0.824	-0.193	0.380	-0.001	0.998	-0.106	0.605
PRX3	*Prdx3*	0.266	-0.107	0.511	0.132	0.391	0.166	0.306	0.171	0.234
PRX5	*Prdx5*	-0.083	0.021	0.892	-0.019	0.897	-0.041	0.789	-0.007	0.962
PSEN1	*Psen1*	-0.026	-0.026	0.820	0.078	0.477	-0.049	0.677	0.013	0.896
PTEN	*Pten*	0.131	0.001	0.995	-0.097	0.595	0.069	0.717	0.041	0.807
SCP2	*Scp2*	-0.808	-0.096	0.729	-0.584	0.028	-0.608	0.031	-0.742	0.002
SDHA	*Sdha*	0.185	-0.084	0.658	-0.239	0.185	0.027	0.886	0.013	0.937
SDHB	*Sdhb*	0.462	0.127	0.474	-0.026	0.876	0.195	0.271	0.193	0.220
SDHC	*Sdhc*	0.632	-0.009	0.957	0.101	0.502	0.244	0.121	0.251	0.073
SDHD	*Sdhd*	0.735	-0.042	0.850	-0.024	0.909	0.411	0.063	0.435	0.028
SDS	*Sds*	0.552	-0.177	0.474	0.353	0.130	0.513	0.035	0.445	0.042
SIRT1	*Sirt1*	0.214	0.016	0.938	0.066	0.732	-0.119	0.560	0.299	0.092
SLC27A1	*Slc27a1*	0.243	0.426	0.232	0.558	0.098	0.507	0.153	0.413	0.195
SLC27A2	*Slc27a2*	-0.093	0.095	0.659	-0.196	0.340	-0.106	0.622	-0.149	0.434
SLC27A4	*Slc27a4*	-0.326	-0.168	0.379	-0.070	0.699	-0.309	0.109	-0.298	0.078
SLC27A5	*Slc27a5*	0.118	-0.290	0.277	-0.112	0.657	-0.093	0.727	0.005	0.982
SUCLA2	*Sucla2*	0.370	0.007	0.963	-0.121	0.409	0.114	0.461	0.183	0.181
SUCLG1	*Suclg1*	0.279	-0.007	0.963	0.015	0.923	0.156	0.331	0.137	0.338
Synucleinα	*Snca*	-0.087	0.131	0.862	1.040	0.130	0.415	0.575	0.818	0.210
TFAM	*Tfam*	0.426	-0.001	0.992	-0.054	0.709	0.217	0.150	0.217	0.105
TPI1	*Tpi1*	0.483	-0.182	0.331	0.011	0.951	0.104	0.577	0.331	0.045
TRAK1	*Trak1*	0.678	0.125	0.502	0.095	0.591	0.419	0.023	0.301	0.068
TRX2	*Txn2*	0.583	0.027	0.862	0.236	0.109	0.181	0.242	0.340	0.014
TRXR2	*Txnrd2*	0.093	-0.187	0.271	-0.124	0.437	-0.015	0.931	0.033	0.825
UCP2	*Ucp2*	-0.133	0.204	0.479	0.582	0.033	0.177	0.540	-0.190	0.458
UQCR10	*Uqcr10*	0.369	0.246	0.170	0.020	0.907	0.319	0.074	0.419	0.008
UQCRB	*Uqcrb*	0.516	0.178	0.401	-0.102	0.618	0.259	0.226	0.308	0.106
UQCRC1	*Uqcrc1*	0.507	-0.064	0.712	-0.068	0.684	0.090	0.606	0.228	0.140
UQCRC2	*Uqcrc2*	0.688	0.012	0.944	-0.043	0.795	0.194	0.263	0.331	0.032
UQCRFS1	*Uqcrfs1*	0.618	0.012	0.942	-0.067	0.660	0.212	0.181	0.320	0.023
Xanthine oxidase	*Xdh*	0.107	0.077	0.634	0.158	0.303	-0.013	0.937	0.036	0.799

Table S10. Expression levels of genes involved in H2S production and signaling pathway correlated with the increase in calorie restriction (CR) and their gene expression at each level of CR relative to 12h ad libitum intake.

			10CR		20CR		30CR		40CR	
Symbol	**Gene Symbol**	**r**	**logFC**	**p**	**logFC**	**p**	**logFC**	**p**	**logFC**	**p**
CBS/CBSL	*Cbs*	-0.549	-0.626	0.021	-0.500	0.050	-0.701	0.010	-0.565	0.016
CRY1	*Cry1*	0.785	0.676	0.138	1.026	0.018	1.333	0.003	1.800	0.000
CRY2	*Cry2*	0.441	0.071	0.687	0.056	0.741	0.189	0.284	0.159	0.308
CTH	*Cth*	0.550	0.268	0.302	0.461	0.063	0.550	0.034	1.054	0.000
PER1	*Per1*	0.849	0.284	0.455	0.544	0.132	0.868	0.021	1.301	0.000
PER2	*Per2*	0.724	0.671	0.039	0.828	0.008	1.028	0.002	0.950	0.001
SIRT1	*Sirt1*	0.214	0.016	0.938	0.066	0.732	-0.119	0.560	0.299	0.092
FGF21	*Fgf21*	-0.076	0.369	0.614	0.588	0.399	-0.948	0.215	-0.960	0.146

Table S11. Expression levels of genes involved in xenobiotic metabolism correlated with the increase in calorie restriction (CR) and their gene expression at each level of CR relative to 12h ad libitum intake.

			10CR		20CR		30CR		40CR	
Symbol	**Gene Symbol**	**r**	**logFC**	**p**	**logFC**	**p**	**logFC**	**p**	**logFC**	**p**
ABCA1	*Abca1*	-0.518	-0.087	0.602	-0.172	0.280	-0.230	0.169	-0.264	0.073
ABCG1	*Abcg1*	-0.038	0.130	0.615	0.320	0.190	0.041	0.873	-0.302	0.192
ABCG5	*Abcg5*	0.286	0.287	0.179	0.106	0.604	0.276	0.196	0.139	0.464
ABCG8	*Abcg8*	-0.078	-0.054	0.805	-0.279	0.179	-0.140	0.522	-0.319	0.097
AE2	*Slc4a2*	0.109	0.029	0.861	0.205	0.185	-0.107	0.518	0.010	0.945
AHR	*Ahr*	0.468	-0.012	0.957	0.117	0.564	0.293	0.166	0.422	0.025
ALAS1	*Alas1*	0.595	0.988	0.033	1.105	0.013	1.421	0.002	0.913	0.030
ALDH1A1	*Aldh1a1*	-0.379	0.234	0.324	-0.117	0.606	-0.105	0.660	-0.037	0.860
ALDH1A7	*Aldh1a7*	-0.034	0.029	0.894	0.172	0.401	0.144	0.504	-0.002	0.991
ALDH3A2	*Aldh3a2*	0.595	0.450	0.133	0.489	0.088	0.771	0.010	0.882	0.001
ANKRA2	*Ankra2*	-0.150	0.140	0.518	-0.085	0.685	0.060	0.782	-0.153	0.436
ApoA1	*Apoa1*	-0.468	-0.682	0.033	-0.354	0.239	-0.588	0.066	-0.797	0.004
ApoB	*Apob*	-0.239	0.044	0.827	-0.174	0.358	-0.202	0.313	-0.057	0.747
APOC2	*Apoc2*	0.073	0.211	0.366	0.551	0.013	0.171	0.464	0.218	0.293
APOE	*Apoe*	-0.364	-0.248	0.238	-0.216	0.277	-0.331	0.116	-0.233	0.207
ARNT	*Arnt*	0.457	0.085	0.566	0.091	0.519	0.273	0.063	0.201	0.126
ASBT	*Slc10a2*	-0.623	-0.542	0.345	-0.396	0.463	-1.162	0.049	-1.764	0.001
BAAT	*Baat*	-0.151	0.050	0.809	-0.180	0.358	-0.015	0.943	0.163	0.372
BACS	*Slc27a5*	0.118	-0.290	0.277	-0.112	0.657	-0.093	0.727	0.005	0.982
BSEP	*Abcb11*	-0.627	-0.395	0.138	-0.610	0.016	-0.552	0.039	-0.446	0.055
CAR	*Nr1i3*	0.691	0.674	0.140	0.656	0.133	1.327	0.004	1.153	0.005
CAT	*Cat*	-0.805	-0.091	0.700	-0.470	0.039	-0.487	0.043	-0.668	0.001
CCRP	*Dnajc7*	0.217	-0.023	0.850	-0.153	0.183	-0.004	0.971	0.020	0.853
CD14	*Cd14*	-0.154	0.506	0.365	0.982	0.064	-0.159	0.782	-0.274	0.589
CES3	*Ces3a*	-0.924	-0.247	0.769	-1.607	0.051	-2.929	0.002	-4.669	0.000
ChREBP	*Mlxipl*	-0.493	-0.236	0.412	-0.743	0.007	-0.638	0.028	-0.520	0.040
c-Jun	*Jun*	-0.025	-0.027	0.943	0.834	0.017	-0.052	0.891	-0.014	0.966
CPT1A	*Cpt1a*	0.390	0.173	0.452	0.285	0.193	0.300	0.191	0.191	0.352
c-RAF	*Raf1*	-0.299	-0.165	0.253	-0.215	0.116	-0.278	0.055	-0.247	0.052
CRM-1	*Xpo1*	-0.081	-0.079	0.647	-0.266	0.104	-0.171	0.323	-0.136	0.372

CUL3	*Cul3*	0.353	0.026	0.864	-0.092	0.531	-0.025	0.870	0.187	0.169
CYP1A2	*Cyp1a2*	-0.687	-0.123	0.821	-0.924	0.078	-1.176	0.036	-2.285	0.000
CYP1B1	*Cyp1b1*	-0.231	0.206	0.729	-0.544	0.347	-0.757	0.223	-1.001	0.067
CYP27A1	*Cyp27a1*	-0.004	-0.562	0.060	-0.470	0.095	-0.280	0.345	-0.157	0.546
CYP2A6	*Cyp2a5*	0.169	1.206	0.015	1.435	0.003	1.390	0.005	1.171	0.009
CYP2B6	*Cyp2b10*	-0.133	1.602	0.277	4.118	0.008	1.852	0.213	3.296	0.024
CYP2C8	*Cyp2c39*	0.876	0.691	0.457	2.302	0.011	3.947	0.000	4.260	0.000
CYP3A5	*Cyp3a11*	0.415	0.541	0.169	1.047	0.005	0.772	0.049	1.286	0.000
CYP3A7	*Cyp3a13*	0.611	0.099	0.736	0.829	0.003	0.649	0.025	1.007	0.000
CYP4A14	*Cyp4a14*	0.822	2.801	0.015	4.426	0.000	5.538	0.000	6.391	0.000
CYP4A22	*Cyp4a10*	0.830	1.612	0.047	2.220	0.005	3.406	0.000	4.024	0.000
CYP7A1	*Cyp7a1*	0.394	0.316	0.485	0.865	0.045	1.275	0.005	1.275	0.002
CYP8B1	*Cyp8b1*	-0.679	-0.942	0.103	-1.523	0.006	-1.690	0.005	-2.072	0.000
ERK5	*Mapk7*	-0.087	0.035	0.909	0.106	0.709	-0.127	0.682	-0.082	0.765
FASN	*Fasn*	-0.367	-1.511	0.008	-1.297	0.014	-0.592	0.280	-1.562	0.001
FBP1	*Fbp1*	0.117	-0.036	0.851	-0.076	0.681	0.079	0.682	0.065	0.702
Fetuin B	*Fetub*	-0.149	-0.354	0.192	0.252	0.325	-0.229	0.398	-0.330	0.165
FGFR4	*Fgfr4*	-0.490	-0.152	0.465	-0.059	0.765	-0.399	0.058	-0.441	0.017
FOXO1	*Foxo1*	0.603	0.236	0.302	0.322	0.139	0.382	0.094	0.681	0.001
FOXO2	*Foxo3*	0.168	-0.019	0.924	-0.241	0.220	-0.120	0.562	0.015	0.933
FTL	*Ftl1*	0.220	0.118	0.549	0.193	0.301	0.164	0.402	0.214	0.220
FXR	*Nr1h4*	0.190	0.053	0.792	-0.168	0.379	0.148	0.460	0.106	0.548
G6PC	*G6pc*	0.183	-0.646	0.195	-0.285	0.543	0.167	0.733	0.657	0.133
GCLC	*Gclc*	-0.388	0.246	0.368	0.017	0.948	-0.571	0.041	-0.504	0.038
GR	*Nr3c1*	*0.055*	0.191	0.265	-0.069	0.671	0.075	0.664	-0.030	0.845
GSTM1	*Gstm2*	0.284	0.024	0.914	0.454	0.031	0.354	0.109	-0.020	0.917
GSTM2	*Gstm7*	-0.344	-0.306	0.099	-0.338	0.054	-0.342	0.065	-0.385	0.018
HDAC4	*Hdac4*	0.193	-0.153	0.629	0.013	0.966	0.018	0.953	0.128	0.642
HDAC5	*Hdac5*	-0.265	-0.543	0.005	-0.505	0.006	-0.435	0.025	-0.343	0.043
HL	*Lipc*	-0.575	-0.320	0.323	-0.763	0.014	-0.649	0.047	-0.784	0.006
HMGCS2	*Hmgcs2*	0.412	0.102	0.677	-0.066	0.779	0.183	0.455	0.356	0.102
HNF1α	*Hnf1a*	0.203	-0.285	0.066	-0.149	0.306	-0.277	0.074	0.115	0.392
HNF4α	*Hnf4a*	0.338	-0.104	0.665	0.075	0.744	-0.060	0.802	0.316	0.139
HO-1	*Hmox1*	0.117	-0.006	0.985	0.739	0.020	-0.080	0.813	0.241	0.418
IGFBP1	*Igfbp1*	0.377	0.089	0.878	1.118	0.042	0.318	0.581	1.199	0.022
IL-1	*Il1b*	-0.231	-1.102	0.055	-0.394	0.447	-1.195	0.040	-0.497	0.304
INSR	*Insr*	0.507	0.106	0.572	-0.076	0.670	0.153	0.414	0.245	0.141
IRAK	*Irak1*	-0.245	0.026	0.842	0.080	0.521	-0.091	0.486	-0.013	0.908
KEAP1	*Keap1*	0.076	0.009	0.946	-0.022	0.857	0.008	0.950	0.084	0.452
LBP	*Lbp*	0.527	-0.388	0.206	0.429	0.136	0.184	0.543	0.919	0.001
LPL	*Lpl*	-0.185	0.763	0.208	0.938	0.107	-0.668	0.285	-0.623	0.250
LRH-1	*Nr5a2*	0.161	-0.111	0.515	-0.169	0.297	-0.105	0.537	0.106	0.481
MAF	*Maf*	0.259	0.052	0.748	0.210	0.175	0.236	0.146	0.176	0.223
MD-2	*Ly96*	-0.313	-0.231	0.436	-0.253	0.368	-0.798	0.011	-0.412	0.122
MDR1	*Abcb1a*	0.576	1.621	0.014	2.488	0.000	2.378	0.000	2.826	0.000
MDR3	*Abcb4*	0.260	0.286	0.150	0.303	0.110	0.114	0.568	0.310	0.080
MEK5	*Map2k5*	0.099	-0.098	0.545	0.004	0.978	-0.200	0.220	-0.058	0.687
MEKK1	*Map3k1*	-0.017	0.233	0.317	0.167	0.452	-0.016	0.946	0.145	0.486
MGMT	*Mgmt*	0.011	0.128	0.611	0.040	0.868	0.215	0.390	-0.103	0.651
MRP2	*Abcc2*	0.241	0.209	0.333	0.190	0.355	0.132	0.543	0.139	0.470
MRP3	*Abcc3*	0.083	0.231	0.420	0.632	0.020	0.669	0.019	0.092	0.718
MRP4	*Abcc4*	0.073	1.657	0.007	2.157	0.000	0.988	0.108	1.217	0.030
MTTP	*Mttp*	0.098	-0.256	0.280	-0.348	0.121	-0.111	0.638	0.052	0.801

MYD88	*Myd88*	0.040	-0.245	0.162	-0.095	0.564	-0.174	0.318	0.009	0.954
NFκBp65	*Rela*	-0.300	-0.150	0.371	-0.134	0.396	-0.409	0.016	-0.292	0.049
NR0B2	*Nr0b2*	-0.288	-0.450	0.261	-0.159	0.673	-0.627	0.120	-0.554	0.114
NRF2	*Nfe2l2*	-0.139	-0.035	0.828	-0.105	0.491	-0.146	0.365	-0.057	0.687
NTCP	*Slc10a1*	0.248	-0.190	0.627	-0.560	0.135	-0.021	0.958	-0.033	0.924
OATP4	*Slco1b2*	-0.407	0.083	0.834	-0.513	0.178	-0.394	0.326	-0.677	0.054
OSTB	*Slc51b*	0.578	0.160	0.838	1.659	0.023	1.641	0.031	2.322	0.001
PAPSS2	*Papss2*	0.585	0.133	0.603	0.265	0.276	0.622	0.014	0.321	0.157
PEPCK	*Pck2*	0.047	0.229	0.534	0.905	0.008	0.269	0.464	0.047	0.886
PERK	*Eif2ak3*	-0.206	0.109	0.663	-0.187	0.438	-0.587	0.024	-0.329	0.145
PGC-1α	*Ppargc1a*	0.806	-0.172	0.624	0.249	0.452	0.623	0.071	1.064	0.001
PGC-1β	*Ppargc1b*	0.189	0.051	0.824	-0.193	0.380	-0.001	0.998	-0.106	0.605
PKLR	*Pklr*	-0.281	-0.556	0.146	-0.928	0.011	-0.253	0.505	-0.495	0.137
PLTP	*Pltp*	-0.122	-0.973	0.005	-0.269	0.404	-0.156	0.647	-0.992	0.001
PON1	*Pon1*	0.017	-0.150	0.613	-0.284	0.315	-0.070	0.813	-0.008	0.974
PPAR	*Ppara*	0.257	-0.004	0.987	-0.055	0.811	0.114	0.637	-0.037	0.864
PPARγ	*Pparg*	-0.012	0.249	0.483	0.534	0.113	0.024	0.947	-0.111	0.729
PXR	*Nr1i2*	0.805	0.306	0.204	0.498	0.030	0.782	0.001	0.783	0.000
RARα	*Rara*	-0.358	0.048	0.765	0.051	0.739	-0.203	0.217	-0.363	0.013
RXRα	*Rxra*	0.348	-0.026	0.890	-0.001	0.996	0.041	0.828	0.135	0.420
SCD1	*Scd1*	-0.123	-0.561	0.125	-0.670	0.053	-0.278	0.444	-0.438	0.169
SDC1	*Sdc1*	0.257	-0.136	0.497	0.441	0.020	0.208	0.297	0.375	0.035
SITPEC	*Ecsit*	0.136	0.053	0.751	-0.119	0.457	-0.069	0.683	0.111	0.451
SMRT	*Ncor2*	-0.095	-0.029	0.872	0.219	0.197	-0.123	0.495	-0.074	0.643
SOD3	*Sod3*	-0.247	-0.172	0.466	0.149	0.501	-0.314	0.186	-0.498	0.017
SR-BI	*Scarb1*	0.155	-0.154	0.397	0.015	0.930	-0.146	0.422	0.125	0.438
SRC-1	*Ncoa1*	0.269	-0.018	0.903	-0.090	0.507	0.104	0.465	0.194	0.123
SREBP1	*Srebf1*	-0.463	-0.260	0.435	-0.102	0.745	-0.343	0.304	-0.914	0.002
SULT2A1	*Sult2a3*	0.570	0.000	1.000	0.000	1.000	4.322	0.017	6.585	0.001
SUMO1	*Sumo1*	0.202	0.335	0.047	0.142	0.380	0.341	0.044	0.180	0.235
TEBP	*Ptges3*	-0.223	0.113	0.432	0.002	0.991	0.056	0.700	-0.021	0.869
TLR4	*Tlr4*	-0.006	-0.007	0.979	0.146	0.576	0.044	0.875	0.005	0.986
TRAF2	*Traf2*	-0.004	0.326	0.163	0.400	0.071	0.112	0.638	0.206	0.330
TRAF6	*Traf6*	0.420	0.135	0.414	0.082	0.601	0.150	0.365	0.383	0.009
UGT1A1	*Ugt1a1*	0.670	-0.010	0.972	0.310	0.249	0.523	0.063	0.805	0.001
UGT1A9	*Ugt1a9*	0.427	0.722	0.114	0.776	0.075	1.007	0.027	1.313	0.002
VLDLR	*Vldlr*	0.784	0.798	0.260	1.420	0.036	2.706	0.000	2.917	0.000
XAP2	*Aip*	-0.276	-0.335	0.083	0.042	0.815	-0.139	0.465	-0.453	0.008